ENERGY DISSIPATION IN HEAVY ION COLLISIONS

By

BETYLDA MARY JYRWA

DEPARTMENT OF PHYSICS
SCHOOL OF PHYSICAL SCIENCES

A THESIS
SUBMITTED IN FULFILMENT OF THE
REQUIREMENT FOR THE DEGREE OF

DOCTOR OF PHILOSOPHY

To

THE NORTH-EASTERN HILL UNIVERSITY
SHILLONG - 793001
MEGHALAYA, INDIA

NOVEMBER, 1984

"For it is He who gave me unerring knowledge of what exists, to know the structure of the world and the activity of the elements."

(Wisdom 7 : 17)

DEDICATED TO

MY MOTHER

Whose encouragement and affection has been a source of inspiration for this thesis.

CERTIFICATE

I certify that the dissertation entitled 'ENERGY DISSIPATION IN HEAVY ION COLLISIONS' submitted by Miss Betylda Mary Jyrwa in fulfilment of the requirements for the degree of DOCTOR of Philosophy is the outcome of a study undertaken by the candidate. I certify that the sources from which ideas have been borrowed have been duly referred to.

The material in this dissertation has not been presented to for award of a degree in any University before.

This dissertation may be placed before the examiners for evaluation and necessary formalities.

I certify that this dissertation is worth of consideration by the examiners.

Y.S.T. RAO,
Supervisor,
Physics Department,
North Eastern Hill University,
SHILLONG.

NOVEMBER 5, 1984.

ACKNOWLEDGEMENTS

I wish to express my deep gratitude to Dr. Y.S.T. Rao, Reader, Physics Department, North Eastern Hill University for supervision and constant guidance provided throughout my work and without which the thesis could not have been completed.

I am greatly indebted to Dr. V.S. Ramamurthy, Dr. R.K. Chaudhury, Mrs. Rekha Govil for the necessary training I received at the B.A.R.C. Computer, Bombay. I also express my thanks to the then Governor of Assam and Meghalaya Shri P. Malhotra, Colonel C.M. Chadda, Director, Survey of India (N.E.C.) for their kind permission to have access to the computer facility at the Survey of India, 80 Party (N.E.C.).

Major N. Chandra, Mr. T. Phillipose, Mr. P. Khongwang and Mr. Biswas have rendered invaluable services towards running the programmes successfully. I am grateful to all of them.

In respect of the illustrations, I am thankful to Major Gercha, Mrs. Tiewla, Mrs. Kharbuki from the Survey of India for sparing no pains to complete the graphs successfully.

I extend my gratitude to Mother Anne, Principal, St. Mary's College, Shillong for the permission to take up the research work, and the University Grants Commission for the financial assistance in my research works.

Finally, I take this opportunity to extend my gratitude to Mr. K.K.S. Shabong for taking keen interest in typing and Mr. M. Lakiang for cutting the stencils.

B.M. Jyrwa.

CONTENTS

CHAPTER 0

INTRODUCTION

0.1 Hartree-Fock Theory.

The Hartree-Fock Theory is an approximation which has been developed to study the many Fermion system in an independent particle approximation. The nuclear wave function is an antisymmetrized product of the single particle wave functions to satisfy the Fermi Dirac statistics. The independent particle wavefunctions are obtained by solving Schrodinger equation in a mean single particle potential.

Hartree-Fock Theory has been used in nuclear physics since its introduction in 1962. The first calculations were done by Ullah et al[1]. Several methods to improve the theory have since been introduced. They include Density Dependent Hartree-Fock[2], Brueckner Hartree-Fock,[3, 4, 5] Multiconfigurational Hartree-Fock[6] and many others.

0.2 Symmetry Projection.

Sometimes the Hartree-Fock wavefunction Ψ_{HF} does not possess the symmetries of the Hamiltonian, e.g. even in the case of the Hamiltonian commuting with the parity operator Ψ_{HF} need not have a good parity. Symmetry (Parity) projection on Ψ_{HF} give an improved description of the physical state.

Projection of parity [7, 8] and angular momentum from nuclear wavefunctions has been used extensively in the study of deformed nuclei and of nuclear rotational spectra.

0.3 Inclusion of Pairing.

Closed shell nuclei have a large energy gap between the occupied and unoccupied single particle energy levels and hence the Hartree-Fock description is expected to be good. However, for a typical open shell nucleus, the corresponding energy gap is not appreciably large and such a description is not adequate. In such cases the Hartree-Fock solution is 'soft' i.e. not very stable.

With several nucleons in the open shell, even a deformed Hartree-Fock wavefunction is not very stable.

The Hamiltonian with pairing was solved originally by Bardeen, Cooper and Schiffer to explain the phenomenon of superconductivity [10]. But for nuclear purposes, the Bogoliubov-Valatin method of quasiparticle is more suitable [11, 12, 13]. A quasi-particle creation operator is a mixture of a particle creation operator and a hole annihilation operator. The single particle states and the mixing parameters are coupled by combining the Hartree-Fock Theory procedure with the B.C.S. procedure.

0.4 Time Dependent Hartree-Fock Theory (TDHF).

In order to describe the time varying systems, one has to extend the stationary Hartree-Fock Theory to include time dependence.

The TDHF theory seeks a time dependent determinental wavefunction and demands that the operator $\left(i\frac{\partial}{\partial t} - H\right)$ should not create any one particle - one hole excitations.

There are equivalent formulations of arriving at a time dependent determinental wave function. The formalism was established more than fifty years back[14], and was used in the adiabatic limit to describe nuclear vibrations and rotations. More recently in the last ten years it was being used for the study of Heavy Ion Collisions[18].

The self-consistent mean-field-theory, instead of being static, is of time varying type. The TDHF wave function is a normalised determinental wave function Ψ_T, made up of time dependent single particle wave functions :

$$\Psi_T = \frac{1}{\sqrt{N}} \det\left[\Psi_1(x_1,t), \Psi_2(x_2,t) \cdots\cdots \Psi_N(x_N,t)\right] \qquad \text{-----(0.1)}$$

The exact wave function Ψ_{ex} satisfies the Time Dependent Schrodinger equation :

$$\left(i\frac{\partial}{\partial t} - H\right)\Psi_{ex} = 0 \qquad \text{-----(0.2)}$$

H, the many-body Hamiltonian in the notation of second quantization is written as :

$$H = \sum_{\alpha,\beta} T_{\alpha\beta}\, a_\alpha^\dagger a_\beta + \frac{1}{2} \sum_{\substack{\alpha,\beta \\ \gamma,\delta}} \langle \alpha,\beta | V | \gamma\delta \rangle\, a_\beta^\dagger a_\alpha^\dagger a_\delta a_\gamma \qquad \text{-----(0.3)}$$

The TDHF equations follow from the requirement [9] :

$$\delta \int dt\, \psi_T^\dagger \left(i\frac{\partial}{\partial t} - H \right) \psi_T = 0 \qquad \text{-----(0.4)}$$

The linear Schrodinger equation for the N-particle system is replaced by N coupled non-linear differential equations for the N occupied orbitals $\psi_i(\bar{r},t)$:

$$i\frac{\partial}{\partial t}\psi_i(\bar{r},t) = \frac{\delta \langle \psi_T | H | \psi_T \rangle}{\delta \psi_i^*(\bar{r},t)} \qquad \text{-----(0.5)}$$

$i = 1, 2, \ldots N$

Equation (0.5) conserves several quantities like the expectation values of the energy, H, the total momentum, the total angular momentum, and the scalar product of the single particle wave functions, $\langle \psi_i | \psi_j \rangle = \delta_{ij}$. From equation (0.3) it is obvious that the Hamiltonian H consists of the kinetic energy plus a local central two body potential. Subsequently we use the notation of one body density Matrix : $\rho(\bar{r},\bar{r}',t) = \sum_{i=1}^{N} \psi_i(\bar{r},t)\, \psi_i^*(\bar{r}',t)$

where the diagonal elements yield the particle density, and the kinetic energy density is given by :

$$\tau(\bar{r},t) = \bar{\nabla}_{\bar{r}} \cdot \bar{\nabla}_{\bar{r}'} \rho(\bar{r},\bar{r}';t)\Big|_{r=\bar{r}'}$$

Then variation of :

$$\langle \Psi_T|H|\Psi_T\rangle = \int d^3\bar{r}\frac{\hbar^2}{2m}\tau(\bar{r},t) + \frac{1}{2}\int d^3r\, d^3r' \rho(\bar{r},t) V(\bar{r}-\bar{r}')\rho(\bar{r}',t) - \frac{1}{2}\int d^3r \int d^3r' \left|\rho(\bar{r},\bar{r}';t)\right|^2 V(\bar{r}-\bar{r}') \quad (0.6)$$

as required by equation (0.5) would yield the required TDHF equations :

$$i\frac{\partial}{\partial t}\psi_i(\bar{r},t) = -\frac{\hbar^2}{2m}\nabla^2\psi_i(\bar{r},t) + \int d^3r' V(\bar{r}-\bar{r}')\rho(\bar{r}',t)\psi_i(\bar{r},t) - \int d^3r' V(\bar{r}-\bar{r}')\rho(\bar{r},\bar{r}',t)\psi_i(\bar{r}',t) \quad ----(0.7)$$

Leaving aside the third term on the right side of (0.7), the single particle wave functions are obtained from a Schrodinger equation where the potential is evolved by the mean field generated by the instantaneous nuclear density. The third term is the exchange term as required by the Pauli Principle.

0.5 Improvements on TDHF.

For a long time, the application of TDHF theory was restricted to the study of small amplitude slow collective motions[19]. TDHF was used to derive Random Phase Approximation (RPA) equations. In case the Hamiltonian and the wavefunction can be parametrized through a slowly varying collective co-ordinate q, in the adiabatic limit, one can obtain the expression for collective potential and Kinetic

energies. Depending on the nature of the problem, the collective motion can be treated classically or quantally.

0.6 Application of TDHF to Heavy Ion Collision (HIC).

TDHF calculations for Heavy Ion Collisions are being done since 1976[18]. The equations are written in terms of the density matrix in co-ordinate space and a Skyrme like interaction is used to simplify calculations. Calculations are done for several mass ranges and to demonstrate phenomena like fusion, Deep Inelastic Collision, giant multipole resonances, fission and compound nucleus formation. TDHF approximation is used in situations in which the strongly interacting fermion systems are far from equilibrium.

It has been observed that several other methods viz. (resonating groups[20], adiabatic TDHF[21], fluid dynamics[22] and RPA[23] etc.) have their own drawbacks e.g. the resonating group method is applicable to light nuclei, the RPA being a linearized version of TDHF is applicable only to small amplitude disturbances. Again it may be mentioned that the ATDHF is limited to the description of low-lying excitations in the case of large amptitude motion[24]. Fimally the application of fluid dynamics is very limited since the validity of approximations used can be determined only by testing them by a more complete microscopic theory[25]. A number of works[26, 27] have been carried out

on TDHF method to seek if it is the correct mean field theory. The above works[26, 27] have confirmed that TDHF is the true mean field theory for the calculation of one-body observables.

When the TDHF calculations have been compared with experimental results, it is seen that the TDHF approximation does not give a comprehensive description of nuclear reactions, but instead an exclusive picture of nuclear collisions[27]. This is because the detailed channel information is prohibited. Nevertheless one can conclude that there is a good agreement between theory and experiment for reactions which result in fusion or Deep Inelastic Collisions (DIC)[28].

0.7 Plan of the present Thesis.

Herein we propose to test the TDHF theory on the basis of an exactly solvable microscopic model.

Several calculations have been done on the basis of TDHF theory. Yet its validity has not been tested. This motivated us to verify its veracity, by using an exactly solvable model based on the Lipkin-Meshkov-Glick Hamiltonian[29], and finally comparing the results with those obtained from TDHF.

The detailed formalism, calculations, and results are presented in Chapter I. Chapter II deals with the application of symmetry Projected Time Dependent Hartree-Fock Theory (PTDHF) to an isolated nucleus and the subsequent interesting results. In Chapter III the TDHF theory has been extended to include pairing, where the Time Dependent Hartree-Fock Bogoliubov equations are given explicitly. Finally, Chapter IV gives the conclusions.

CHAPTER I

TEST OF TIME DEPENDENT HARTREE-FOCK THEORY USING A MODEL

1.1 Introduction.

In order to facilitate the study of the validity TDHF approximation, we have introduced an exactly solvable microscopic Hamiltonian based on the Lipkin model[29]. It consists of :

$$H = T + H_A + H_B + H_{int} \qquad \text{----------} (1.1)$$

Where T represents the kinetic energy of motion restricted to one dimension. The nucleons of each nucleus A and B interact a Lipkin like interaction given by :

$$\left.\begin{aligned} H_A &= \varepsilon L_3 + V\left(L_1^2 + L_2^2\right) \\ H_B &= \varepsilon S_3 + V\left(S_1^2 - S_2^2\right) \end{aligned}\right\} \qquad \text{--------} (1.2)$$

The nuclei A and B also interact with each other in a similar manner given by $H_{int} = V\left[L_+ S_+ + L_- S_-\right] a_1 \delta(x)$ ------ (1.3)

where $\left[2m/\hbar^2 = 1\right]$; $L_+ = \sum_m a^\dagger_{m+1} a_{m-1}$; $L_- = L_+^\dagger$

and $L_3 = \sum_{m,\sigma} \sigma\, a^\dagger_{m\sigma} a_{m\sigma}$ -------- (1.4)

The exact calculations of the energy loss, probability distribution etc. are presented in Appendix A. If the interaction V is neglected, the ground state is $|L_3 = -J\rangle$. It can be shown that if A is a single particle Hermitian operator $\left[A = \sum_{i,j} A_{ij}\, a_i^\dagger a_j\right]$

Then $\psi = \exp(iA)\,|L_3 = -J\rangle$ ---------- (1.5)

is also a determinental wavefunction. The most general

non-trivial wavefunction can be written as :

$$\Psi_{TDHF} = \exp[X]\,|\,L_3 = -J\rangle \qquad \text{-------- (1.6)}$$

Where $\exp X = \exp\left[-i/2\,(\sigma\cdot\hat{n})\theta\right]$

and $X = -i\theta\left[J_y \cos\phi + J_x \sin\phi\right] = -\eta J_+ + \eta^* J_-$ if

$\eta = \theta/2\; e^{-i\phi}$, (θ, ϕ)

indicate the direction of the maximal spin.

1.2 Motivation for Time Dependent Hartree-Fock.

The exact calculations (Appendix A) gave som interesting results. With a short ranged interaction, (either) nucleus gets excited to a state with energy $\mathcal{E}_i$ with a probability P_i that is almost Maxwell Boltzmann type, i.e. is proportional to $\exp(-\beta\mathcal{E}_i)$. We show that the TDHF theory also predicts a similar exponential distribution law approximately and thus has a good chance of being accurate. From equation (1.6) the wavefunction can be expanded in terms of the complete set of states $|\,M\rangle$, where $-J \le M \le J$. For weaker interaction, i.e. $(N-1)V/\mathcal{E} \ll 1$, the eigen states of H_A can be approximated by $|M\rangle$ themselves.

Then we have

$$\Psi_{TDHF} = e^X\,|J\rangle = \sum_M \binom{2J}{J+M}^{1/2} \left(\cos\theta/2\right)^{J+M} \left(e^{-i\varphi}\sin\theta/2\right)^{J-M} |M\rangle \qquad \text{-------- (1.7)}$$

But since the ground states is $|L_3 = -J\rangle$

$$\Psi_{TDHF} = e^X\,|-J\rangle = \sum_M \binom{2J}{J+M}^{1/2} \left(\sin\theta/2\right)^{J+M} \left(e^{-i\varphi}\cos\theta/2\right)^{J-M} |M\rangle \qquad \text{-------- (1.8)}$$

The probability of excitation to the state $|M\rangle$

$$P_M = |\langle \psi_{TDHF} | M \rangle|^2$$

or $$\ln P_M \simeq \ln C - 2M \cot\frac{\theta}{2} - M^2\frac{(1-2J)}{J^2} \quad \text{---(1.9)}$$

Where equation (1.9) has been evaluated using the Stirling formula $N! = \sqrt{2\pi N}\left(N/e\right)^N$

From equation (1.9) it is seen that C is a constant, independent of M. For most of the values of $M\left(|M| < J/2\right)$ the last term on the right side of equation (1.9) can be neglected. For $\theta = 0.1, 0.55, 1.00$, the dependence of P_M on M is shown in figure (1.1), (1.2) and (1.3), and listed in tables (1.1), (1.2) and (1.3).

The linear distribution suggests that there is a possibility that the TDHF prediction might agree with the exact results and given the basis for the expectation that the model serves as a testing ground for the adequacy of TDHF approximation.

1.3 Calculation of energy loss.

When the nuclei A and B are well separated so that the interaction between them can be neglected, the wavefunction of the system can be written in terms of the wavefunction of relative motion and the intrinsic motion of isolated nuclei. (The centre of mass motion is already separated out).

For an isolated Lipkin nucleus, from arguments given earlier, the Hartree-Fock like state is parametrized

by a complex parameter $\eta = \frac{\theta}{2} e^{-i\phi}$

The ground state is given by $\eta_0 = 0.5236$

$\left(\because \cos\theta = \frac{1}{(N-1)V/\varepsilon} \right)$ and $\phi = 0$. In this calculation

$\frac{(N-1)V}{\varepsilon} = 2.00$, If the incident relative momentum is k , the incident wave is given by

$$\Psi_{inc} = I_0 e^{ikx} \left| \eta_0(A)\, \eta_0(B) \right\rangle \text{ ------ (1.10a)}$$

The reflected and transmitted wavefunction are given by

$$\Psi_R = R e^{ik'x} \left| \eta'(A)\, \eta'(B) \right\rangle \text{ ------ (1.10b)}$$

and $$\Psi_T = T e^{ik''x} \left| \eta''(A)\, \eta''(B) \right\rangle \text{ ---- (1.10c)}$$

From energy conservation we have

$$\frac{k^2}{2m} + 2W(\eta_0) = \frac{k'^2}{2m} + 2W(\eta') = \frac{k''^2}{2m} + 2W(\eta'')$$

Where the Hartree-Fock energy $\bar{W}(\bar{\eta})$ is (1.12)

$$W(\eta) = -J\cos\theta - J\chi\cos\theta(1-\cos^2\theta) \text{ -- (1.12)}$$

$$\left(\chi = (N-1)V/\varepsilon \,,\ \varepsilon = 1,\ N = 8 \right)$$

For simplicity, we use the result that, since $\phi = 0$ to start with, it will remain zero throughout.

The final wave function can be written from the continuity condition as follows :

$$\psi = I_0 \phi_{inc} + R\phi_r - T\phi_t \quad \text{------(1.13)}$$

where

$$\left.\begin{aligned} \phi_{inc} &= e^{-i\theta_i L_y}|L\rangle\, e^{-i\theta_i S_y}|S\rangle \\ \phi_r &= e^{-i\theta_r L_y}|L\rangle\, e^{-i\theta_r S_y}|S\rangle \\ \phi_t &= e^{-i\theta_t L_y}|L\rangle\, e^{-i\theta_t S_y}|S\rangle \end{aligned}\right\} \text{---(1.14)}$$

Taking the norm of (1.13) and using the relations $R = r_1 + i r_2$ and $T = t_1 + i t_2$ we get the following relations :

$$I_0^2 + (r_1^2 + r_2^2) + (t_1^2 + t_2^2) + 2I_0 r_1 \cos^{4J}\left(\frac{\theta_i - \theta_r}{2}\right) - 2I_0 t_1 \cos^{4J}\left(\frac{\theta_i - \theta_t}{2}\right)$$

$$- 2(r_1 t_1 + r_2 t_2)\cos^{4J}\left(\frac{\theta_t - \theta_r}{2}\right) = 0$$

$$\text{------} \quad (1.15)$$

Now we take the derivative of (1.15) with respect to r_1, r_2, t_1 and t_2 individually, we arrive at the following relations :

$$r_1 = t_1 \cos^{4J}\left(\frac{\theta_t - \theta_r}{2}\right) + I_0 \cos^{4J}\left(\frac{\theta_i - \theta_r}{2}\right) = 0 \quad \text{----(1.16a)}$$

$$r_2 - t_2 \cos^{4J}\left(\frac{\theta_t - \theta_r}{2}\right) = 0 \quad \text{----(1.16b)}$$

$$t_1 - I_0 \cos^{4J}\left(\frac{\theta_i - \theta_r}{2}\right) - r_1 \cos^{4J}\left(\frac{\theta_t - \theta_r}{2}\right) = 0 \quad \text{----(1.16c)}$$

$$t_2 - r_2 \cos^{4J}\left(\frac{\theta_t - \theta_r}{2}\right) = 0 \quad \text{---(1.16d)}$$

From the boundary condition on the derivative of ψ we get

$$i\left[k_t T \phi_t - \left\{k_0 I_0 \phi_{inc} - k_r R \phi_r\right\}\right] - \left\{a_1\left(L_+ S_+ + L_- S_-\right) \phi_t T\right\} = 0 \quad \text{----(1.17)}$$

where

$$a = \frac{mV}{\hbar^2} a_1$$

On taking the norm of (1.17) we get :

$$k_t^2 TT^* + k_t k_r \left(T\phi_t, R^* \phi_r^*\right) - k_t k_0 T I_0 \left(\phi_t, \phi_{inc}^*\right)$$

$$- iT^* k_t T a_1^2 \left(\phi_t, V a_1 \phi_t^*\right) + k a_1 k_t R T^* \left(\phi_r, \phi_t^*\right)$$

$$+ k_r^2 RR^* - k_r k_0 R I_0 \left(\phi_r, \phi_{inc}^*\right) - i a_1 k_r R T^*$$

$$\left(\phi_r, V\phi_t^*\right) - k_0 I_0 k_t T^* \left(\phi_{inc}, \phi_t^*\right)$$

$$- k_r I_0 k_0 R^* \left(\phi_{inc}, \phi_r^*\right) + k_0^2 I_0^2 + i a_1 k_0 I_0 T^*$$

$$\left(\phi_{inc}, V\phi_t^*\right) + i a_1 T T^* k_t \left(V\phi_t, \phi_t^*\right) +$$

$$i a_1 T R^* k_r \left(V\phi_t, \phi_r^*\right) - i a_1 T k_0 I_0 \left(V\phi_t, \phi_{inc}^*\right)$$

$$+ a_1^2 TT^* \left(V\phi_t, V^*\phi_t^*\right) = 0 \quad \text{-----} \quad (1.18)$$

On using

$$e^x J_+ e^{-x} = -J_3 \sin\theta + \left(\frac{1+\cos\theta}{2}\right) J_+ + J_- \left(\frac{\cos\theta - 1}{2}\right)$$

$$e^x J_- e^{-x} = -J_3 \sin\theta + \left(\frac{1+\cos\theta}{2}\right) J_- + J_+ \left(\frac{\cos\theta - 1}{2}\right)$$

$$\text{-------} \quad (1.19)$$

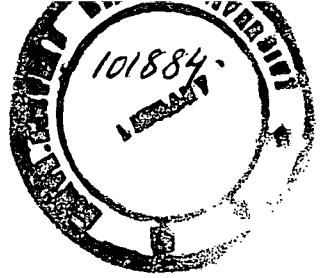

equation (1.18) turn out to be

$$k_t^2(t_1^2+t_2^2)+k_r^2(r_1^2+r_2^2)+k_0^2 I_0^2$$

$$+a^2(t_1^2+t_2^2)\left[2J^2\left\{\sin^4\theta_t\left\{J^2+(J-\tfrac{1}{2})^2-J\right\}\right.\right.$$

$$\left.\left.+2(J-\tfrac{1}{4})\sin^2\theta_t\right\}+1\right]+2k_tk_r\cos^{4J}\left(\frac{\theta_r-\theta_t}{2}\right)$$

$$(r_1t_1+r_2t_2)-2k_tk_0I_0t_1\cos^{4J}\left(\frac{\theta_i-\theta_t}{2}\right)-$$

$$2k_rk_0I_0r_1\cos^{4J}\left(\frac{\theta_i-\theta_r}{2}\right)-4ak_r(r_1t_2-r_2t_1)$$

$$\cos^{4J-2}\left(\frac{\theta_t-\theta_r}{2}\right)(1-\cos\theta_r\cos\theta_t)+4I_0k_0$$

$$at_2J^2\cos^{4J-2}\left(\frac{\theta_t-\theta_i}{2}\right)(1-\cos\theta_i\cos\theta_t)$$

------ (1.20)

From the equations (1.16a), (1.16b) and (1.16c), (1.16d)

we get

$$r_2=t_2,\quad k_r=k_t,\quad \theta_r=\theta_t,\ \text{and}$$

$$r_1=t_1-I_0\cos^{4J}\left(\frac{\theta_i-\theta_t}{2}\right)$$

Using the above conditions in equation (1.20) we obtain

$$k_t^2\left(t_1^2+t_2^2\right)+k_t^2\left\{t_1^2+I_0^2\cos^{8J}\left(\frac{\theta_i-\theta_t}{2}\right)\right.$$

$$\left.-2t_1I_0\cos^{4J}\left(\frac{\theta_i-\theta_t}{2}\right)+t_2^2\right\}+k_0^2I_0^2+$$

$$a^2\left(t_1^2+t_2^2\right)(c+1)+2k_t^2\left\{t_2^2+t_1\left\{t_1-I_0\right.\right.$$

$$\left.\left.\cos^{4J}\left(\frac{\theta_i-\theta_t}{2}\right)\right\}\right\}-2k_tk_0I_0t_1\cos^{4J}\left(\frac{\theta_i-\theta_t}{2}\right)$$

$$-2k_0k_tI_0\left\{t_1-I_0\cos^{4J}\left(\frac{\theta_i-\theta_t}{2}\right)\right\}-4a$$

$$k_t\left\{\left\{t_1-I_0\cos^{4J}\left(\frac{\theta_i-\theta_t}{2}\right)\right\}t_2-t_1t_2\right\}$$

$$\sin^2\theta_t+4I_0k_0at_2J^2\cos^{4J-2}\left(\frac{\theta_t-\theta_i}{2}\right)$$

$$\left(1-\cos\theta_i\cos\theta_t\right)=0 \qquad \text{-----(1.21)}$$

where

$$C=2J^2\left[\sin^4\theta_t\left\{J^2+\left(J-\frac{1}{2}\right)^2-J\right\}+2\left(J-\frac{1}{4}\right)\sin^2\theta_t\right]$$

On differentiating (1.21) with respect to 't_1', and equating it to zero we get

$$\left\{4k_t^2+a^2(c+1)\right\}t_1=\left(2k_t^2+k_tk_0\right)I_0\cos^{4J}$$

$$\left(\frac{\theta_i-\theta_t}{2}\right)+k_tk_0I_0 \qquad \text{-----(1.22)}$$

Similarly on differentiating (1.21) with respect to t_2

we get

$$\left\{4k_t^2 + a^2(c+1)\right\}t_2 = -2aI_0\cos^{4J-2}\left(\frac{\theta_i-\theta_t}{2}\right)$$
$$\left\{\frac{k_t}{4}\sin^2 2\theta_t + k_0 J^2\left(1-\cos\theta_i\cos\theta_t\right)\right\} \quad ----(1.23)$$

Equation (1.21) can further be simplified as

$$\left(t_1^2+t_2^2\right)\left\{4k_t^2 + a^2(c+1)\right\} - 2t_1k_t\left\{2k_t\right.$$
$$\left.\cos^{4J}\left(\frac{\theta_i-\theta_t}{2}\right) + k_0\left(1+\cos^{4J}\left(\frac{\theta_i-\theta_t}{2}\right)\right)\right\}$$
$$+ 4at_2\left\{k_t\cos^{4J}\left(\frac{\theta_i-\theta_t}{2}\right)\sin^2\theta_t + k_0J^2\cos^{4J-2}\right.$$
$$\left.\left(\frac{\theta_i-\theta_t}{2}\right)\left(1-\cos\theta_i\cos\theta_t\right)\right\} + k_t^2\cos^{8J}\left(\frac{\theta_i-\theta_t}{2}\right)$$
$$+ k_0^2 + 2k_0k_t\cos^{4J}\left(\frac{\theta_i-\theta_t}{2}\right) = 0 \quad ----(1.24)$$

Using equations (1.22) and (1.23) one solves for t_1, and t_2 and substitute them in equation (1.24) which is the equation to be minimized and the best value of θ_t is to be determined.

Having obtain the minimum value of θ_t we substitute it in the equation (1.12) and then we take the difference between the ground state $\left(\cos\theta = \frac{1}{2}\right)$ and the excited states we obtain the required energy loss for various values of θ_t.

1.4 Improvements on TDHF results.

From figure (1.4) - (1.8) and table 1.4 - 1.8 it is seen that there is some difference between the energy loss calculated from the exactly solvable model and that obtained from TDHF. Hence we try to improve TDHF approxi-

mation with the help of projection technique in the following way.

We know from equation (1.6) the TDHF wave function can be written as $\Psi_\alpha = A\Psi_+ + B\Psi_-$ -----(1.25)

i.e. a linear combination of odd and even parity. Consequently we may write

$$\Psi_\pm = N_\pm\left(\Psi_\alpha \pm \Psi_{-\alpha}\right) \text{ -------} (1.26)$$

The normalization constant $N_\pm$ can be determined from the conditions

$$\left(\Psi_\alpha, \Psi_\alpha\right) = 1$$

$$\left(\Psi_+, \Psi_+\right) = 1$$

and $$\left(\Psi_-, \Psi_-\right) = 1$$

Thereby having obtained $N_\pm$ we use it in equation (1.26) and consequently we calculate A and B which are to be substituted in equation (1.25) thereby we obtain

$$\Psi_\alpha = \sqrt{\frac{1+(\cos\theta)^{2J}}{2}}\,|\,\Psi_+\rangle + \sqrt{\frac{1-(\cos\theta)^{2J}}{2}}\,|\,\Psi_-\rangle \text{ -----} (1.27)$$

Having obtained this parity projection we now proceed to calculate the energy loss in the following manner :

Let $$E_1 = \langle \Psi^+_{\alpha\,inc} | H | \Psi^+_{\alpha\,inc}\rangle \text{ -----} (1.28)$$

denote the incoming energy states.

While E_2 and E_3 are the outgoing states where

$$E_2 = \langle \Psi^{+}_{\alpha\,out} | H | \Psi^{+}_{\alpha\,out} \rangle A^2 \quad \text{-----(1.29)}$$

and

$$E_3 = \langle \Psi^{+}_{\alpha\,out} | H | \Psi^{-}_{\alpha\,out} \rangle B^2 \quad \text{---(1.30)}$$

Thus improvements are made on the energy loss in the following way, we project the Hartree-Fock energy E_{HF} from equation (1.12) by multiplying it by [30] :

$$\left[1 + \frac{(\cos\theta_t)^{2J-2} \times \sin^2\theta_t}{1 + (\cos\theta_t)^{2J}} \right]$$

$$E_1' = E_{HF}\left[1 + \frac{(\cos\theta_t)^{2J-2} \sin^2\theta_t}{(1 + (\cos\theta_t)^{2J})} \right] \text{-----(1.31)}$$

similarly the even and odd parity is projected by multiplying the energy E_{HF} obtained for a particular θ_t from equation (1.12) by

$$\left[1 + \frac{(\cos\theta_t)^{2J-2}(\sin^2\theta_t)}{1 + (\cos\theta_t)^{2J}} \right]\left(\frac{1 + (\cos^{2J}\theta_t)}{2} \right)$$

$$+ \left[1 - \frac{(\cos\theta_t)^{2J-2}(\sin\theta_t)^2}{(1 - \cos^{2J}\theta_t)} \right]\left(\frac{1 - (\cos^{2J}\theta_t)}{2} \right) \text{------(1.32a)}$$

Thereby we obtain

$$E_2' = E_{HF}\left[\left\{1+\frac{(\cos\theta_t)^{2J-2}(\sin^2\theta_t)}{(1+(\cos\theta_t)^{2J}}\right\}\left(1+\frac{(\cos^{2J}\theta_t)}{2}\right)+\left\{1-\frac{(\cos\theta_t)^{2J-2}\sin^2\theta_t}{(1-\cos^{2J}\theta_t)}\right\}\left(\frac{1-\cos^{2J}\theta_t}{2}\right)\right] \quad ------ (1.32b)$$

Finally we obtain the projected energy loss by subtracting equation (1.32b) from equation (1.31).

1.5 Probability Distribution.

A probability distribution calculation had been done for several values of the incident momentum by using the states obtained from the exactly solvable model.

However the need to compare the above probabilities and those obtained from TDHF, somewhat motivated us to take an overlapp of the TDHF states obtained from equation (1.8) with the exact ones. In this way we are able to draw several conclusions as given in the next section.

1.6 Conclusion.

Based on the TDHF, PTDHF and the model as given in Appendix A, detailed numerical calculations have been performed on the variation of the energy loss for several incident momenta (K_0) and different ranges of the interaction parameter (λ). A brief discussion for each individual

21

interaction is given below.

When the interaction is very weak, (e.g. $\lambda = 0.1$) the energy loss decreases monotonically as a function of the incident momentum; in all, in the three cases, i.e. exact, TDHF, PTDHF, the trend is the same; however the average value of the energy loss obtained from the TDHF calculation is less than that of the exact calculation by a factor of 3. On the other hand the average values of the energy loss obtained from PTDHF calculations overestimate the exact calculations by a factor of 9 . (Fig 1.4). Hence one can conclude that for weak interactions, both the approximations, (i.e. TDHF and PTDHF) do not seem to be adequate.

As the interaction increases (e.g. $\lambda = 0.5$), though the trend is still the same as in the above case, yet there is some improvement, overall in the sense that the average energy loss from the TDHF theory underestimates the exact calculation by a factor of 1.4, while there is a reasonable agreement between the PTDHF and exact calculations especially in the range of low momenta i.e. $5 < k_0 < 23$; however beyond $K = 23$, there is a slight overestimation of the PTDHF over the exact calculation, nevertheless one can conclude that the PTDHF theory is a much better approximation to the exact calculation of the energy loss. (Fig 1.5).

With the interaction increased to $\lambda = 1.00$ the features improve, the TDHF underestimates by a factor of 1.3 while $k_0 < 23$; however beyond $k_0 = 23$, there is a slight overestimation of the PTDHF over the exact

calculation, nevertheless one can conclude that the PTDHF theory is a much better approximate to the exact calculation of the energy loss.

Moreover
With the interaction increased to $\lambda = 1.00$ ~~the features improve, the TDHF underestimates by a factor of 1.3 while~~ the average PTDHF improves it by 1.12, in other words, there is an excellent agreement between the results of PTDHF theory and those obtained from the exact calculation as the momenta k_0 exceed 10.

With the interaction $\lambda = 2.00$, the pattern is more or less the same, in the region $5 < k_0 < 26$, but beyond the value of $k_0 = 26$, both the TDHF and PTDHF results exhibit a steep fall on the other hand the results of the exact calculation continue decreasing slowly, as was the case in the above interactions.

For a high interaction $\lambda = 4.5$, the exact calculation exhibit a peak around $5 < k_0 = 8$, while the curve falls off steeply for $5 < k_0 < 8$ and it decreases monotonically for $k_0 > 8$; on the other hand no such peaks are seen in the TDHF and PTDHF calculations. The average results underestimate the exact calculations by a factor of 2 while the PTDHF results somewhat improve the TDHF theory but not to a high degree of accuracy. Hence the study of energy loss, from the exact calculation, TDHF and PTDHF approximations shows that the above theories are not good when the interaction is very weak $(\lambda = 0.1)$ and also when

the interaction is high. ($\lambda = 3.5$) For the latter the pattern is the same as that for $\lambda = 4.5$. On the other hand there is relatively good agreement between the exact calculations and the two theories for medium interactions e.g. $\lambda = 0.5$, 1.00 etc.

The results of the probability distribution are given in figures $1.9 - 1.24$ and listed in tables 1.4-1.9 A comparison is made between the logarithms of the probability distribution obtained from the exact calculations and the TDHF approximations.

For very weak interactions, i.e. $\lambda = 0.1$ and small values of the incident momentum (K_0) the probability distribution based on the exact calculations, follow a single Boltzmann distribution while those of TDHF approximation are distributed in a parabolic curve. With the increase of the incident momentum (K_0) the exact probability distribution follow two straight lines. Only the probability for the ground state of both TDHF and exact calculation agree excellently, while there is a bad agreement throughout. As the interaction increases to $\lambda = 0.5$, the pattern remains the same though for low incident momentum $K_0 = 5$, for the exact calculation there are two straight lines each for odd-odd and even-even states similarly there are two parabolas for the TDHF calculation. Therefore there is no agreement between them, as the incident momentum K_0 increases (e.g. $K_0 = 35.00$) there is a good agreement for the ground state. The results of TDHF calculations are distributed in

a single parabola, while the results the exact calculations follow a single Boltzmann distribution.

As the interaction λ is increased to 1.00, the features do not change much, except that for small incident momentum $k_0 = 5.00$, the exact calculations follow a single Boltzmann distribution, there is an excellent agreement between the TDHF calculation and exact ones for the odd state 5.04. For $k_0 > 20.00$, there are two straight lines for the exact calculations.

With the interaction increased to $\lambda = 2.00$, the exact calculations, are distributed in a single straight line for all values of the incident momentum (k_0), while the TDHF calculations follow a single parabolic curve for $k_0 = 8$, and for $k_0 > 8$, there are two parabolic curves, one interesting feature here, is that the two curves somewhat get closer for positive states, i.e. the curvature decreases and approaches the line obtained from the exact calculations, thereby producing a relatively good agreement between the TDHF and exact calculations.

When the interaction is increased to 3.50, for low values of the incident momentum $5 \leq k_0 < 15.00$, there is a bad agreement between the TDHF and exact calculations for $k_0 > 15$, the latter follow a single straight line and the former is in two parabolic curves. However for $k_0 = 17.00$, and the odd eigenstate -5.04 exhibits an excellent agreement. With higher incident momentum (k_0) there is a good

agreement for the positive eigenvalues between the TDHF and the exact calculations.

Finally when the interaction is increased to $\lambda = 4.5$, the exact calculations split into two straight lines and the TDHF calculations also follow two parabolic paths, except that for high incicent momentum (e.g. $K_0 = 10$) the two parabolic curves almost merge on the positive side of the eigenvalues and there is relatively a good agreement.

The presence of such random features above, leads one to investigate the possibility of a phase transition.

Figures 1.25 - 1.36 display a difference in the logarithms of the probability distribution obtained from the exact and TDHF calculations as the function of the various incident momenta for all the states beginning with the ground state, at different ranges of the interaction parameter.

From the figures it is evident that for very weak interaction $\lambda = 0.1$, the curves are smooth, in both cases odd and even. With the increase of the interaction to $\lambda = 0.5$ a peak is evident around the incident momentum $K_0 = 22.00$ for the ground state -5.37 , while the rest of the curves are smooth.

For the interaction $\lambda = 1.00$ a peak appears for the odd eigenstates 1.76 and 5.04 around $15 < K_0 < 20$, the rest of the curves vary smoothly. For the interaction parameter $\lambda = 2.00$, the curves decrease exponentially for

26

the higher even and odd states, while the low lying states vary smoothly.

With the interaction increased to $\lambda = 3.50$, the peaks are seen for the even eigenstates with eigenvalues 0.00, 3.24 and 5.37 around $k_0 = 8$ while the other curves vary smoothly. Again the odd eigenstate decreases exponentially, except for the state 1.76 a peak appears at $k_0 = 15$, while the other curves vary smoothly.

Finally with the interaction parameter $\lambda = 4.50$, the peaks are seen for the higher even eigenstates with eigenvalues 0.00, 3.24 and 5.37 around $7 < k_0 \leq 10$, while the low lying states vary smoothly on the other hand for the odd states, the curves decrease exponentially while the lowest odd state with eigenvalue -5.04 vary smoothly.

The presence of such sharp peaks leads one to conclude that there is a possibility of a phase transition since at those instances there is more than one minimum value for the transmitted angle θ_t.

CHAPTER II

PROJECTED TIME DEPENDENT HARTREE-FOCK THEORY APPLIED TO AN ISOLATED LIPKIN LIKE SYSTEM.

2.1 Introduction.

In the previous chapter we have seen the results of TDHF in a collision of two Lipkin like systems. One of the significant results was the explanation of the exponential probability distribution. But as seen in the Appendix (A) in some cases the odd parity state behave differently from the even parity states and a single distribution function is not appropriate.

This motivated us to propose a procedure of incorporating the symmetry properties of the Hamiltonian in the Time Dependent Hartree-Fock formalism.

From the defination of symmetry operator $[S, H]$, one can find simultaneous eigenstates of S and H. If an approximate model eigenfunction Φ of H is not an eigenstates of S, repeated operation of S on Φ will result in a set of wave functions where Φ, $S\Phi$, $S^2\Phi$ - - - - - usually span a manifold of finite dimension. One can construct linear combination (ψ_k) of these wave functions that are eigenfunctions of S.

In most of the open shell nuclei, the search for a Hartree-Fock state usually leads to a Hartree-Fock single particle potential that is not spherically symmetric. Hence the single particles wave function or the many body wave-

function obtained from Hartree-Fock calculation are not eigenfunctions of angular momentum operator. However this Hartree-Fock state can conceptually be regarded as describing the intrinsic state of the nucleus. Quite often, the Hartree-Fock potential has axial symmetry and in such cases the component of the total angular momentum along the symmetry axis K, is a good quantum number.

It is possible to project out wavefunctions ϕ_J, that are eigenfunction of the total angular momentum J, by using the generator co-ordinate approach through the usual rotation matrices.

$$\Psi^J_M \simeq \int d\Omega \, D^J_{MK}(\Omega) \, \Phi_K(\Omega) \text{ ------ } (2.1)$$

The projected wavefunction is of considerable importance. Since the wavefunction has the symmetry properties desired by the Hamiltonian, it is usually a better representation of the eigenstate of H. Further, since all the with different values of Ψ^J_M, are generated from the same intrinsic state Φ_K, they all correspond to different collective rotational states of the same intrinsic state and thus do correspond to the members of collective rotational band connected through highly enhanced $E2$ transitions etc. These states Ψ_K, represent a band of eigenstates of H. An example is the rotational states projected out of a deformed Hartree-Fock solution.

Thus to take the desired symmetry in the mean field approximation, we describe the state of the system obtained

by projection of an appropriate symmetry from the determinental wave function.

2.2 Time Independent Projected Hartree-Fock Theory.

Whenever a Hartree Fock solution ψ_{HF} breaks a symmetry present in the original Hamiltonian, as in the case of deformed nuclei where the rotational invariance is broken, then ψ_{HF} does not have a good angular momentum. If we want to improve on the Hartree-Fock approximation to satisfy certain symmetry properties of the original Hamiltonian (Rotational symmetry), then we project wavefunctions of the desired symmetry from the Hartree-Fock solution. By this we get an improved result. The procedure is done in the following way; Let $\psi_{HF}(\kappa, 0)$ be a Hartree-Fock wave function describing an axially symmetric deformed nucleus with symmetry axis along the z -axis and which is an eigenstate of J_z with eigenvalue k . Let $\psi_{HF}(\kappa, \Omega)$ be the same wave function with orientation given by the Euler angles $\Omega(\alpha, \beta, \gamma)$. If $D^{I}_{KM}\Omega$ is a rotation matrix element. Then the trial wavefunction can be represented as

$$\psi_{KIM} = \int d\Omega\, \psi_{HF}(\kappa, \Omega)\left(D^{I}_{MK}(\Omega)\right) \text{----} (2.2)$$

In the above equation, ψ_{KIM} is an eigenstate of J^2 and J_z with eigenvalues $I(I+1)$ and M . The intrinsic state $\psi_{HF}(\kappa, 0)$ is not an eigenstate of angular momentum, while the projected states correspond to collective motion of the system satisfying the desired symmetry.

The method of projecting linear and angular momenta was first studied by Griffin and Wheeler[41] and by Peierls and Yoccuz[42]. The results predicts definite values of the kinetic energies of rotation, though the prediction of the centre of mass motion was incorrect. However this discrepancy was removed by Peierls and Thouless[43] with the help of a second generator co-ordinate.

It was seen by Verhaar[44] that when $\beta \simeq \bar{\kappa}$, one gets an energy spectrum of rotational model form in a deformed nuclei. The calculation of moment of inertia and other quantities is also possible.

Instead of carrying out projection after variation of the intrinsic wave function ψ_{HF} (i.e. HFP) one can also first project out states of good angular momentum, then we vary the intrinsic wave function so as to minimize the energy, i.e. PHF. This method was used by Rouhaninejad and Yoccuz[45] and it was seen to give much better results than the HFP theory.

2.3 Application to the Lipkin Hamiltonian.

We illustrate the use of the projection technique using a Lipkin Hamiltonian[30, 40]. The Hartree-Fock like independent particle wavefunction can be parametrized (as already mentioned) through χ :

$$\psi_{HF} = e^{\chi} \left| M = -J \right\rangle \text{ --------(2.3)}$$

As already mentioned, the Hamiltonian conserves the parity P. But Ψ_{HF} is not an eigenfunction of P. The two projected wavefunctions (unnormalised) are :

$$\Psi_{\pm} = \left(e^{x} \pm e^{-x}\right) \left| M = -J \right\rangle \quad ----- (2.4)$$

and

$$E_{\pm} = \frac{\langle \Psi_{\pm} | H | \Psi_{\pm} \rangle}{\langle \Psi_{\pm} | \Psi_{\pm} \rangle}$$

$$= \langle \Psi_{HF} | H | \Psi_{HF} \rangle \frac{1 \pm \sin^{2}\theta \left(\cos\theta\right)^{2J-2}}{\left(1 \pm \left(\cos\theta\right)^{2J}\right)} \quad ---(2.5)$$

When PHF calculations on the Lipkin model were done by Agassi et al[30], it was found that for $\chi \gg 1$ the projection technique does not improve results appreciably. This is because of the near degeneracy of the odd-even states. But for smaller values of $\chi \left(1 < \chi < 1.5\right)$, the HFP results are considerably better than HF results. However, the odd parity excitation energy differs appreciably from the exact value.

On the other hand the PHF calculations of Parikh[40] et al show substantial improvement in the ground state energy and leads to good results even for $\chi < 1$. However, they have not studied the odd parity states.

On calculating the odd eigenvalues it is found that the PHF calculations agree with the exactly calculated values when $\chi < 1$. This is depicted in figure (2.1) and listed in table (2.1). Around $\chi > 1$, i.e. $\chi = 1.077$, the HFP has

not improved the accuracy, only it has changed the sign of errors.

Further it was seen that for odd parity states, the deformation parameter χ varies smoothly, unlike the even parity states where χ has steep variation around $\chi \simeq 1.7$. This is displayed in figure (2.2) and shown in table (2.2).

The phase transition which appeared in the Hartree-Fock solution at $\chi = 1$, has now disappeared by projection.

From the figure (2.3) it is clear that the excitation energy obtained from PHF calculation are considerably better than the results obtained by Parikh et al [40], through the use of other approximation theories : Random Phase Approximation (RPA), exact one particle hole (EXPH) equation method, and the renormalized RPA.

As expected for larger values of χ, (say $\chi > 1.5$) the projection makes very little difference and hence the excitation energy predicted by PHF is bound to be much smaller than the exact value. Thus Parikh et al [40] have established that for $\chi \gg 1$, it is immaterial whether one projects before or after variation or indeed whether one projects at all.

2.4 Projected Time Dependent Hartree-Fock Theory.

The above projected Hartree-Fock theory has been generalised to include time dependent problems by inducing some symmetries in the Time Dependent Hartree-Fock equations:

$$\langle a_p^\dagger a_h \Psi_{TDHF} \left| \left(i\frac{\partial}{\partial t} - H \right) \right| \Psi_{TDHF} \rangle = 0 \qquad \text{-----(2.6)}$$

in the following manner. By replacing the determinental wave function by a projected component of the determinental wave functions :

$$\langle a_p^\dagger a_h \Psi_{PTDHF} \left| \left(i\frac{\partial}{\partial t} - H \right) \right| \Psi_{TDHF} \rangle = 0 \qquad \text{-----(2.7)}$$

On using equation (1.7) one may write :

$$e^{2x} |J\rangle = \sum_M \binom{2J}{J+M}^{1/2} (\cos\theta)^{J+M} \left(e^{-i\phi} \sin\theta \right)^{J-M} |M\rangle \qquad \text{-----(2.8)}$$

Then equations (2.7) can be written as follows :

$$\langle -J | J_- \left(e^x + e^{-x} \right) \left(i\frac{\partial}{\partial t} - H \right) \left(e^x + e^{-x} \right) | -J \rangle = 0 \qquad \text{-----(2.9)}$$

Thus equation (2.9) produce $2p-2h$ excitations only and not $1p-1h$ excitation.

2.5 Application of PTDHF to the Lipkin Model.

Hereby we apply the projected time-dependent Hartree-Fock formalism given in the last section to study the Lipkin Hamiltonian. From equation (2.9) the projected time-dependent Hartree-Fock wave function can be written as follows :

$$\langle \Psi_2 \left| \left(i\frac{\partial}{\partial t} - H \right) \right| \Psi_1 \rangle = 0 \qquad \text{------(2.10)}$$

$$\Psi_1 = \left\{ e^{\left(-\eta J_+ + \eta^* J_-\right)} \pm e^{\left(\eta J_+ - \eta^* J_-\right)} \right\} \left| \Psi_{TDHF} \right\rangle \qquad \text{------(2.11)}$$

$$\Psi_2 = \left(e^{-\eta J_+ + \eta^* J_-} \pm e^{\eta J_+ - \eta^* J_-} \right) a_p^\dagger a_h \left| \Psi_{TDHF} \right\rangle \qquad \text{------(2.12)}$$

These equations can be simplified as follows :

We introduce the rotations

$$X = -\eta J_+ + \eta^* J_-$$

One may also write equation (2.10) as :

$$\left\langle \left(e^X + e^{-X}\right)\left(J_+ \Psi_{TDHF}\right) \right| i\frac{\partial}{\partial t} - H \left| \left(e^X + e^{-X}\right) \Psi_{TDHF} \right\rangle = 0 \qquad \text{------(2.13)}$$

Now the state e^X given by equation (1.7) contains both even and odd M values. On the other hand the state $\left(e^X \pm e^{-X}\right)\left|M=-J\right\rangle$ has state with only even or odd M values.

One can rewrite equation (2.13) as follows :

$$\langle J \left| J_+ e^X \left(i\frac{\partial}{\partial t} - H \right) \left(e^X + e^{-X}\right) \right| J \rangle = 0 \quad \text{or,}$$

$$\left\langle J-1 \left| e^X i\frac{\partial}{\partial t}\left(e^X + e^{-X}\right) \right| J \right\rangle = \left\langle (J-1) \left| e^X H \left(e^X + e^{-X}\right) \right| J \right\rangle \qquad \text{------(2.14)}$$

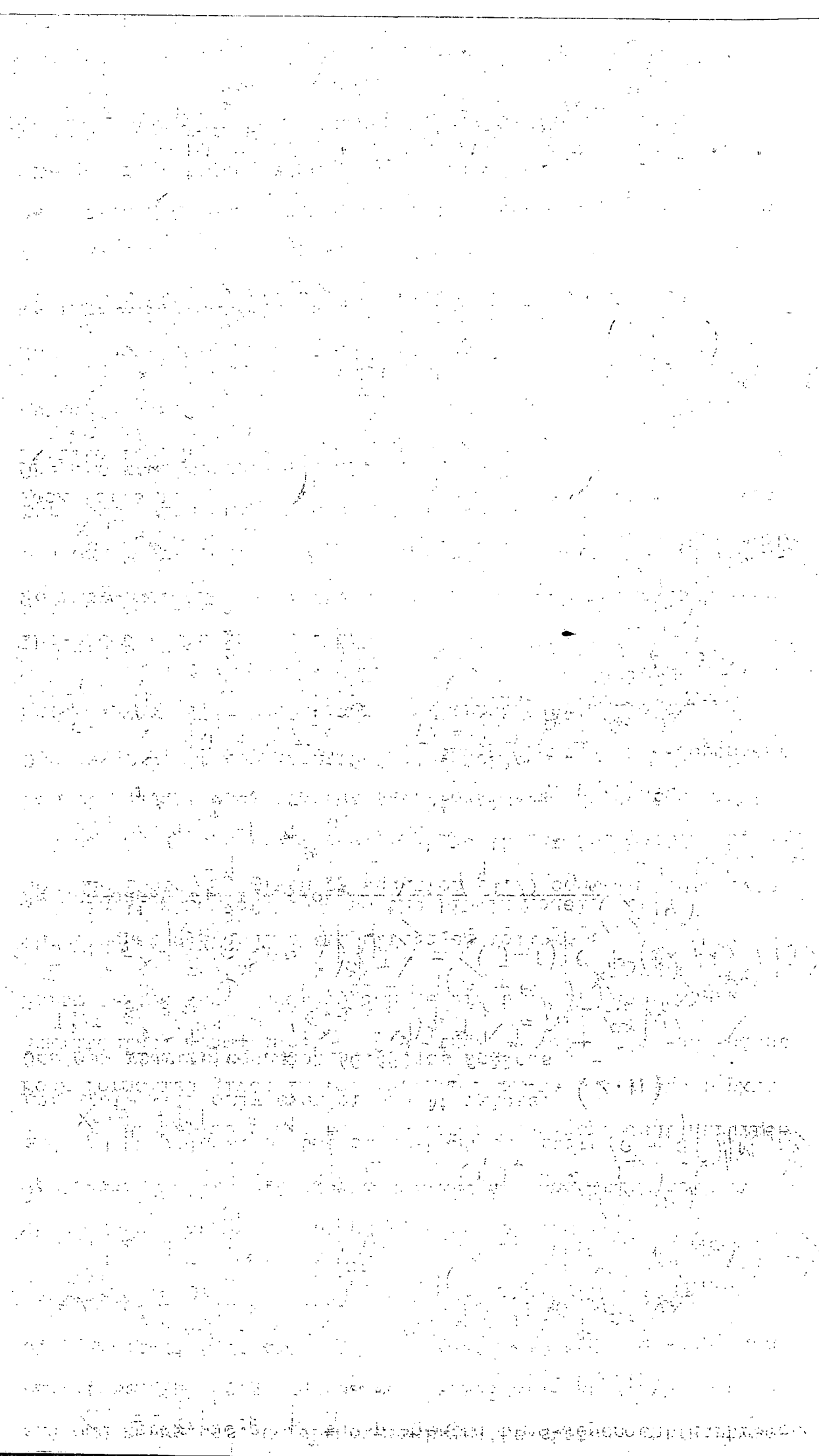

In order to simplify equation (2.14) we use the following equations :

$$e^{\chi} J_3 e^{-\chi} = J_3 \cos\theta + \frac{1}{2}\sin\theta\, e^{i\phi} J_+ + \frac{1}{2}\sin\theta\, e^{-i\phi} J_- \quad \text{---(2.15a)}$$

$$e^{\chi} J_+ e^{-\chi} = -J_3 \sin\theta\, e^{-i\phi} + \frac{1}{2}(1+\cos\theta) J + \frac{1}{2}(\cos\theta - 1)\, e^{-2i\phi} J_- \quad \text{---(2.15b)}$$

$$e^{\chi} J_- e^{-\chi} = -J_3 \sin\theta\, e^{i\phi} + \frac{1}{2}(1+\cos\theta) J_- + \frac{1}{2}(\cos\theta - 1)\, e^{2i\phi} J_+ \quad \text{---(2.15c)}$$

Now the left hand side of equation (2.14) is

$$\left\langle J-1 \left| e^{\chi} i\frac{\partial}{\partial t} e^{\chi} \right| J \right\rangle + \left\langle J-1 \left| e^{\chi} i\frac{\partial}{\partial t} e^{-\chi} \right| J \right\rangle$$

On using relations like

$$\frac{\partial}{\partial t}(e^{\chi}) = \lim_{\delta \to 0} \dot{\phi} \left[\frac{e^{\chi(\phi+\delta)} - e^{\chi(\phi)}}{\delta} \right] \quad \text{or,}$$

$$\frac{\partial}{\partial t}(e^{\chi}) = \lim_{\delta \to 0} \dot{\phi} \left[\frac{e^{\chi(\phi+\delta)}\, e^{-\chi(\phi)} - 1}{\delta} \right] e^{\chi(\phi)}$$

where $e^{\chi(\phi+\delta)}$ is like a rotational operator similarly for $e^{-\chi\phi}$

With the help of equations (2.15) the left side of equation (2.14) turn out to be

$$\dot{\phi}\sin\theta\left[\frac{1}{2} + (\cos\theta)^{2J-2}\left\{\left(J-\frac{1}{2}\right) - J\cos\theta\right\}\right]$$

On using the Lipkin Hamiltonian[29] in the right hand side of equation (2.14) and evaluating terms like $J_1, J_2, J_3, J_1^2, J_3^2$, $(J_1 J_2 + J_2 J_1)$, $(J_2 J_3 + J_3 J_2)$ and $(J_1 J_3 + J_3 J_1)$.

These operators can change the M values of the state on which they operate by 0 , 1 or 2 only and hence the equation (2.14) is further simplified and finally we obtain the time dependent equations as follows :-

$$\dot{\xi} = \frac{V\sin 2\phi\left[2(\xi)^{2J+5} + \{(-8J-8)\xi + \xi^3(12J+14) + \xi^5(4J^2-8J+8)\}\right]}{2\xi\{J(1-\xi^2)-1\}} \qquad ----(2.16a)$$

$$\dot{\phi} = \frac{-(J-1)(1-\xi^2)2\xi + V\cos 2\phi\left[(1+\xi^2) + \{(2J^2-5J+3)\right.}{-\sqrt{1-\xi^2}\left[0.5+(\xi)^{2J-2}\{(J-0.5)-J\xi\}\right]}$$

$$\left. + \xi^2(-8J^2+28J-5) + \xi^4(10J^2-45J+4) + \xi^6(-4J^2+22J)\}\right]$$

$$---(2.16b)$$

where $\xi = \cos\theta$

which are the differential equations to be solved interatively. The results are given in section 2.7.

2.6 TDHF results of Lipkin Model.

Griffin et al[39] have studied the TDHF solutions of the LMG[29] model, and they have established the presence of a ground state phase transition when the interaction parameter $\chi = 1$, in the sense that when the interaction parameter $\chi < 1$, there are only open curves in the $(\theta - \phi)$ space pertaining to rotations. On the other hand when the interaction parameter $\chi > 1$, there exist both open and closed loops, the latter being associated with librations, in other words two types of TDHF solutions exist simultaneously for strong interactions, viz (a) those portrayed

by closed loop trajectories (librations), which are doubly degenerate, and (b) those shown by open, periodic rotations which are non degenerate.

2.7 General theory of the Projected Time Dependent Hartree-Fock equations.

From the proceeding section, it is seen that the PTDHF equations are of the form

$$\dot{\theta} = P(\theta, \phi) \quad ----- (2.17)$$

$$\dot{\phi} = Q(\theta, \phi) \quad ---- (2.18)$$

The above equations are autonomous as P and Q do not depend on time explicitly.

If $\theta(t)$ and $\phi(t)$ are solutions of equation (2.17) and (2.18), the oriented curve described by the moving point $\theta = \theta(t)$ and $\phi = \phi(t)$, in the phase space, as t increases, is called a (phase) trajectory of the system.

There are three basic types of trajectories -

(a) non closed or open curves,

(b) closed (cycles) curves : when the trajectory along which the moving point passes through the same point,

(c) rest point or stationary point :

The trajectory consists of a single point.

If our interest is confined to the qualitative nature of orbits, i.e. the category from the above three

under which they can be classified. The equations (2.17) and (2.18) are to be re-written as

$$\frac{d\theta}{d\phi} = \frac{P(\theta,\phi)}{Q(\theta,\phi)} \qquad \text{------(2.19)}$$

Any point (θ,ϕ) for which the two functions $P(\theta,\phi)$ and $Q(\theta,\phi)$ do not vanish simultaneously is called an ordinary point with respect to the differential equation. On the other hand a point (θ_0,ϕ_0) for which

$$P(\theta_0,\phi_0) = Q(\theta_0,\phi_0) = 0$$

is called a singular or a stationary point. The asymptotic behaviour of the trajectories in the neighbourhood of a singular point determines the type of equilibrium represented by the singular point.

Expanding the right hand side of equations (2.17) and (2.18) in the neighbourhood of the stationary point (θ_0,ϕ_0) we obtain

$$\dot{\theta} = B(\phi-\phi_0) \qquad \text{------(2.20)}$$

$$\dot{\phi} = D(\theta-\theta_0) \qquad \text{------(2.21)}$$

where the dots refer to terms of higher orders relative to $\theta-\phi_0$ and $\phi-\phi_0$ and

$$\left.\begin{aligned} B &= P'_{\phi}(\theta_0,\phi_0) \\ D &= \theta'_{\theta}(\theta_0,\phi_0) \end{aligned}\right\} \qquad \text{---------(2.22)}$$

To solve the equations (2.20) and (2.21), we make a transformation by $\theta \longrightarrow \theta_0 + \theta$, $\phi \longrightarrow \phi_0 + \phi$. Thus we obtain

$$\left.\begin{aligned} \dot{\theta} &= B\phi \\ \dot{\phi} &= D\theta \end{aligned}\right\} \quad \text{-------(2.23)}$$

From equation (2.23), if the product BD is negative, we obtain an oscillatory system whereby the trajectories are not intersecting the point. Such an isolated point may be terms as a node. However, if the product BD is positive, we get open curves.

2.8 Results of the Projected Time Dependent Hartree-Fock equations.

The Projected Time Dependent Hartree-Fock equations are given in equations (2.16) as

$$\dot{\xi} = \frac{V \sin 2\phi\left[2(\xi)^{-2J+5} + \left\{(-8J-8)\xi + \xi^3(12J+14) + \xi^5(4J^2-8J+8)\right\}\right]}{2\xi\left\{J(1-\xi^2)-1\right\}}$$

$$= F(\xi,\phi) \quad \text{---------(2.24)}$$

$$\dot{\phi} = \frac{-(J-1)(1-\xi^2)2\xi + V\cos 2\phi\left[(1+\xi^2) + \left\{(2J^2-5J+3)\xi^2(-8J^2+28J-5) + \xi^4(10J^2-45J+4) + \xi^6(-4J^2+22J)\right\}\right]}{\sqrt{1-\xi^2}\left[0.5 + (\xi)^{-2J-2}\left\{(J-0.5) - J\xi\right\}\right]}$$

$$= G(\xi,\phi) \quad \text{----------(2.25)}$$

Owing to the presence of 2ϕ in the right side of equations (2.24) and (2.25) there exist a translatory symmetry between $0 < \phi < \pi$ and $\pi < \phi < 2\pi$. There is also a reflection symmetry about $\phi = \pi/2$
In the neighbourhood of the singularities (ξ_0, ϕ_0) the equations can be written in analogy with equation (2.20) and (2.21). It is seen that the above equations (2.24) and (2.25) give rise to four singularities whose positions depend on the strength of the interaction brought in through the term in the above **equations.**

The isolated or stationary points are evaluated in the following way.

The right hand side of equation (2.24) vanishes if $\phi = 0, \pi/2$ for all values of ξ and nowhere else. The numerator of equation (2.25) can be written in the form

$$N_1 = -6\xi(1-\xi^2) + V(16 - 20\xi^2 - 16\xi^4 + 24\xi^6)$$

On using the Newton-Raphson method of approximation one obtains the fixed or stationary points as $(\xi_1, 0)$, $(\xi_2, 0)$, $(-\xi_1, \pi/2)$, $(-\xi_2, \pi/2)$
where $0.9 < \xi_1 < 1$ and $0.09 < \xi_2 < 0.6$
for $0.25 < NV/\varepsilon < 2.5$
In the above case the points $(-\xi_2, \pi/2)$ and $(\xi_1, 0)$ are nodes whereas for the points $(\xi_2, 0)$ and $(-\xi_1, \pi/2)$ the trajectories are open curves. The above points are displayed in table (2.3).

From the equations (2.24) and (2.25) it is evident that the right side of (2.25) is infinity for $\xi = 0, \pm \frac{\sqrt{3}}{2}$ for all values of ϕ other than 0 and $\pi/2$, in which case the right side of (2.25) vanishes. On the other hand $\dot{\phi}$ is finite at $\xi = 0$ and at $\xi = \pm \sqrt{3}/2$

Near the line $\xi = 0$, the trajectories cross it normally with those in the region $0 \leq \phi \leq \pi/2$ being in an upward direction and those lying between $\frac{\pi}{2} < \phi \leq \pi$ going in a downward direction, thereby indicating that the velocity or the rate of change of ξ is very fast.

Just below and above the lines $\xi = \pm \sqrt{3}/2$, the curves turn away from the line, thereby it can be termed as a repeller.

From equation (2.25), $\dot{\phi}$ is infinity for $\xi = \pm 1$, however $\dot{\xi}$ is finite at such points.

For $\xi = -1$, one may write

$$\frac{d\phi}{d\xi} = (1+\xi)^{-1/2}/c$$

On integration $$c\phi + \alpha = 2\sqrt{1+\xi}$$

or $$(1+\xi) \simeq \frac{1}{2} c^2 (\phi - \phi_0)^2$$

Hence the curves will approach $\xi = -1$ following a parabolic path and depending on C they could either diverge or converge to it, in the sense that for the region $0 \leq \phi \leq \pi/4$ the curves approach the line $\phi = \pi/4$ from the left side while for $\pi/4 < \phi \leq \pi/2$ the orbits approach

the line $\phi = \pi/4$ from the right side. A similar feature is noticed for $\pi/2 < \phi \leq \pi$ For $\rho = 1$,
If one expands the numerator of equation (2.25) as follows :

$$\dot{\phi} = -12\varepsilon + 4v\cos 2\phi(1 - 10\varepsilon)$$

$$= (-12 - 4v\cos 2\phi)\varepsilon + 4v\cos 2\phi$$

Now depending on the step ε and the values of ϕ ranging from $\phi = 0$ to $\phi = \pi$ the right hand side of equation (2.25) could change alternately between positive and negative, thereby changing the direction of the curves.

In general between $\rho_1 < \rho < 0.866$, we get open curves, and a similar feature is noticed in the negative side of ρ .

Around the nodes we get closed elliptical loops which gradually increase in size, as the strength of the interaction increases. However for large interaction and small positive ρ values, one sees that around $\phi = \pi/2$, there are narrow loops i.e. $\dot{\rho} = \rho^{-4}$ while it broadens out in the negative half of ρ or below the line $\rho = 0$.

From figures 2.4–2.9 it is evident that for very small values of the interaction χ one obtains horizontal trajectories. However as the interaction slowly increases, some distinctive features which have not been noticed in the TDHF results (presented by Griffin et al)[39] are evident here in the following sense. There are closed curves

within $-0.5 < \xi < 0.5$. Then beyond that there are open curves. Between $\xi_1 < \xi \leq 0.866$ the curves tend towards the line $\xi = 0.866$, a similar feature is seen on the negative side of ξ after that demarcation, the curves beginning from $\xi = \pm 0.866$ approach the line $\xi = \pm 1$.

Then there are no qualitative changes for different values of the interaction upto $\chi = 1.05$, the only difference is that around the singular points there are closed loops whose width decreases as one approaches the positive values of ξ . A phase transition occurs at $\chi = 1.906$, whereby the upper open curves disappear completely and the trajectories starting from the line $\xi = 0.866$, turn downwards and from a closed curve by enclosing the singular point and returning to the starting point.

However the lower open curves still exists, thereby prompting one to search for a second phase transition which is seen to occur at $\chi = 2.310$. Thereby the trajectories starting from the line $\xi = 0.866$ goes forward and then downwards at $\pi/4 < \phi < \pi$ and they approach the line $\phi = \pi/2$ and finally terminate at $\xi = -0.866$, a similar feature is seen for $0 < \phi \leq \pi/2$ thereby eliminating the possibility of any lower open curves. Finally for $\chi = 2.5$ there are no open curves, and one sees only closed loops.

44

CHAPTER III

TIME DEPENDENT HARTREE-FOCK BOGOLIUBOV EQUATIONS FOR A SOLVABLE MODEL

3.1 Time Dependent Hartree-Fock Bogoliubov General Theory.

The pairing theory was first established by Mayer[31], its wide implications were generally not recognized until the emergence of the BCS[10] theory of superconductivity which was incorporated into nuclear physics by Bohr[32] et al.

Generally, pairing effects the particles in the unfilled shells of the nuclei and the pairing force is a short range interaction. Though pairing does not affect the Binding Energy, yet it plays an important role in yielding collective excitations corresponding to rotational or vibrational states. This is because the short range forces contribute to all the multipole components of the interaction.

The pairing interaction : $g\sum_{\alpha,\beta} a_\alpha^\dagger a_{\bar\alpha}^\dagger a_{\bar\beta} a_\beta$ connects a pair of particles in the $(\alpha, \bar\alpha)$ states with a pair in the $(\beta, \bar\beta)$ states. Here $\bar\alpha$ denotes the time reversed state corresponding to α .

Pairing can be included in the Hartree-Fock theory by generalising the latter to the Hartree Bogoliubov theory. This generalization is brought about by the Bogoliubov -

45

Valatin transformation[33] through the equations :

$$\left.\begin{aligned} \eta_\alpha^\dagger &= u_\alpha a_\alpha^\dagger - v_\alpha a_{\bar\alpha} \\ \eta_{\bar\alpha}^\dagger &= u_\alpha a_{\bar\alpha}^\dagger + v_\alpha a_\alpha \end{aligned}\right\} \text{-----(3.1)}$$

Here $a^\dagger$'s are the Fermion creation operators for particles and $\eta^\dagger$'s are the quasi-particle creation operators. For the transformation to preserve the anti commutation relations :

$$\left.\begin{aligned} \{\eta_\alpha, \eta_\beta^\dagger\} &= \delta_{\alpha\beta} \\ \{\eta_\alpha, \eta_\beta\} &= \{\eta_\alpha^\dagger, \eta_\beta^\dagger\} = 0 \end{aligned}\right\} \text{-----(3.2)}$$

one requires the normalization conditions viz. :

$$u_\alpha^2 + v_\alpha^2 = 1$$

In using a quasi-particle picture, the ground state wave function is no longer a determinental one, but it can be expressed as :

$$\Psi_{g.s} = \eta_1^\dagger \text{-------} \eta_m^\dagger |0\rangle \text{-----(3.3)}$$

Where, $\Psi_{g.s}$ is a quasi-particle vacuum and $|0\rangle$ is a physical vacuum.

The deformed Hartree-Fock orbitals c's are related to the single particle Fermion operators according to the relation :

$$c_\alpha^\dagger = \sum_i u_{\alpha i} a_i^\dagger \qquad \text{-----(3.4)}$$

It is well known that $\Psi_{a.s}$ does not have a definite number of physical particles. Consequently, one uses a

46

Lagrange Multiplier λ in minimizing the Hamiltonian through the equation $H' = H - \lambda n$ where n is the number operator to study the nucleus of N nucleons. The value of λ is brought about by insisting that the expection value of n should be equal to the total number of particles N . (N is the number of the particles in the system).

It is readily seen that the arbitrariness of the single particle wave function can be avoided by introducing the density matrix ρ and the pairing matrix K :

$$\rho_{\alpha\beta} = \langle \Psi_{g.s} | a_\alpha^\dagger a_\beta | \Psi_{g.s} \rangle \text{ ------(3.5)}$$

$$K_{\alpha\beta} = \langle \Psi_{g.s} | g_\beta g_\alpha | \Psi_{g.s} \rangle \text{ -----(3.6)}$$

The necessary conditions to be satisfied by ρ and K are

(1) ρ is Hermitian

(2) $\mathrm{Tr}\,\rho = N$

(3) $\rho^2 - \rho = K K^*$

(4) $K^T = -K$

(5) $\rho K - K\rho^* = 0$

From Pal[34] one may write the Hartree-Fock single

particle Hamiltonian h and the pairing potential Δ as

$$h_{\alpha\beta} = t_{\alpha\beta} + \sum_{\gamma\delta} \langle \alpha\gamma | v | \beta\delta \rangle \rho_{\delta\gamma} \quad \text{-----(3.7)}$$

where

$$t_{\alpha\beta} = \sum_{\alpha,\beta} \langle \alpha | T | \beta \rangle$$

and

$$\Delta_{\alpha\beta} = \frac{1}{2} \sum_{\gamma\delta} \langle \alpha\beta | v | \gamma\delta \rangle K_{\delta\gamma} \quad \text{------(3.8)}$$

3.2 Time Dependent Hartree-Fock Bogoliubov Theory.

It was Koonin and Nix[35] who first formulated the Time Dependent Hartree-Fock Bogoliubov Theory (TDHFB). In the study of Deep Inelastic Heavy Ion Collisions, the damping has been computed by Nix[35], with the help of the total energy obtained from a Time Dependent BCS Theory.

In the Bloch Messiah[36] formulation there is a lack of time reversal symmetry leading to the weakening or vanishing of the energy gap. This defect has been removed by Pal[34] through the use of a suitable symmetry to define degenerate pairs of eigenvalues and eigenstates of the density matrix and the Bloch Messiah representation with the eigenstates as basis. Thereby the Time Dependent equations have been expressed as follows :

$$i\dot{\rho} = [\hat{h}, \rho] + \Delta K^* - K\Delta^* \quad \text{------(3.9)}$$

$$i\dot{K} = \hat{h}K + K\hat{h}^* + \Delta\rho^* + \rho\Delta - \Delta \quad \text{------(3.10)}$$

where

$$\hat{h} = h - \lambda n \quad \text{------(3.11)}$$

3.3 The model for testing validity of Hartree-Bogoliubov method.

The validity of the Hartree Bogoliubov - theory has been ascertained within a special exactly solvable model of the many-body problem.

The model Hamiltonian as used by K. Bleuler and D. Schutte[37], and Agassi[38] is given as follows :

$$H = \sum_{\sigma} \varepsilon_{\sigma} \sum_{\sigma} a^{\dagger}_{m\sigma} a_{m\sigma} -$$

$$\frac{g}{4} \sum_{\substack{m_1,\sigma_1 \\ m_2,\sigma_2}} a^{\dagger}_{m_1\sigma_1} a^{\dagger}_{-m_1\sigma_1} a_{-m_2\sigma_2} a_{m_2\sigma_2} \delta_{m_1} \delta_{m_2}$$

$$- \frac{f}{2} \sum_{\substack{m_1,\sigma_1 \\ m_2,\sigma_2}} a^{\dagger}_{m_1\sigma_1} a^{\dagger}_{m_2\sigma_2} a_{m_2-\sigma_2} a_{m_1-\sigma_1}$$

----- (3.12)

Where $\delta_{m_i} = (-1)^{j-m_i}$, m varies from $-j$ to j, j is a half integer. $\sigma = \pm 1$ denotes the two shells each with the same degeneracy $(\Omega = 2j+1)$, and each can have the same or opposite parity.

The first term in the model Hamiltonian consists of the single particle part. The second term is the pairing interaction which implies the creation of particles (holes) in the two levels with the corresponding creation of holes (particles) in the time reversal state. g is independent of m and σ. The third term is the monopole term which mainly describes the transition of particles (holes) vertically upwards or downwards.

The pairing interaction favours a spherical shell structure, while the monopole interaction favours a so-called parity deformed solution.

3.4 Results of the above model.

The following results are established from the TIHFB formalism as given by Agassi[38].

In the weak coupling limit i.e. $\frac{Nf}{\epsilon} < 1$, it reproduces a vibrational band. In the strong coupling limit, $\frac{Nf}{\epsilon} > 1$, one can distinguish a deformed ground state and a rotational band. Due to the symmetry of the monopole model the rotational band consists of two members only.

The force parameters $\frac{f}{\epsilon}, \frac{g}{\epsilon}$ are so chosen so that

the pairing corelations dominate for small N values, and the ground state is spherical. Whereas for $N = \Omega$ (where the degeneracy $\Omega = 2j + 1$) the ground state is deformed, and the monopole interaction predominates.

As given in Chapter II, the TDHF solution for the Lipkin-Meshkov-Glick (LMG) model has been studied by Griffin et al [39].

It has been established that the TDHF solution is periodic in time. At certain value of the interaction strength χ some ground state phase transition is seen to prevail, i.e. at $\chi = 1$, the Time Independent Hartree-Fock solution undergoes a ground state phase transition. For $\chi < 1$, the system is seen to exhibit the non degenerate rotational symmetry. For $\chi > 1$, there are two types of Time Dependent Hartree-Fock solutions, viz. the nondegenerate rotations as well as the doubly degenerate librations exist.

The TDHF equations are written in terms of coupled differential equations in the following manner :

$$\left.\begin{aligned} \dot{\theta} &= -\epsilon \chi \sin\theta \sin 2\phi \\ \dot{\phi} &= \epsilon (1 - \chi \cos\theta \cos 2\phi) \end{aligned}\right\} \quad ----- (3.13)$$

The effects of Time Dependence in pairing theory have been first considered by Koonin and Nix [35], and several others. The various difficulties are posed by the fact that the wavefunction of the Time Dependent Schrodinger

have been first developed by Koonin and Nix , and several, i.e. at the Time Independent Hartree-Fock solution undergoes a ground state phase transition. ral others. The various difficulties are posed by the fact

that the wavefunction of the Time Dependent Schrodinger For $\lambda < 1$ the system is seen to exhibit the non degenerate rotational symmetry. For $\lambda > 1$ there are two types the pairing correlations dominate for small N values, and the ground state is spherical. Whereas for $N = 12$ (where the

degeneracy $2J - 2J + 1$) the ground state is deformed, and of Time Dependent Hartree-Fock solutions, viz. the nondegenerate rotations as well as the doubly degenerate Libra-

tions exist.

the monopole interaction predominates.

As given in Chapter II, the TDHF solution for the

Lipkin-Meshkov-Glick (LMG) model has been studied by

The TDHF equations are written in terms of coupled

differential equations in the following manner :

Griffin et al

$$\frac{\partial}{\partial t} = -\epsilon \left(\sin\theta \, S_{xx} \, 2\phi \right) \qquad \text{---} \quad (3.15)$$

It has been established that the TDHF solution is

periodic in time. At certain values of the pairing energy strength) some ground state phase transition is seen to

have been first developed by Koonin and Nix , and several, i.e. at the Time Independent Hartree-Fock solution undergoes a ground state phase transition. ral others. The various difficulties are posed by the fact

that the wavefunction of the Time Dependent Schrodinger For $\lambda < 1$ the system is seen to exhibit the non degenerate rotational symmetry. For $\lambda > 1$ there are two types the pairing correlations dominate for small N values, and the ground state is spherical. Whereas for $N = 12$ (where the

degeneracy $2J - 2J + 1$) the ground state is deformed, and of Time Dependent Hartree-Fock solutions, viz. the nondegenerate rotations as well as the doubly degenerate Libra-

tions exist.

the monopole interaction predominates.

As given in Chapter II, the TDHF solution for the

Lipkin-Meshkov-Glick (LMG) model has been studied by

The TDHF equations are written in terms of coupled

differential equations in the following manner :

Griffin et al

$$\frac{\partial}{\partial t} = -\epsilon \left(\sin\theta \, S_{xx} \, 2\phi \right) \qquad \text{---} \quad (3.15)$$

It has been established that the TDHF solution is

periodic in time. At certain values of the pairing energy strength) some ground state phase transition is seen to

equation has to be of mixed time-reversal symmetry while constructing the BCS type. This problem however has been circumvented by Pal[34] with the help of a suitable symmetry.

In analogy with equation (3.13) as obtained by Griffin et al[39] we introduce pairing which essentially requires four differential equations each for $\dot{\theta}$, $\dot{\phi}$, $\dot{\alpha}$, $\dot{\beta}$.

3.5 Method for obtaining TDHFB equations.

The method used in this context essentially consists of substituting equation (3.12) into equations (3.7) and (3.8) so that the Hartree-Fock Hamiltonian can now be written as follows :

$$h_{m\sigma,m'\sigma'} = \delta_{\sigma\sigma'}\varepsilon\delta_{mm'} - [f\rho_{m-\sigma,m'-\sigma'} + g\rho_{-m\sigma,-m'\sigma'}]\delta_{mm'}\delta_{\sigma\sigma'} - f\delta_{mm'}\delta_{\sigma+\sigma'}\sum_{m_3\sigma_3}\rho_{m_3-\sigma_3,m_3\sigma_3} \quad -----(3.14)$$

Again the pairing potential Δ can be written in the form :

$$\Delta_{m\sigma,m'\sigma'} = \frac{1}{2}\delta_{m+m'}\left[-g\mathfrak{S}_m\left(\sum S_{m_2}K_{-m_2\sigma_2,m_2\sigma_2} - fK_{m-\sigma,m'-\sigma'}\right)\right]\delta_{\sigma\sigma'} \quad -----(3.15)$$

The deformed Hartree-Fock creation operators are written in terms of the single particle fermion operators as follows :

$$\left.\begin{aligned} C^{\dagger}_{1m} &= \cos\frac{\theta}{2}a^{\dagger}_{-} + \sin\frac{\theta}{2}e^{-i\phi}a^{\dagger}_{+} \\ C^{\dagger}_{2m} &= -\sin\frac{\theta}{2}e^{-i\phi}a^{\dagger}_{-} + \cos\frac{\theta}{2}a^{\dagger}_{+} \end{aligned}\right\} -----(3.16)$$

The time dependence is essentially brought through the dependence of θ and ϕ on time.

Next the quasi-particle creation operators written in terms of the Hartree-Fock single particles through the canonical transformation as follows :

$$\left.\begin{aligned} \eta_m &= u_m c_m - v_m c_{-m}^{\dagger} \\ \eta_m^{\dagger} &= u_m c_{-m} + v_m c_m^{\dagger} \end{aligned}\right\} \text{-----(3·17)}$$

Using the above equations one calculates ρ and K, Δ and $\hat{h}$. In the matrix language they involve essentially 4 matrices each of dimension 4×4 i.e. states between $m+$, $m-$, $-m+$, $-m-$ $(m > 0)$. Where there are $(2j+1)$, values for m and the second notation after m denotes spin.

It is seen from the transformation equations both Hartree-Fock and Hartree-Bogoliubov that there are six variables viz. θ, ϕ, u_1, v_1, u_2 and v_2. However due to the substitution brought in from the equation $u_1 = \cos\alpha$, $v_1 = \sin\alpha$, $u_2 = \cos\beta$ and $v_2 = \sin\beta$. It is seen that $v_1^2 + v_2^2 = \text{Const} = N/(2j+1)$ and $u_1^2 + v_1^2 = 1$ also $u_2^2 + v_2^2 = 1$, the variables are reduced to 4. The dimensions of the matrices are also reduced to 2 x 2.

From Pal[34] the Time Dependent equations involve on the left side quantities like $\dot{\rho}$ and $\dot{K}$ to be written in terms of $\dot{\theta}$, $\dot{\phi}$, $\dot{\alpha}$ and $\dot{\beta}$.

The equations for ρ, K, Δ and $\hat{h}$ in terms of θ, ϕ, α and β can be written as follows :

ρ Consists of $\begin{bmatrix} \rho_{11} & \rho_{12} & 0 & 0 \\ \rho_{21} & \rho_{22} & 0 & 0 \\ 0 & 0 & \rho_{11} & \rho_{12} \\ 0 & 0 & \rho_{21} & \rho_{22} \end{bmatrix}$

which can be written as $\begin{bmatrix} \rho_1 & 0 \\ 0 & \rho_1 \end{bmatrix}$ where $\rho_1 = \begin{bmatrix} \rho_{11} & \rho_{12} \\ \rho_{21} & \rho_{22} \end{bmatrix}$

essentially

$$\left.\begin{aligned} \rho_{11} &= \sin^2\alpha \sin^2\frac{\theta}{2} + \sin^2\beta \cos^2\theta/2 \\ \rho_{22} &= \sin^2\alpha \cos^2\theta/2 + \sin^2\beta \sin^2\theta/2 \\ \rho_{12} &= \frac{1}{2}\sin\theta\, e^{-i\phi}\left(\sin^2\alpha - \sin^2\beta\right) \\ \rho_{21} &= \frac{1}{2}\sin\theta\, e^{i\phi}\left(\sin^2\alpha - \sin^2\beta\right) \end{aligned}\right\} \quad \text{----- (3.18)}$$

Hence it is seen from equation (3.18) that the diagonal elements ρ_{11} and ρ_{22} are real.

The superscripts R and I mean the real and imaginary parts respectively.

However

$$\left.\begin{aligned}
\rho_{12}^{R} &= \tfrac{1}{2}\sin\theta\cos\phi\left(\sin^2\alpha-\sin^2\beta\right)\\
\rho_{12}^{I} &= -\tfrac{1}{2}\sin\theta\sin\phi\left(\sin^2\alpha-\sin^2\beta\right)\\
\rho_{21}^{R} &= \tfrac{1}{2}\sin\theta\cos\phi\left(\sin^2\alpha-\sin^2\beta\right)\\
\rho_{21}^{I} &= \tfrac{1}{2}\sin\theta\sin\phi\left(\sin^2\alpha-\sin^2\beta\right)
\end{aligned}\right\} \quad \text{------(3.19)}$$

Again $\hat{h}$ can be written as $\begin{bmatrix} \hat{h}_1 & 0 \\ 0 & \hat{h}_1 \end{bmatrix}$

where $h_1 = \begin{bmatrix} \hat{h}_{11} & \hat{h}_{12} \\ \hat{h}_{12} & \hat{h}_{22} \end{bmatrix}$

$$\left.\begin{aligned}
\hat{h}_{11}^{R} &= \tfrac{1}{2}\left\{2\varepsilon+(f-g)(c-2\sin^2\alpha)\cos\theta-(f+g)c\right\}\\
\hat{h}_{22}^{R} &= \tfrac{1}{2}\left\{-2\varepsilon-(f-g)(c-2\sin^2\alpha)\cos\theta-(f+g)c\right\}\\
\hat{h}_{12}^{R} &= -f(2j+1)\sin\theta\cos 2\phi\left(c-2\sin^2\beta\right)\\
\hat{h}_{11}^{I} &= \hat{h}_{22}^{I} = \hat{h}_{12}^{I} = 0\\
\hat{h}_{21}^{R} &= \hat{h}_{12}^{R}
\end{aligned}\right\}$$

------(3.20)

The equations for K can be written as :

$$K = \begin{bmatrix} 0 & K_1 \\ -K_1 & 0 \end{bmatrix}$$

where

$$K_1 = \begin{bmatrix} K_{11} & K_{12} \\ K_{12} & K_{22} \end{bmatrix}$$

$$K_{11} = \frac{S_m}{2}\left\{ \sin 2\alpha \sin^2\frac{\theta}{2}\, e^{-2i\phi} + \sin 2\beta \cos^2 \theta/2 \right\}$$

$$K_{11}^R = \frac{S_m}{4}\left\{ \sin 2\alpha(1-\cos\theta)\cos 2\phi + \sin 2\beta(1+\cos\theta) \right\}$$

$$K_{11}^I = -\frac{S_m}{4}\left\{ \sin 2\alpha(1-\cos\theta)\sin 2\phi \right\}$$

$$K_{22}^R = \frac{S_m}{4}\left\{ (1-\cos\theta)\sin 2\beta \cos 2\phi + (1+\cos\theta) \sin 2\alpha \right\}$$

$$K_{22}^I = \frac{S_m}{4}\left\{ (1-\cos\theta)\sin 2\beta \sin 2\phi \right\}$$

$$K_{12}^R = \frac{1}{4}\sin\theta\, S_m \cos\phi(\sin 2\alpha - \sin 2\beta)$$

$$K_{12}^I = -\frac{1}{4}\sin\theta\, S_m \sin\phi(\sin 2\alpha + \sin 2\beta)$$

$$K_{21}^I = K_{12}^I$$

$$K_{21}^R = K_{12}^R \qquad - - - - - - - - \qquad (3.21)$$

56

similarly one may write $\Delta = \begin{bmatrix} 0 & \Delta_1 \\ -\Delta_1 & 0 \end{bmatrix}$

$$\Delta_{11}^R = \frac{S_m}{8}\left[g(2j+1)\{(1+\cos 2\phi)+\cos\theta(1-\cos 2\phi)\}\right.$$
$$\times(\sin(2\alpha)+\sin(2\beta)) - f\{(1-\cos\theta)\sin 2\beta\cos 2\phi$$
$$\left.+\sin 2\alpha(1+\cos\theta)\}\right]$$

$$\Delta_{11}^I = \frac{S_m}{8}\left[\{g(2j+1)-f\}\sin 2\beta - g(2j+1)\sin 2\alpha\right]$$
$$\sin 2\phi(1-\cos\theta)$$

$$\Delta_{22}^R = \frac{S_m}{8}\left[g(2j+1)\{(1+\cos 2\phi)+\cos\theta(1-\cos 2\phi)\}\right.$$
$$(\sin 2\alpha+\sin 2\beta) - f\{(1-\cos\theta)\sin 2\alpha\cos 2\phi+\sin 2\beta$$
$$\left.(1+\cos\theta)\}\right]$$

$$\Delta_{22}^I = \frac{S_m}{8}\left[\{g(2j+1)+f\}\sin 2\beta - g(2j+1)\sin 2\alpha\right]\sin 2\phi$$
$$(1-\cos\theta)$$

$$\Delta_{12}^R = \Delta_{12}^I = \Delta_{21}^R = \Delta_{21}^I = 0 \quad \text{----(3.22)}$$

Using equations (3.9) and (3.10)

The coupled differential equations which are to be solved :

$$\left.\begin{aligned}
\dot{\rho}^R &= h^R\rho^I - \rho^I h^R - K^R\Delta^I + K^I\Delta^R + \Delta^R K^I - \Delta^I K^R \\
\dot{\rho}^I &= \rho^R h^R - h^R\rho^R - K^R\Delta^R - K^I\Delta^I + \Delta^I K^I + \Delta^R K^R \\
\dot{K}^R &= h^R K^I + K^I h^R + \Delta^R\rho^I + \Delta^I\rho^R + \rho^R\Delta^I + \rho^I\Delta^R \\
&\quad - \Delta^I \\
\dot{K}^I &= -\left[h^R K^R + K^R h^R + \Delta^R\rho^R - \Delta^I\rho^I + \rho^R\Delta^R\right. \\
&\quad \left. - \rho^I\Delta^I - \Delta^R\right]
\end{aligned}\right\} \text{------(3.29)}$$

Hence the problem involves solving the equations for θ, ϕ, α and β respectively.

In Chapter II we have solved the coupled differential equations for θ and ϕ on a two dimensional basis, i.e. we study the trajectories in the $\theta - \phi$ space.

In a similar manner one can solve the above equations for four variables, i.e. $\theta, \phi, \alpha, \beta$ and thus use a four dimensional basis. One can assume initially at $t = 0$, some values of $\theta, \phi, \alpha, \beta$ as $\theta_0, \phi_0, \alpha_0, \beta_0$ and then we solve the equations iteratively and study the trajectories in the four dimensional basis. However the numerical results are not done as yet and thereby the conclusions could not be drawn on the problem.

58

CHAPTER 4

CONCLUSION

4.1 Summary.

The interesting results obtained from the calculations of an exactly solvable model induced a motive for calculating and comparing the results obtained from different approximation theories viz. TDHF and PTDHF with those of the exact calculations. In some cases there arose some ambiguities (e.g. in the occupation probabality distribution), while in the major results (e.g. energy loss) there was some good agreement.

After having done that, we had projected out the desired symmetries of the system, and instead of a single phase transition, we have established the occurence of two phase transitions, which are of considerable importance in the theoretical study of the Heavy Ion Collisions.

Finally the Time Dependent Hartree-Fock Bogoliubov equations have been derived, though the solutions and results have not been calculated.

4.2 Future Prospects.

One hopes that with microscopic quantum mechanical theories the study of energy dissipation will continue to receive serious attention in future. TDHF is certainly a good approximation theory, and with its help one could explain several physical phenomena viz. fission, fusion,

compound nucleus formation and giant multipole resonances.

Davies[46] et al have found that the calculated fragment energies, mean masses, and scattering angles for Deep Inelastic Collisions are in good agreement with experiment. However, the conventional TDHF has some conceptual limitations : (a) It predicts a unique final state and consequently is incapable of describing several reaction (or inelastic) channels; (b) It cannot describe the passage through the classically forbidden barriers; (c) The TDHF wavefunction does not in general satisfy the symmetry requirements of the Hamiltonian; (d) Being variational in nature, the description is not reliable for excited states.

Some of the above constraints have been overcome by several groups[39, 47]. In this thesis we had removed limitation (c) by projecting out the desired symmetry and this yielded some interesting results.

Yet all the above mentioned limitations have not been overcome, so perhaps this itself could present an interesting problem to be solved in future and perhaps the results could be used in interpreting some unexplained features.

The above projection technique could also have been improved if pairing had been taken into account, thereby enabling one to study the various phenomena observed in the nuclear collisions.

Captions to figures

Fig. 1.1 - 1.3 --- The logarithms of the probability distribution $P_M = |\langle \Psi_{TDHF} | M \rangle|^2$ for several values of M.

Fig. 1.4 - 1.8 --- Comparison of the energy loss obtained from the exact calculations, TDHF approximations and PTDHF approximations.

———————— exact

— — — — — — — — TDHF

. . . . . PTDHF

Fig. 1.10 - 1.24 --- The logarithms of the occupation probabilities obtained from exact calculations and TDHF theory.

× × × × × × × × TDHF odd states

. . . . . TDHF even states

— — — — — — — — — TDHF odd even states

—.—.—.— exact odd even states

———————— exact even states

—.—.—.—.—.—.— exact odd states

Fig. 1.25 - 1.30 :-The difference of the occupation probabilities between the exact calculations and those of TDHF theory, for different incident momentum and various interaction parameters.

—.—.—.—.—.— -3.24

.. .. -0.00

— — — — — — — — — — 3.24

× × × × × × × × × × 5.37

.●.●.●.●.●.●.●. -5.37

Fig 1.31 - 1.36 --- The difference of the occupation probabilities between the exact calculation and those of TDHF theory, for different incident momentum and various interaction parameters.

———————— -5.04

– – – – – – – – – – – -1.76

. . . . . 1.76

—.—.—.—.—.— 5.04

Fig. 2.1 : The odd parity excitation energy for various approximation theories viz. HF, PHF and HFP respectively.

Fig. 2.2 : The same as in figure 2.1 but for even parity states.

Fig. 2.3 : The excitation energy from various theories for different values of the interaction strength.

Fig. 2.4 + 2.9 : The trajectories in (θ-ϕ) space for various interaction parameters.

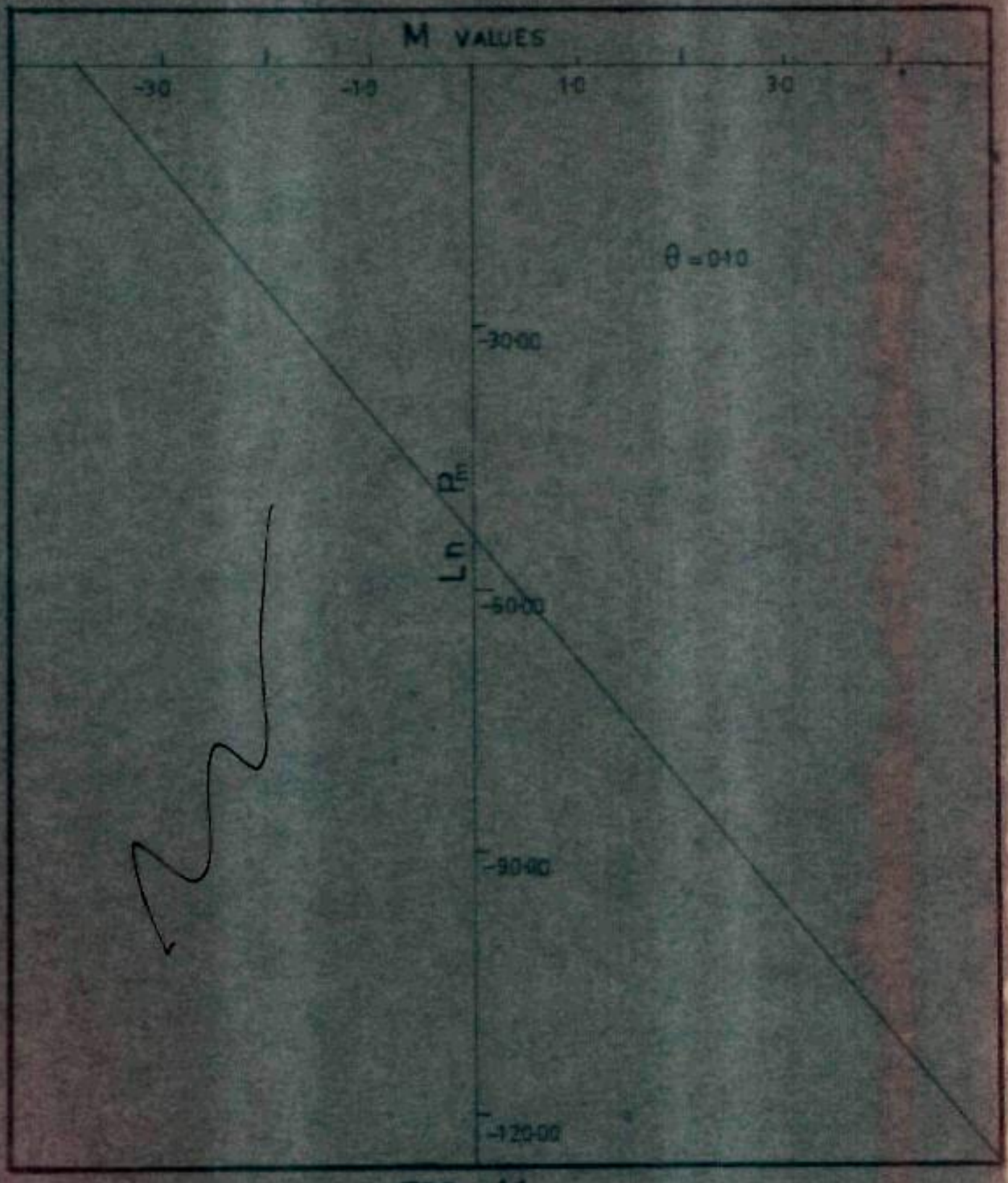

FIG :- 1·1

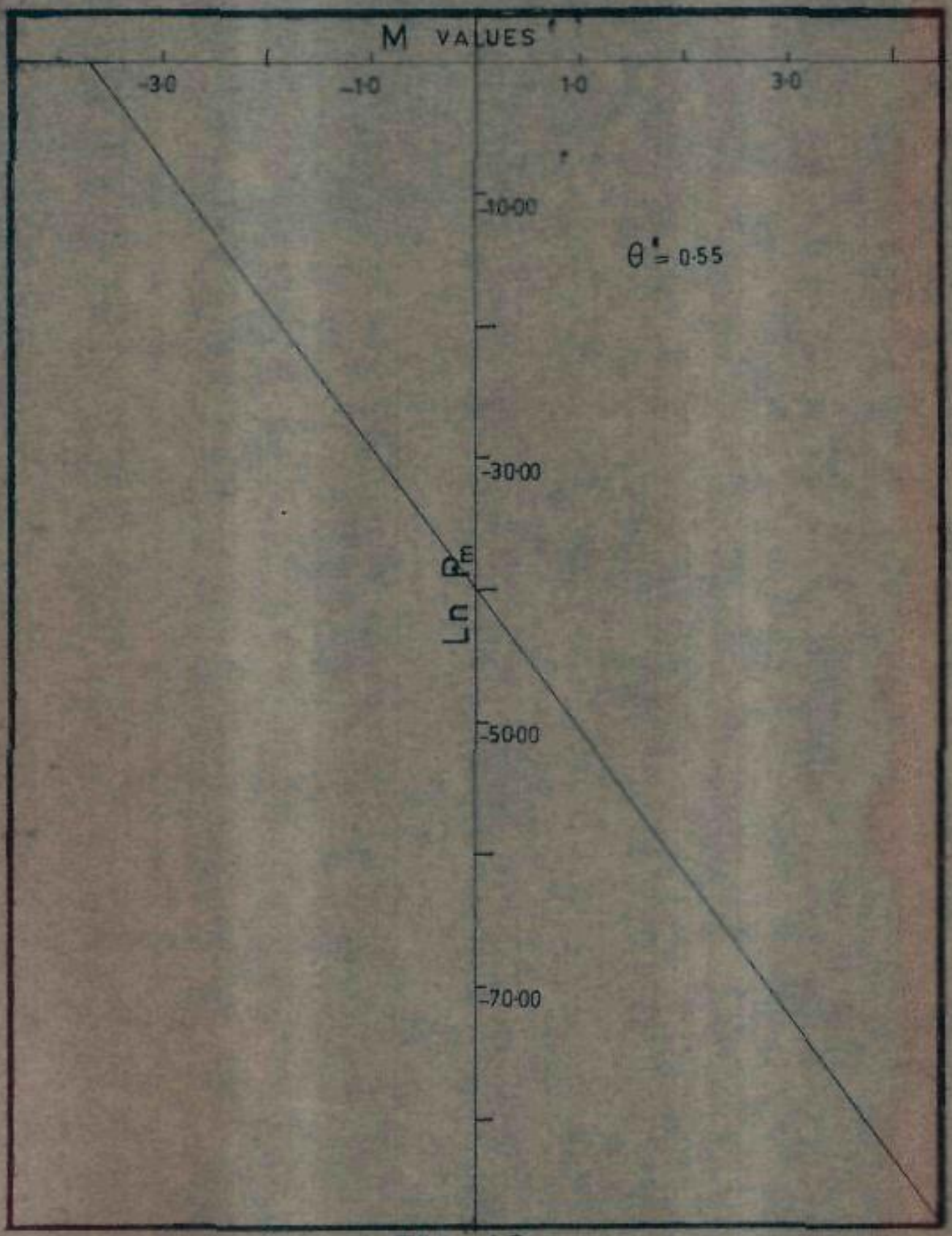

FIG:-1·2

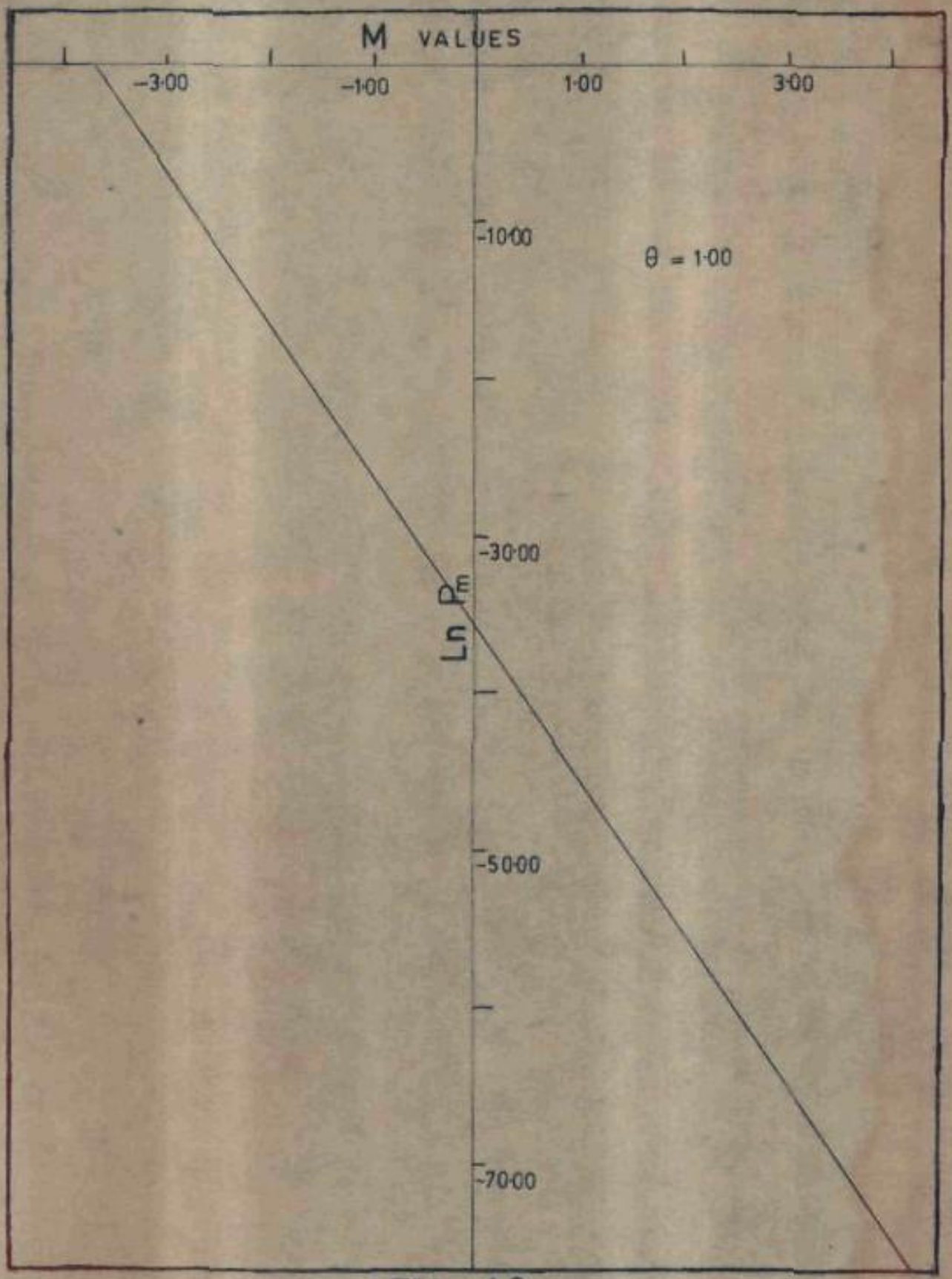

FIG:-1·3

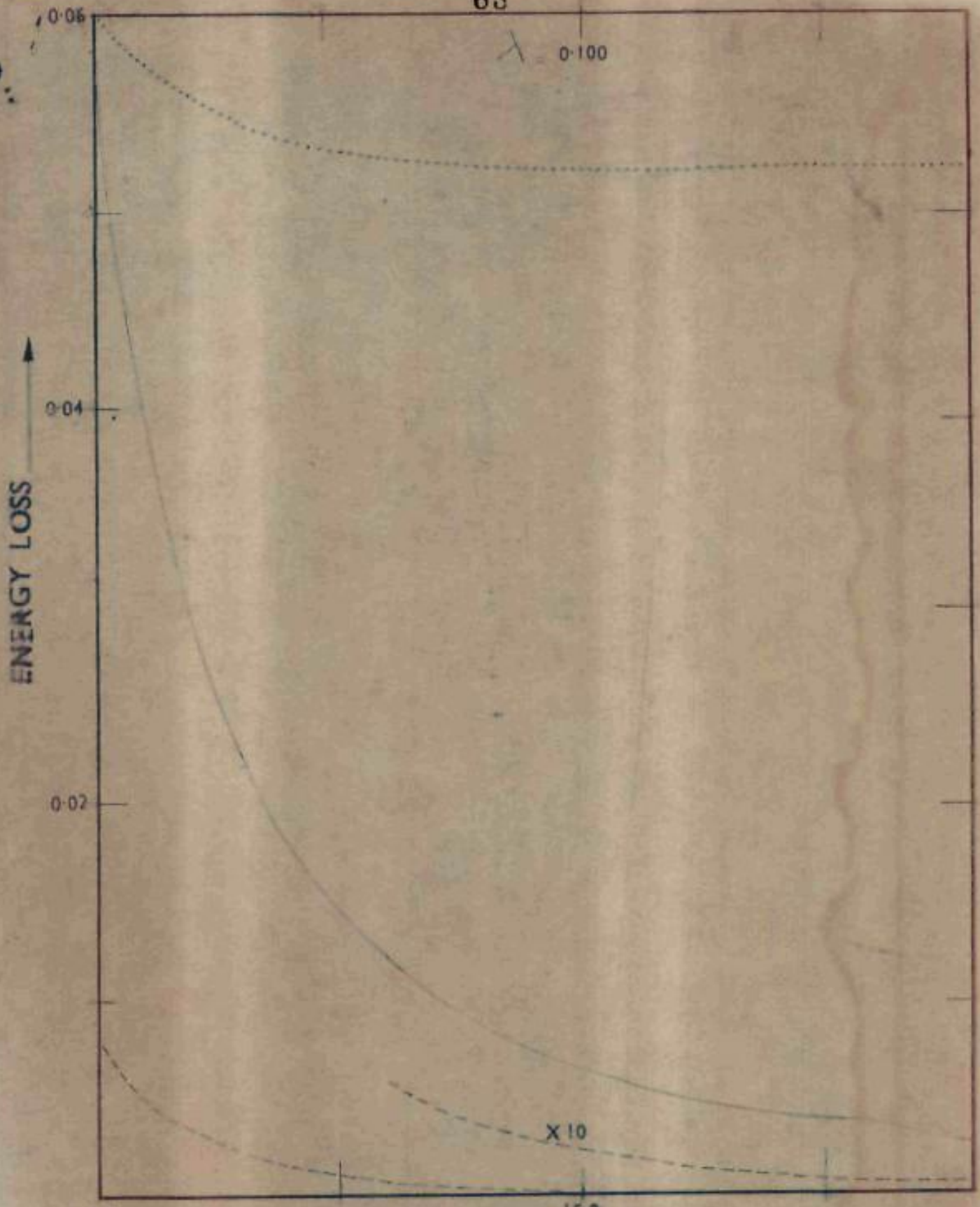

FIG :—1·4

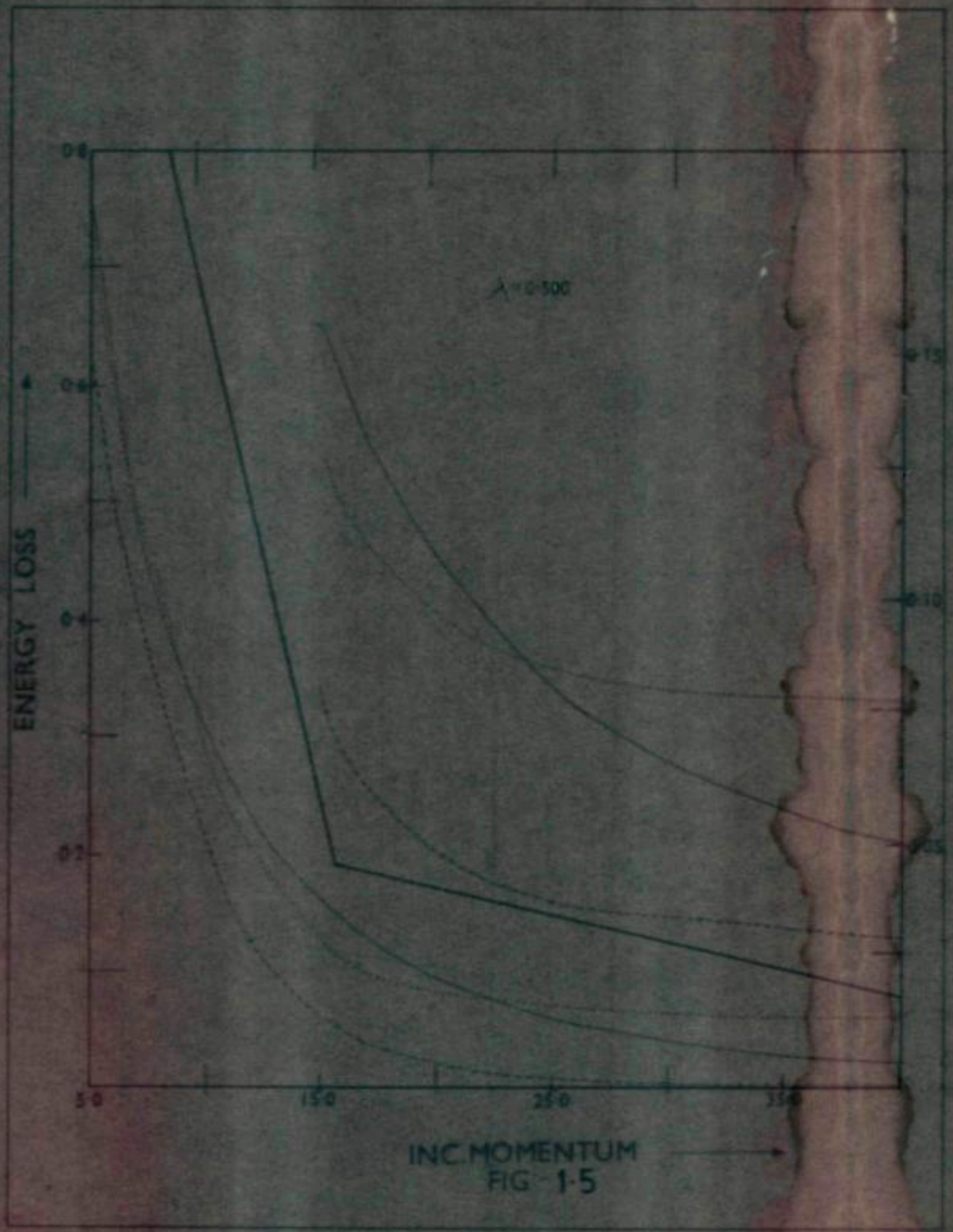
λ = 0·500
ENERGY LOSS
INC. MOMENTUM
FIG 1·5

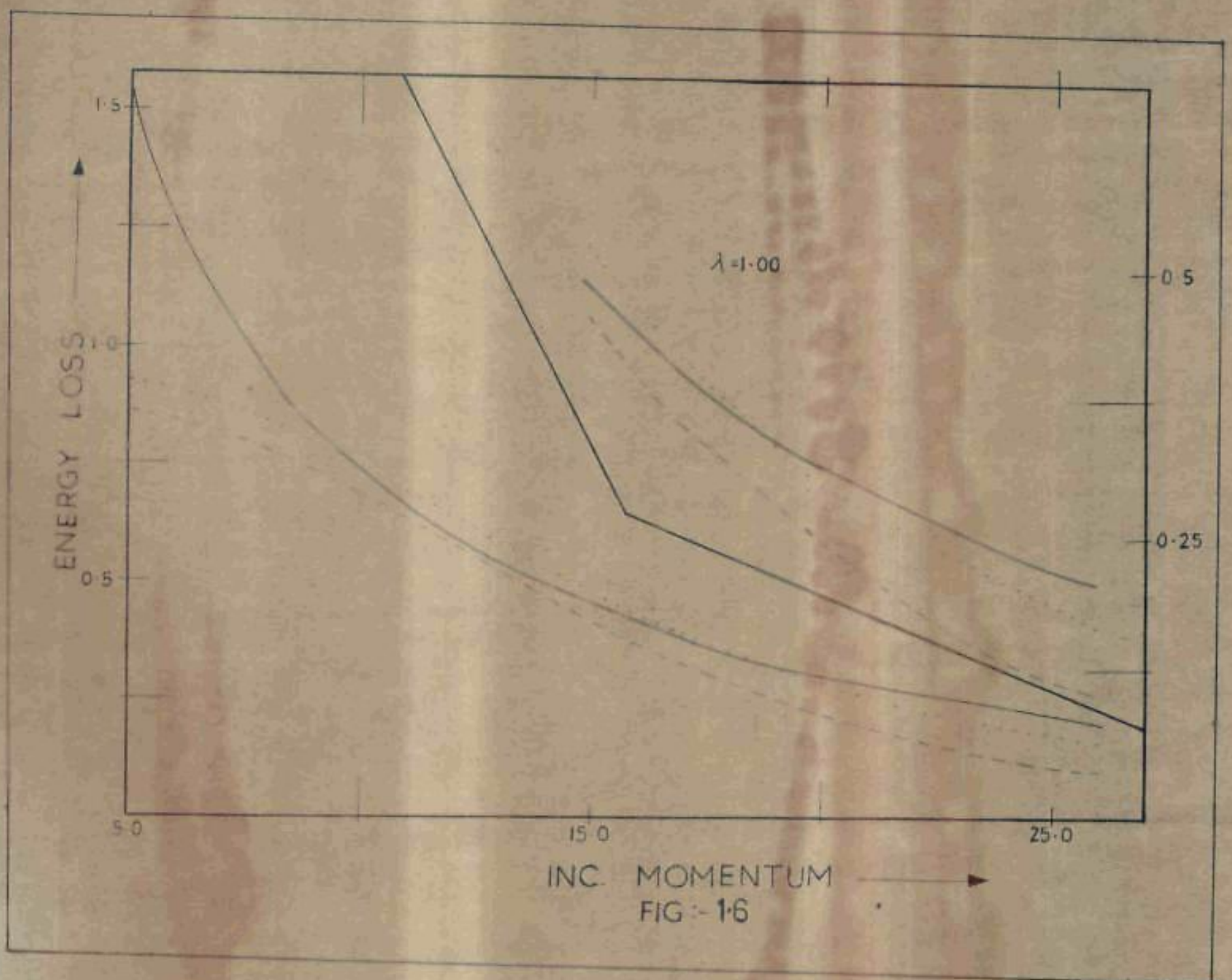

FIG :- 1·6

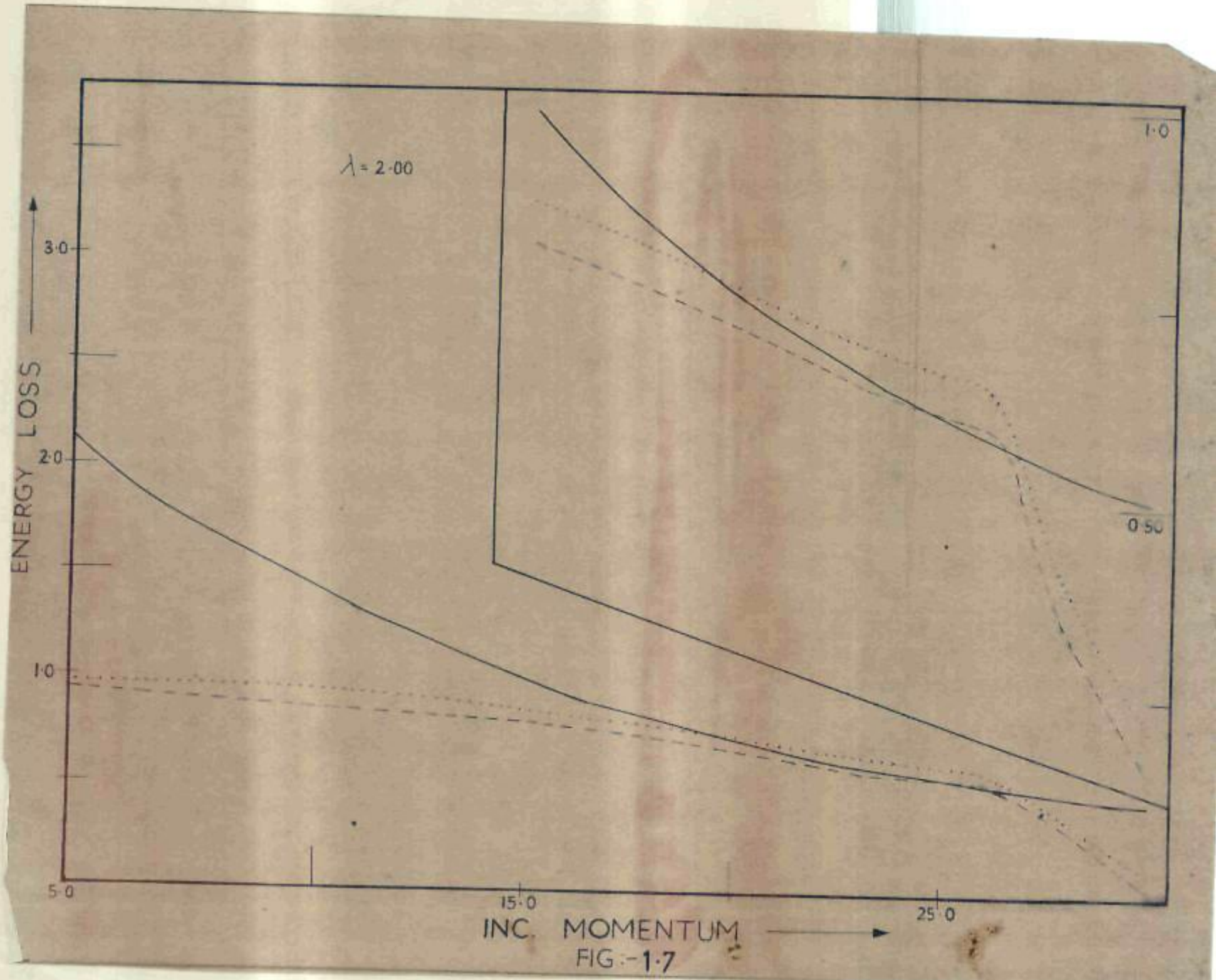

FIG :- 1·7

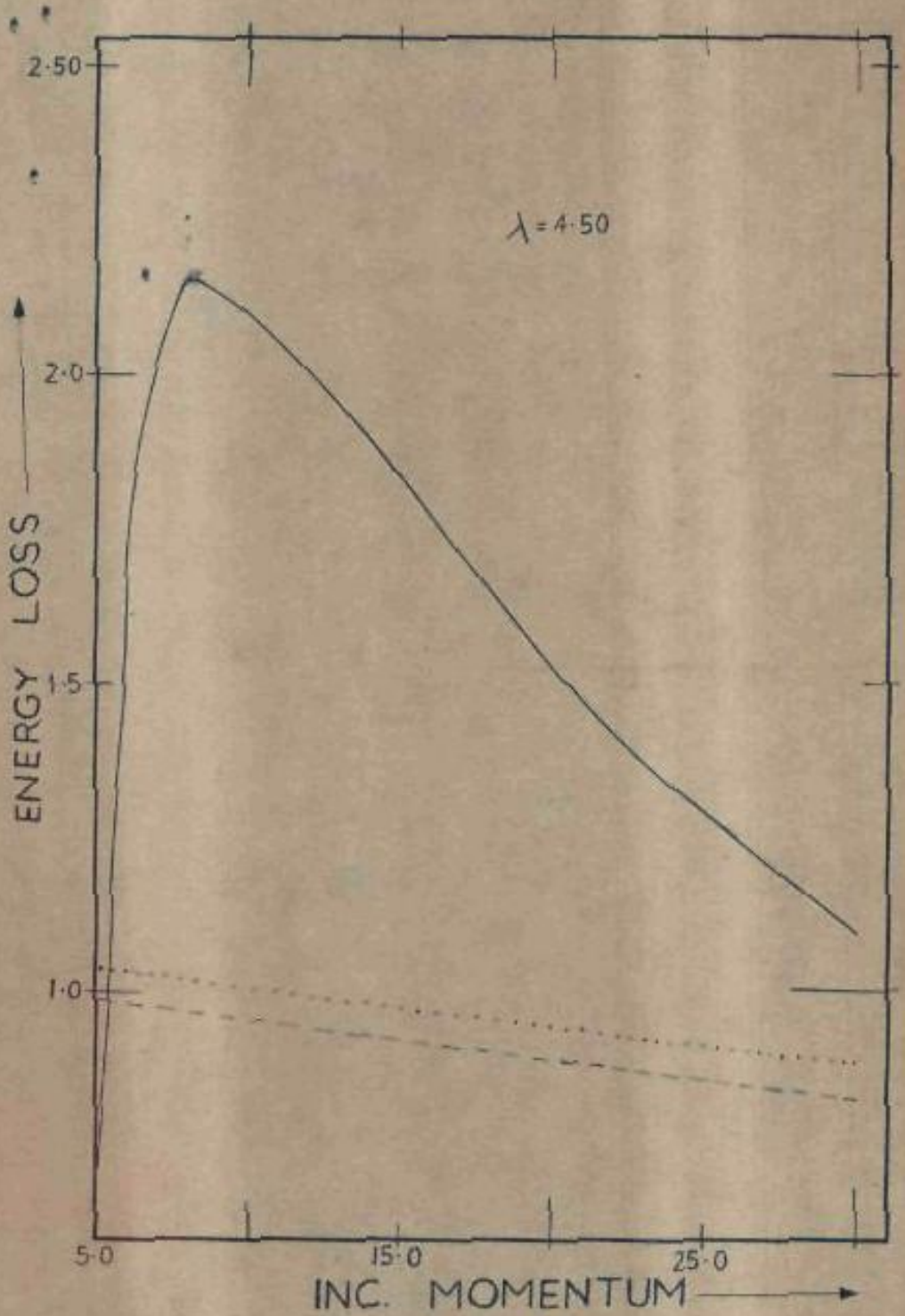

FIG :- 1·8

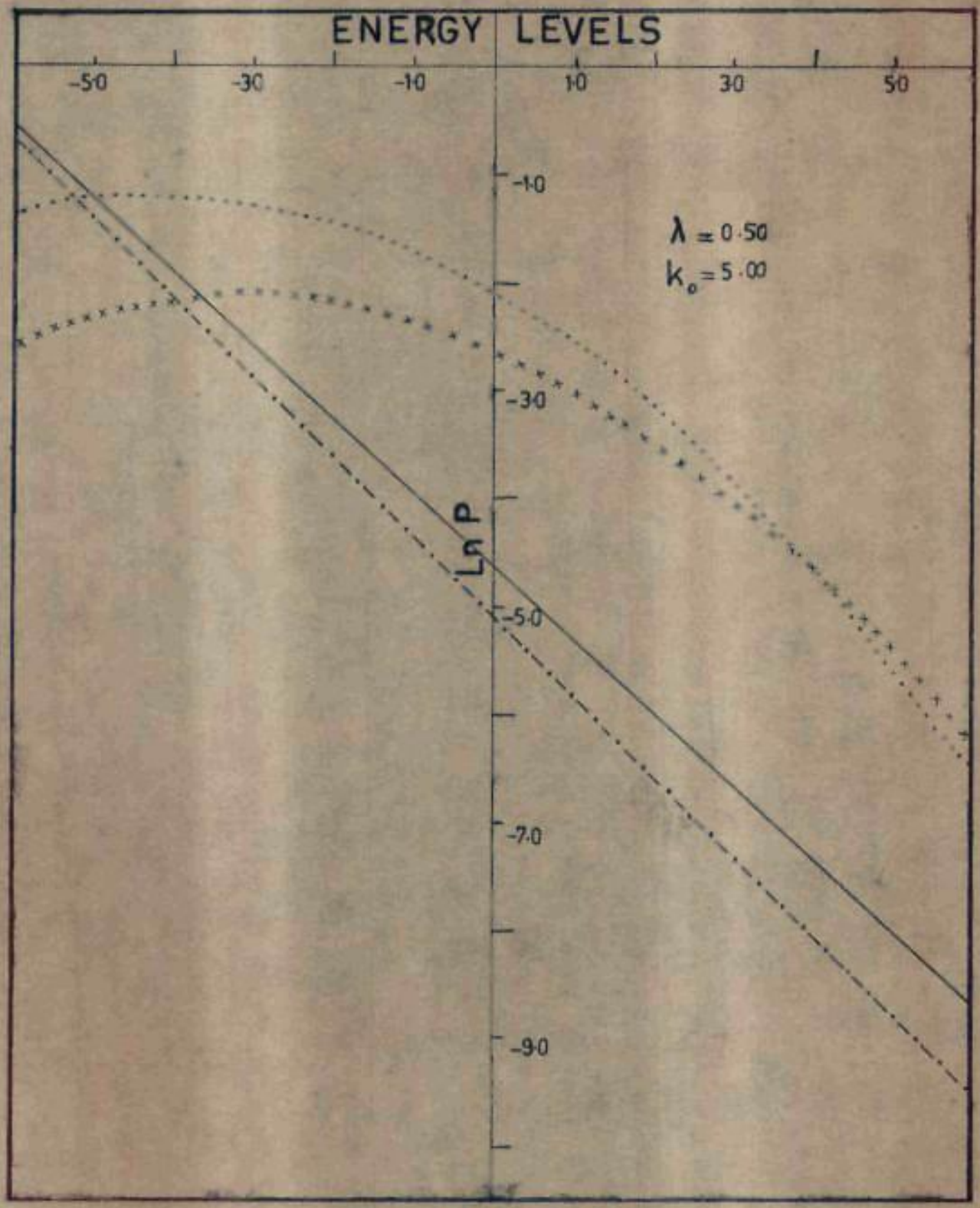

FIG:—19

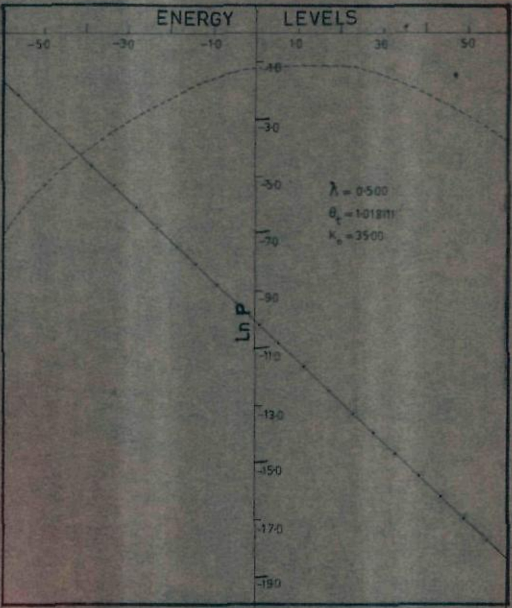

ENERGY LEVELS
-5·0
-3·0
-1·0
1·0
3·0
5·0
-1·0
-3·0
-5·0
-7·0
-9·0
-11·0
-13·0
-15·0
-17·0
-19·0
Ln P
λ = 0·500
θt = 1·018111
Ko = 35·00

FIG : —1·10

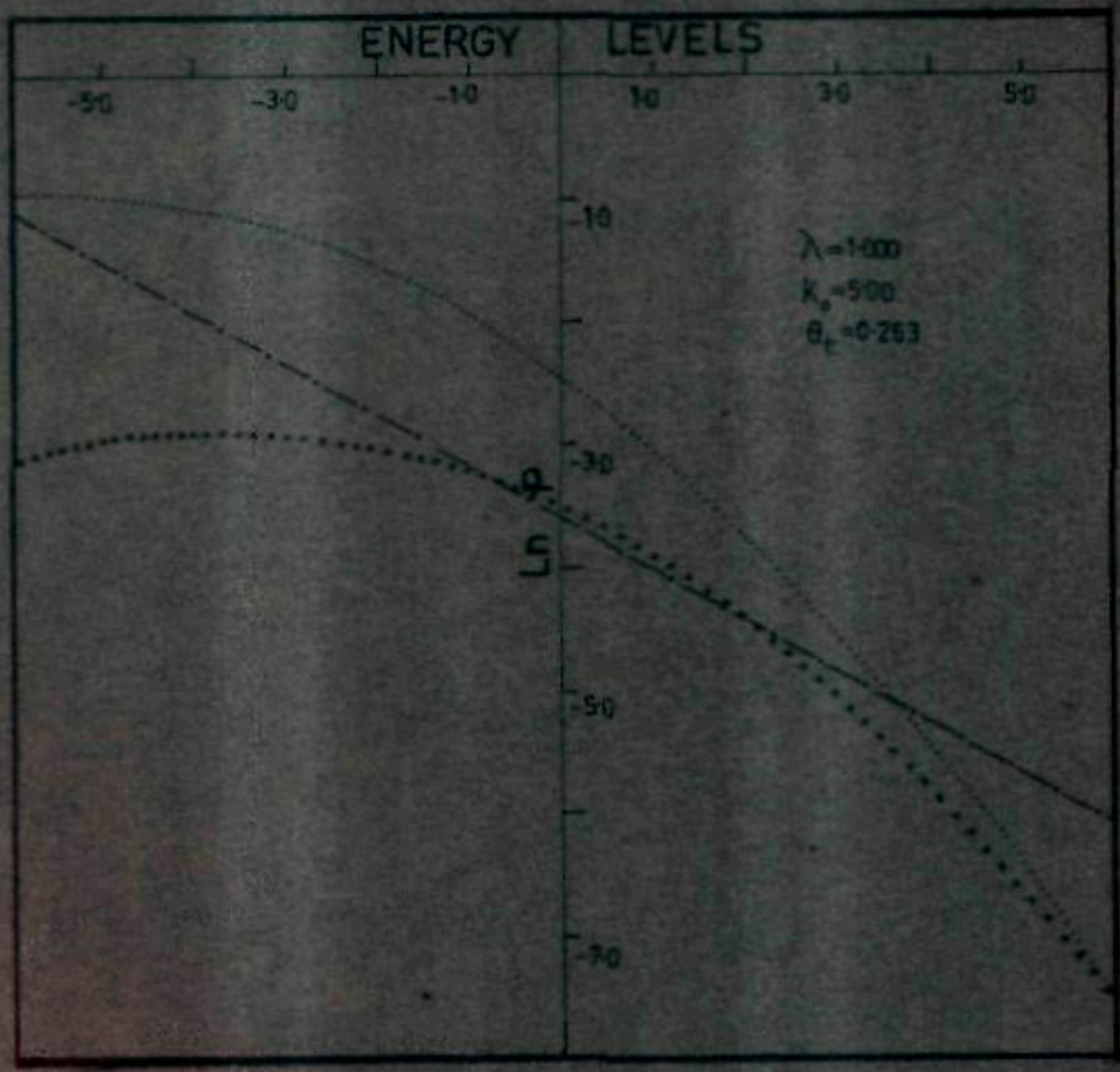
ENERGY LEVELS
-5·0
-3·0
-1·0
1·0
3·0
5·0
-10
-30
-5·0
-7·0
λ=1·000
K₀=5·00
θ_E=0·263
9
5

FIG:-1·11

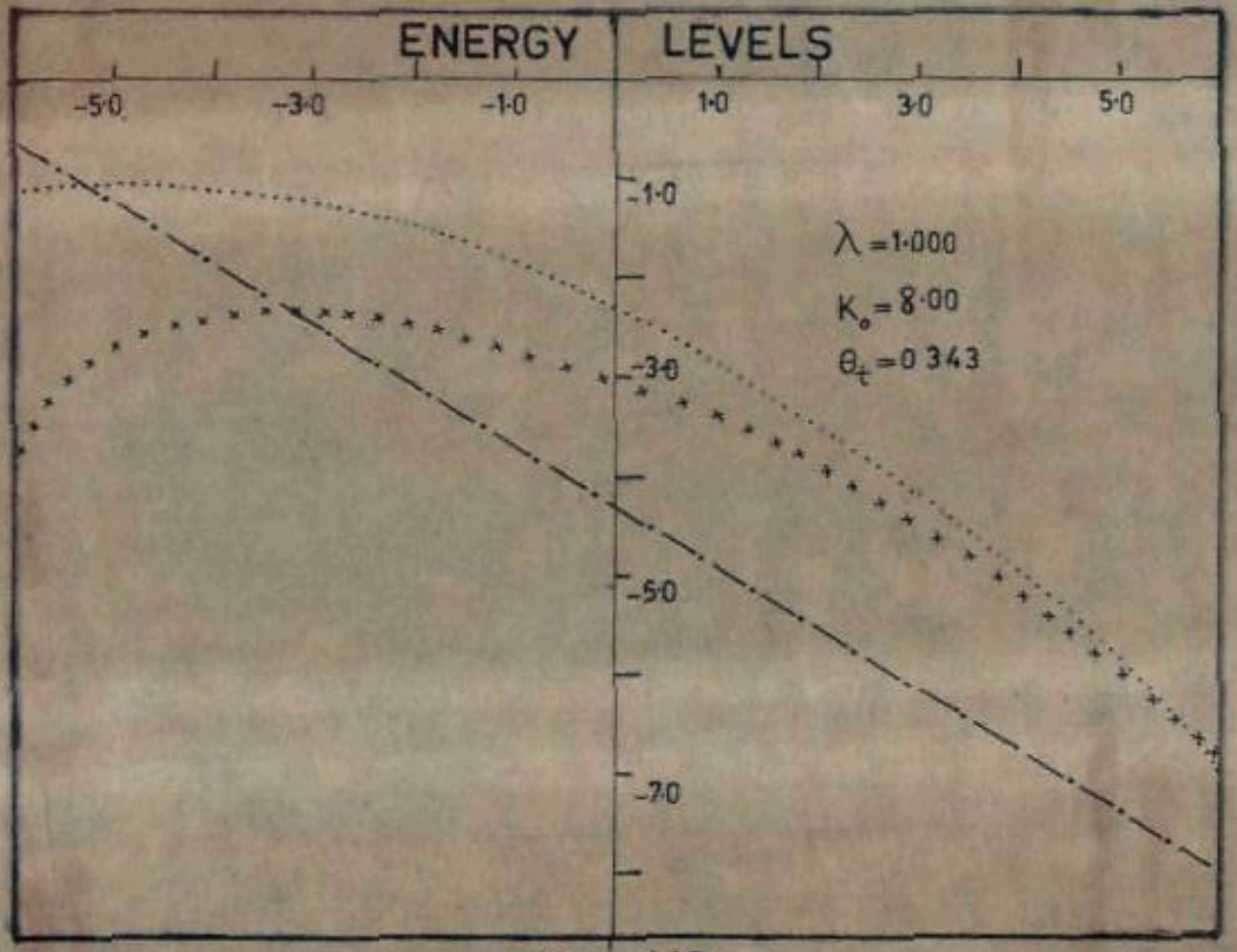

FIG :— 1·12

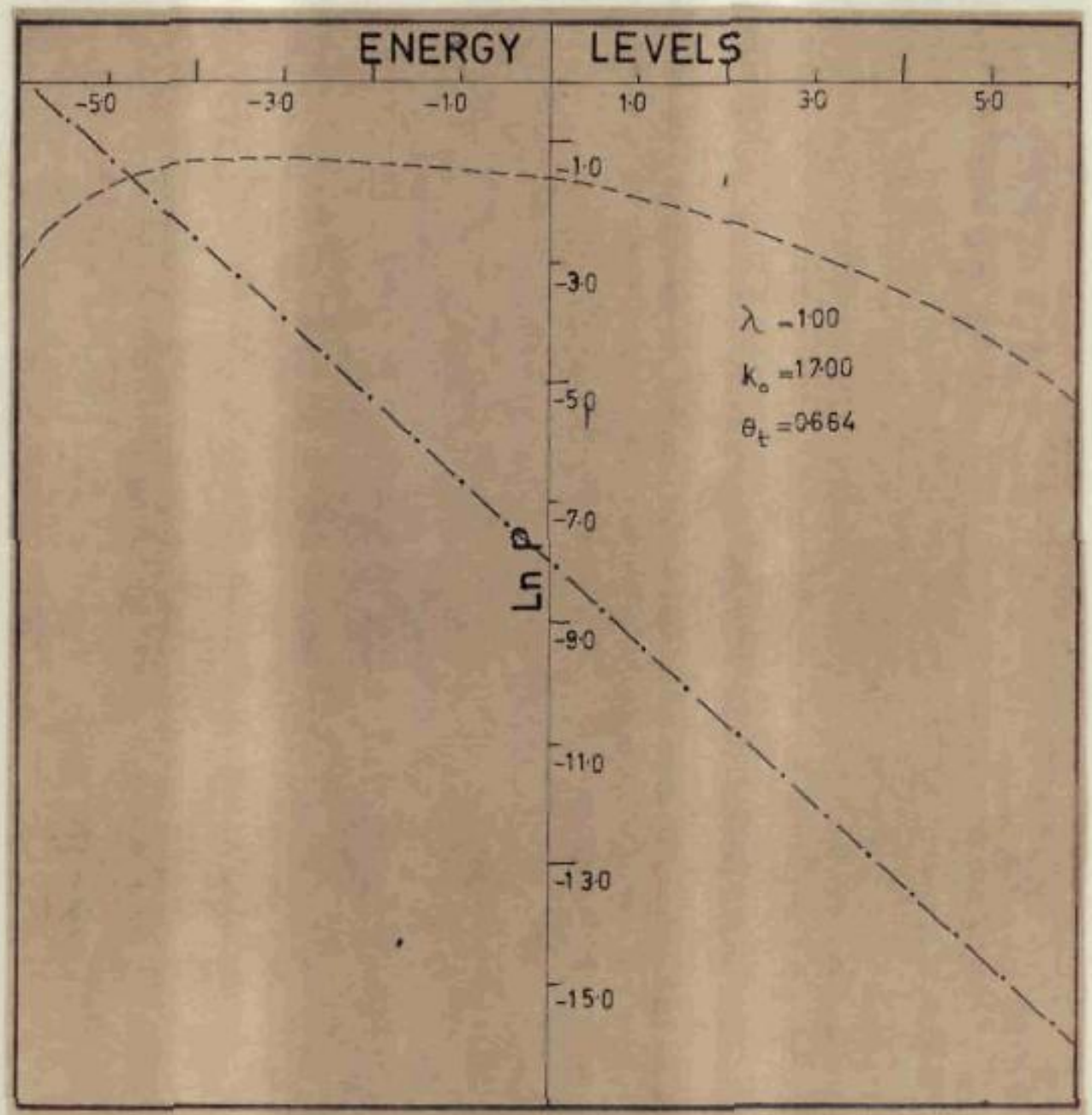
ENERGY LEVELS
-5·0
-3·0
-1·0
1·0
3·0
5·0
-1·0
-3·0
-5·0
-7·0
-9·0
-11·0
-13·0
-15·0
Ln ρ
λ =1·00
K_o =17·00
θ_t =0·664

FIG:- 1·13

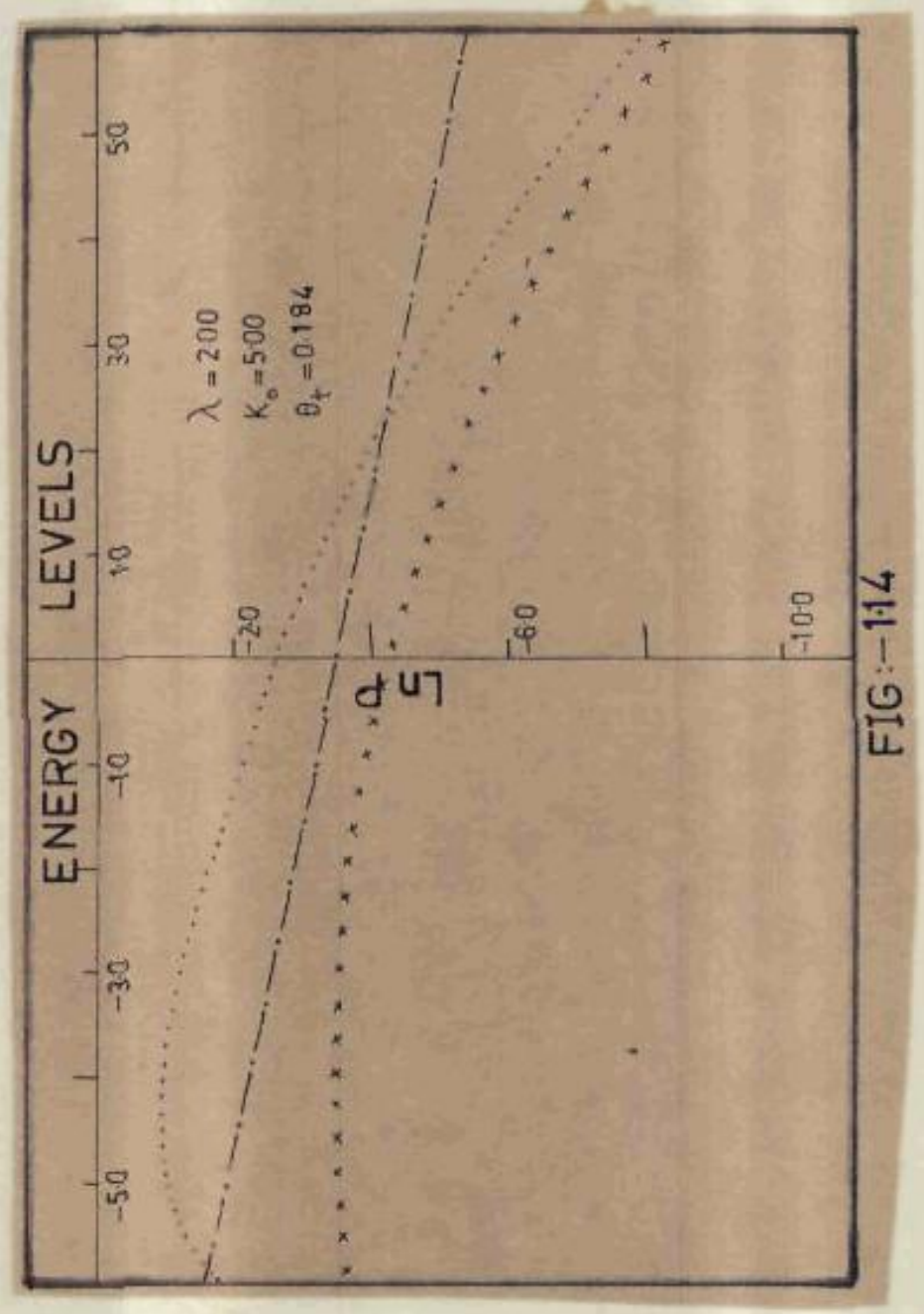
ENERGY LEVELS
-50
-30
-10
10
30
50
-20
-60
-100
$\lambda = 200$
$K_0 = 500$
$\theta_f = 0.184$
Q_5

FIG:-1.14

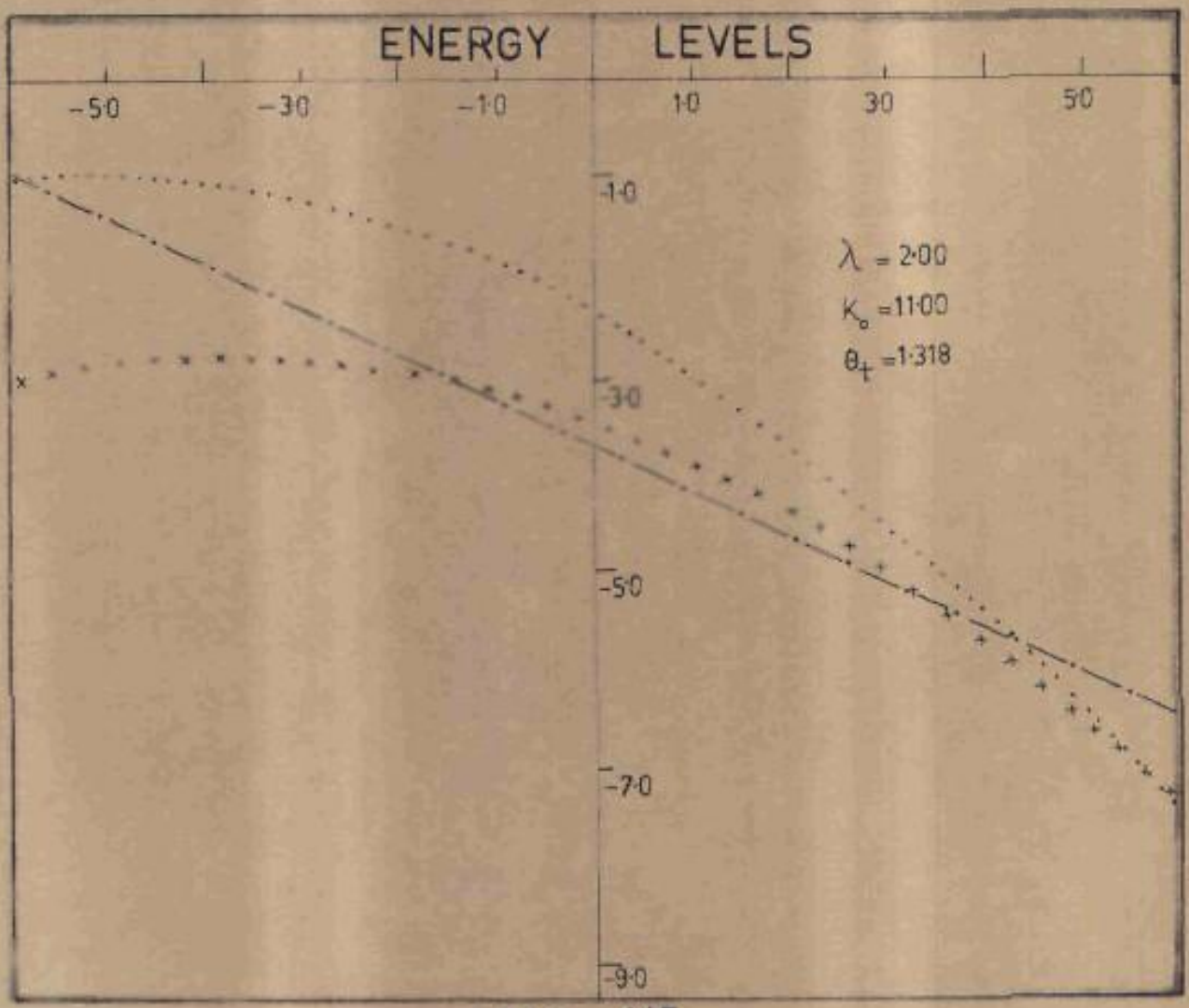
ENERGY LEVELS
-50
-30
-10
10
30
50
-10
-30
-50
-70
-90
λ = 2·00
K₀ =11·00
θt =1·318

FIG :-1·15

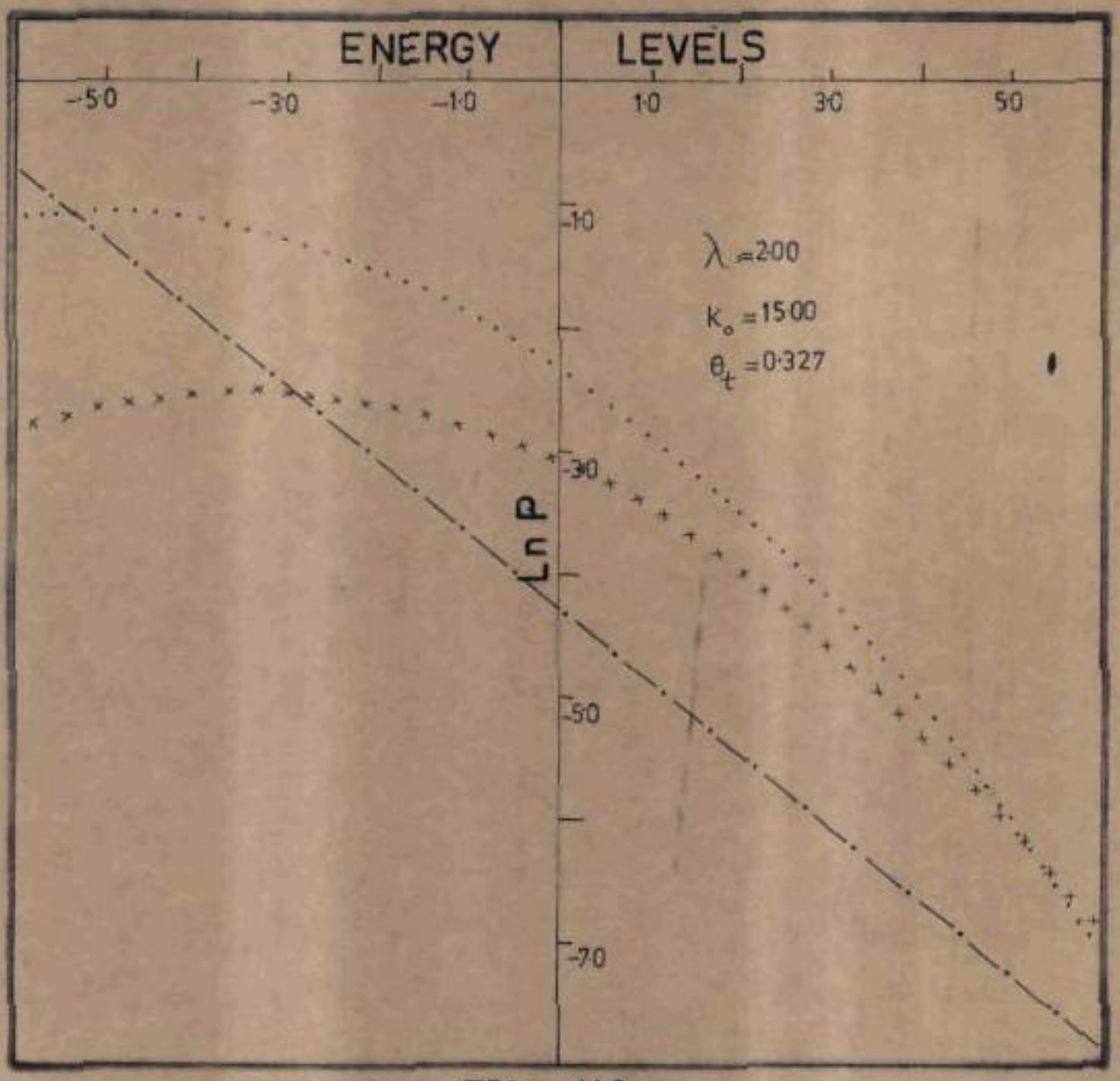
ENERGY LEVELS
-5·0
-3·0
-1·0
1·0
3·0
5·0
-10
-30
-50
-70
Ln P
λ =2·00
K₀ =15·00
θt =0·327

FIG :-116

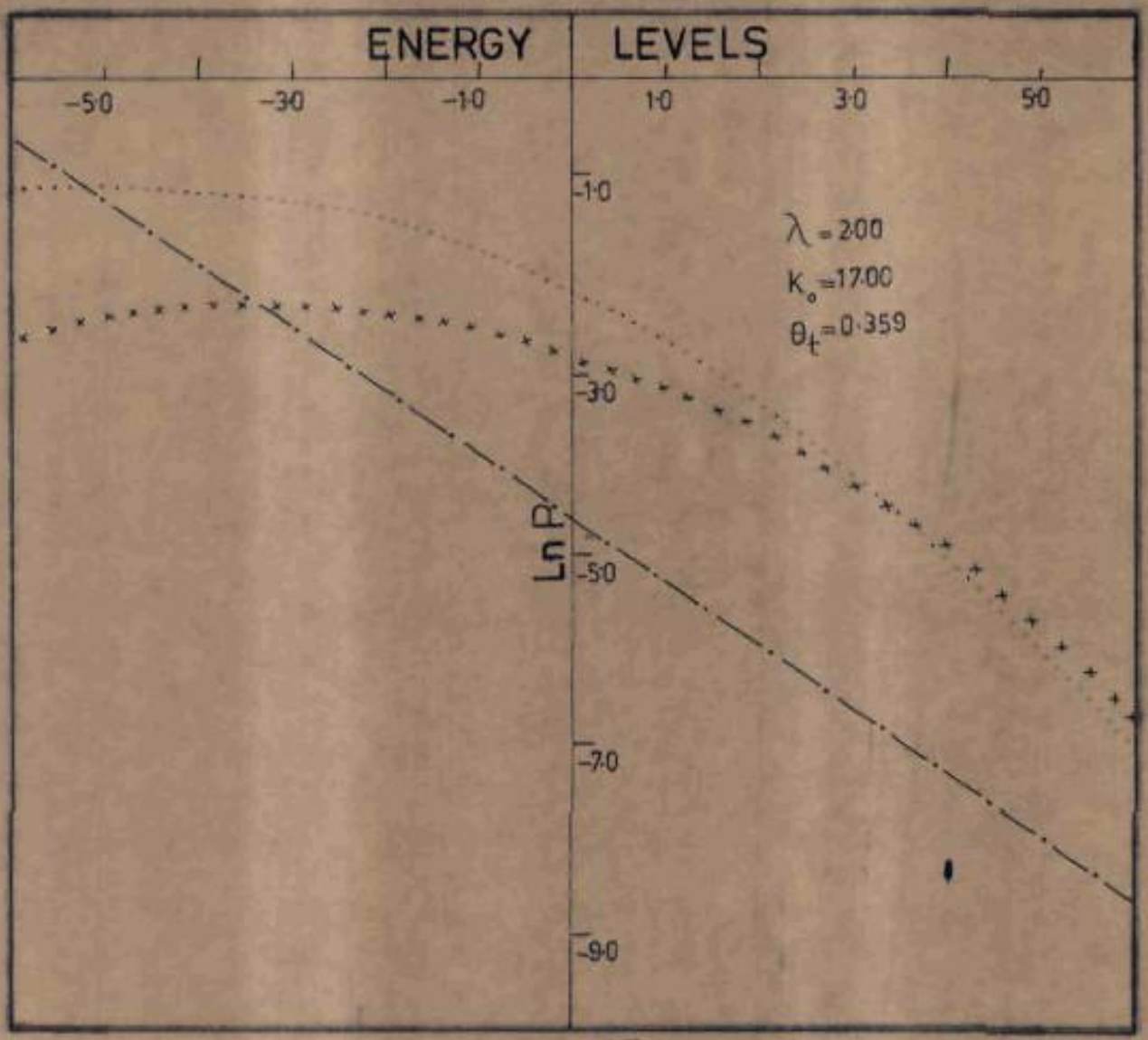
ENERGY LEVELS
-5·0
-3·0
-1·0
1·0
3·0
5·0
-1·0
-3·0
-5·0
-7·0
-9·0
Ln R
λ = 2·00
K₀ = 17·00
θt = 0·359

FIG :-1·17

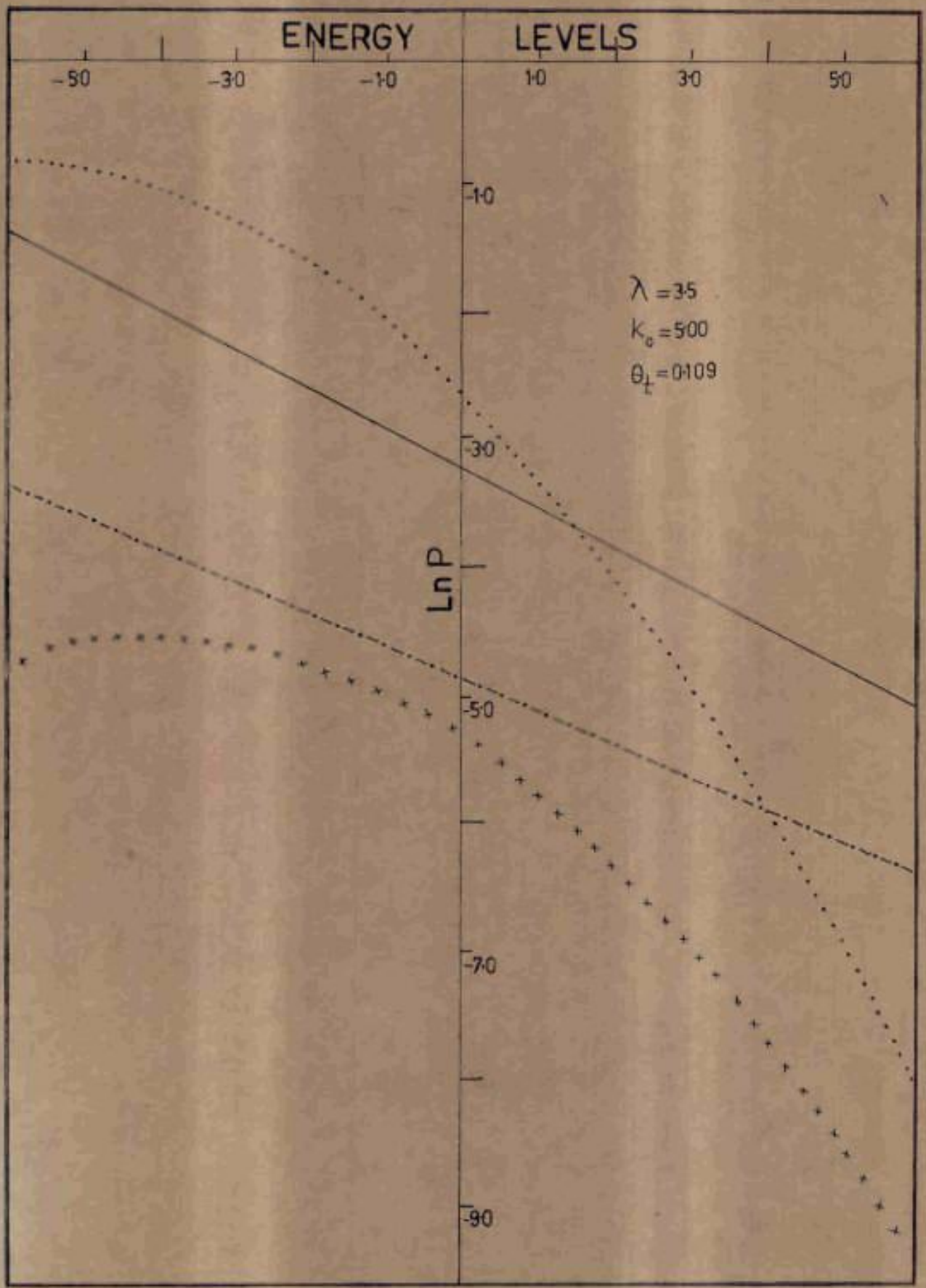
ENERGY LEVELS
-5·0
-3·0
-1·0
1·0
3·0
5·0
-1·0
-3·0
-5·0
-7·0
-9·0
Ln P
λ = 3·5
k_c = 5·00
θ_L = 0·109

FIG :-1·17a

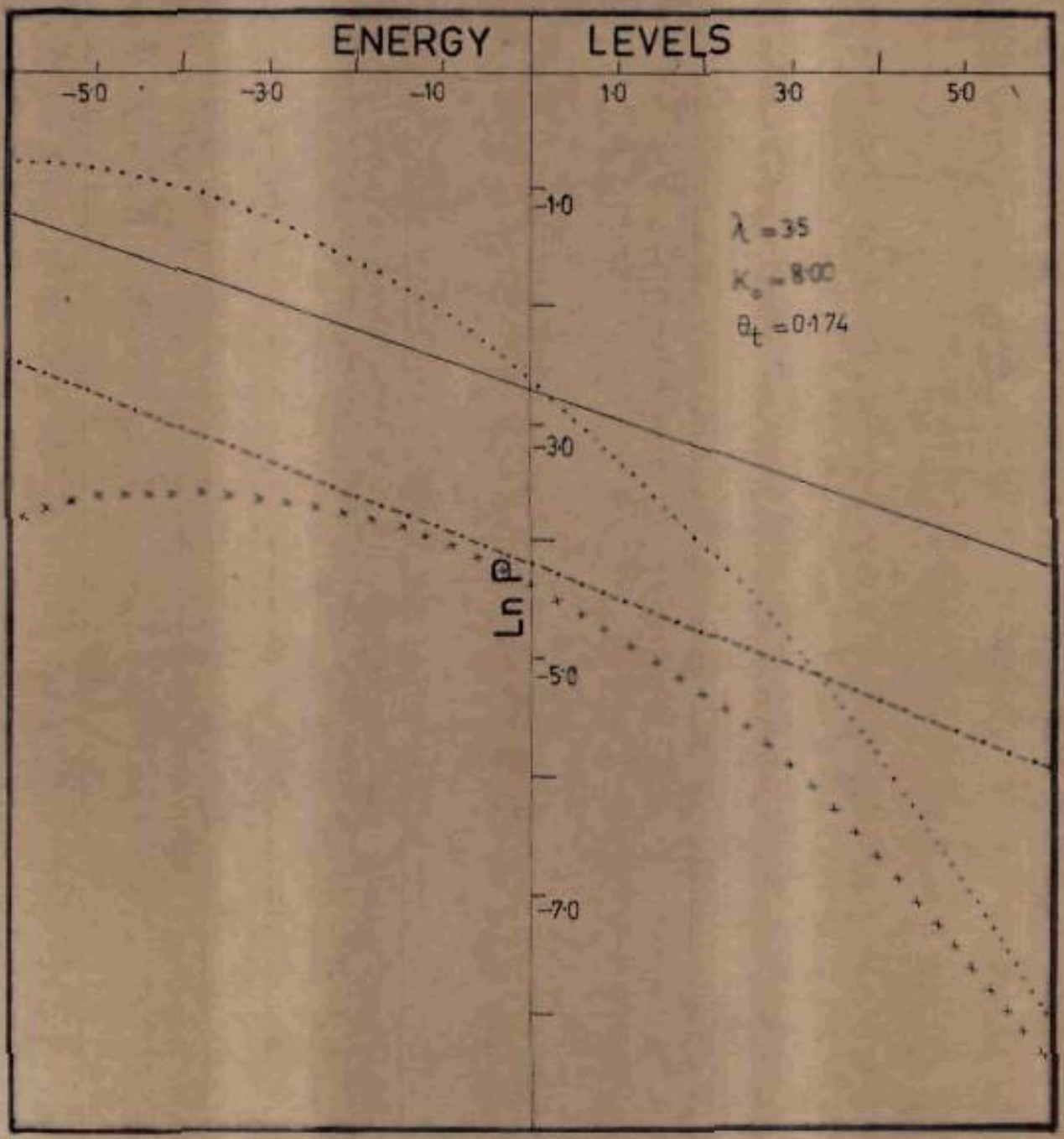

FIG :- 1·18

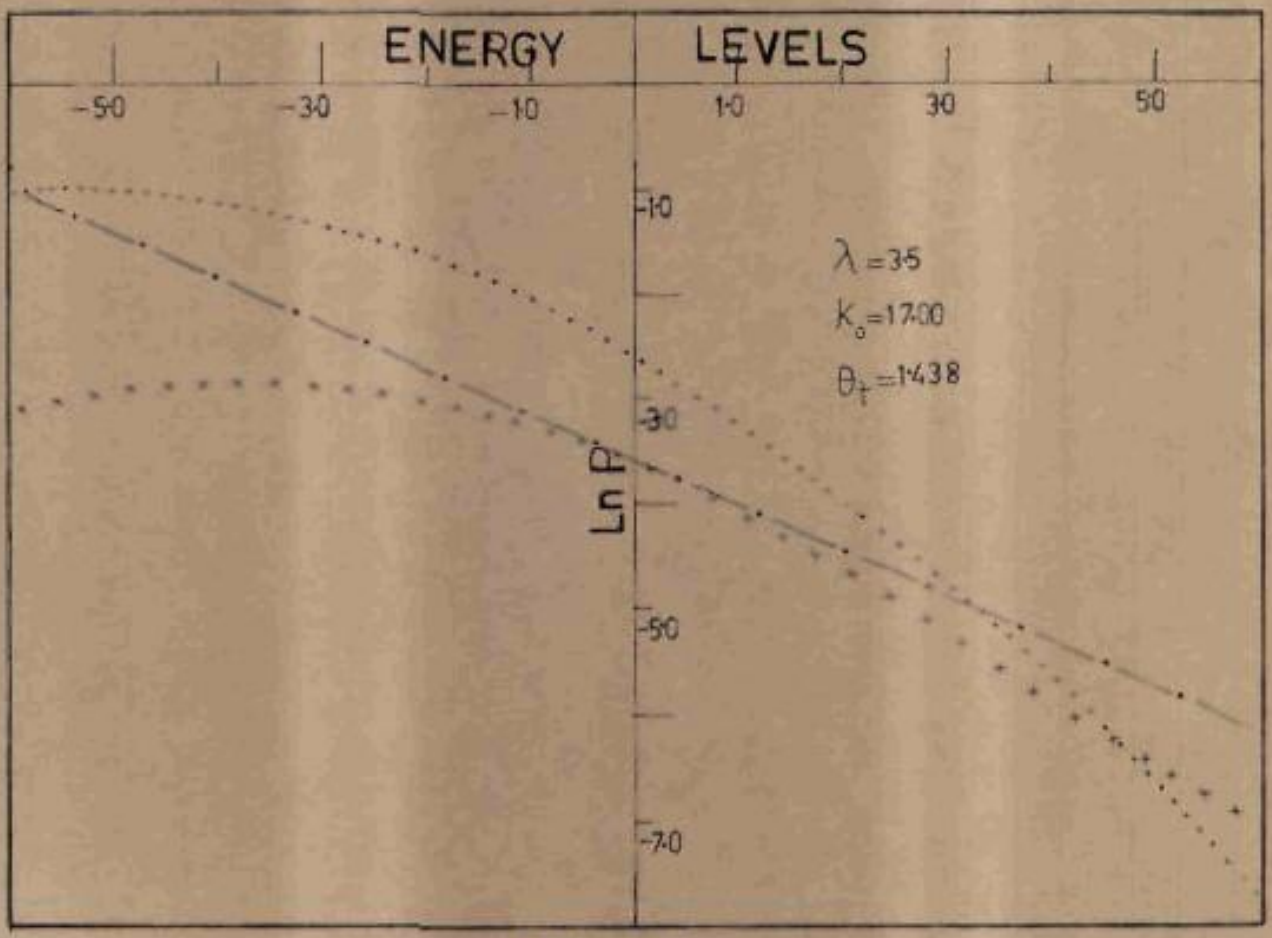
ENERGY LEVELS
-50
-30
-10
10
30
50
-10
-30
-50
-70
Ln P
λ = 3·5
K₀ = 17·00
θf = 1·438

FIG 1·19

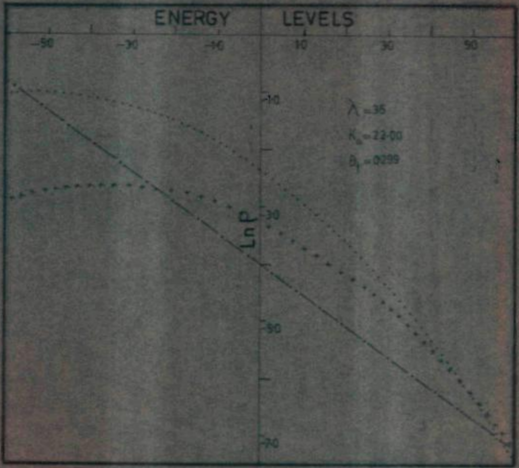
ENERGY LEVELS
-50
-30
-10
10
30
50
-10
-30
-50
-70
Ln P
λ =35
K₀ =22·00
θ₁ =0299

FIG :- 1·20

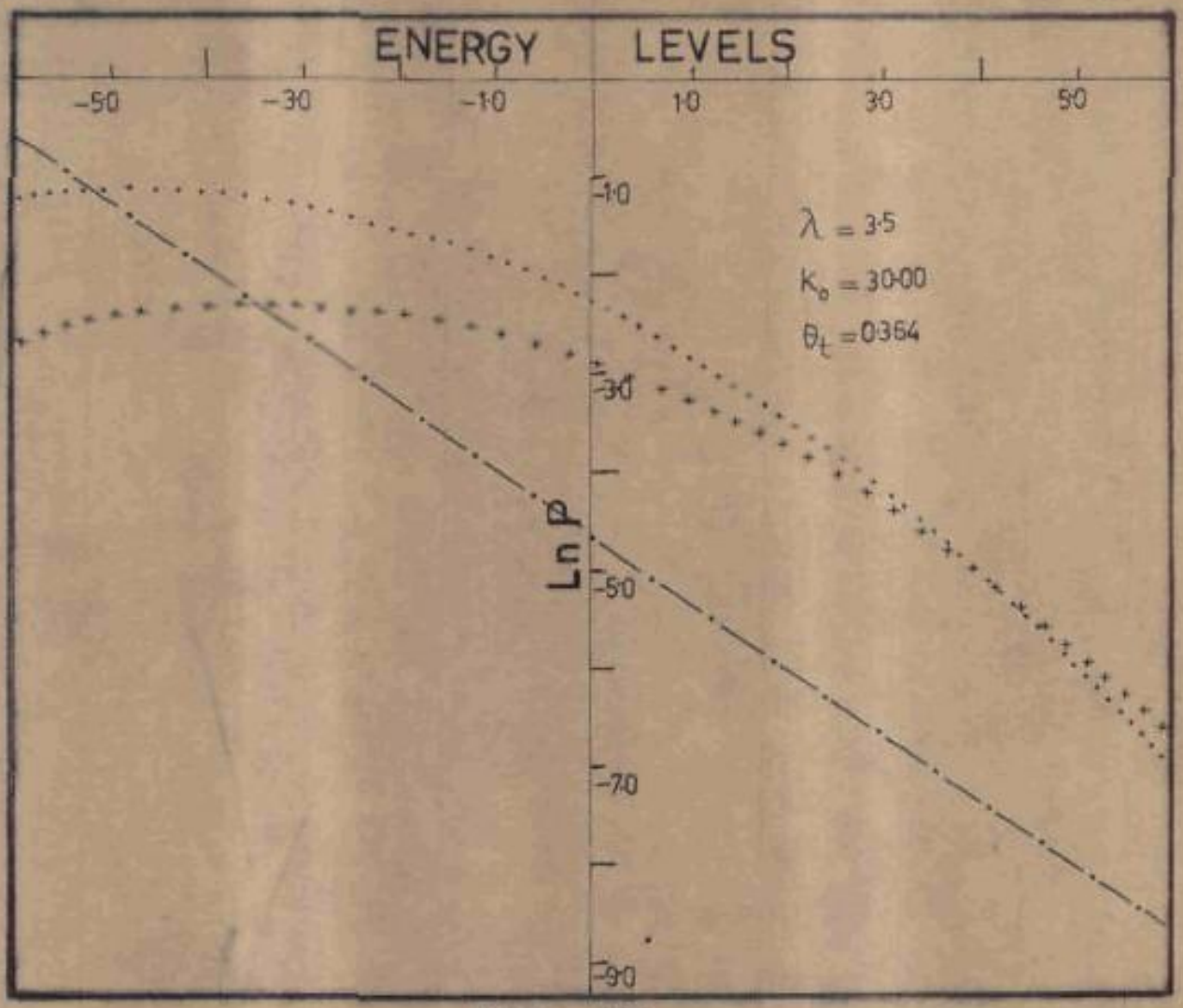
ENERGY LEVELS
-50
-30
-10
10
30
50
-10
-30
-50
-70
-90
Ln P
λ = 3·5
K₀ = 30·00
θ_t = 0·364

FIG :-1·21

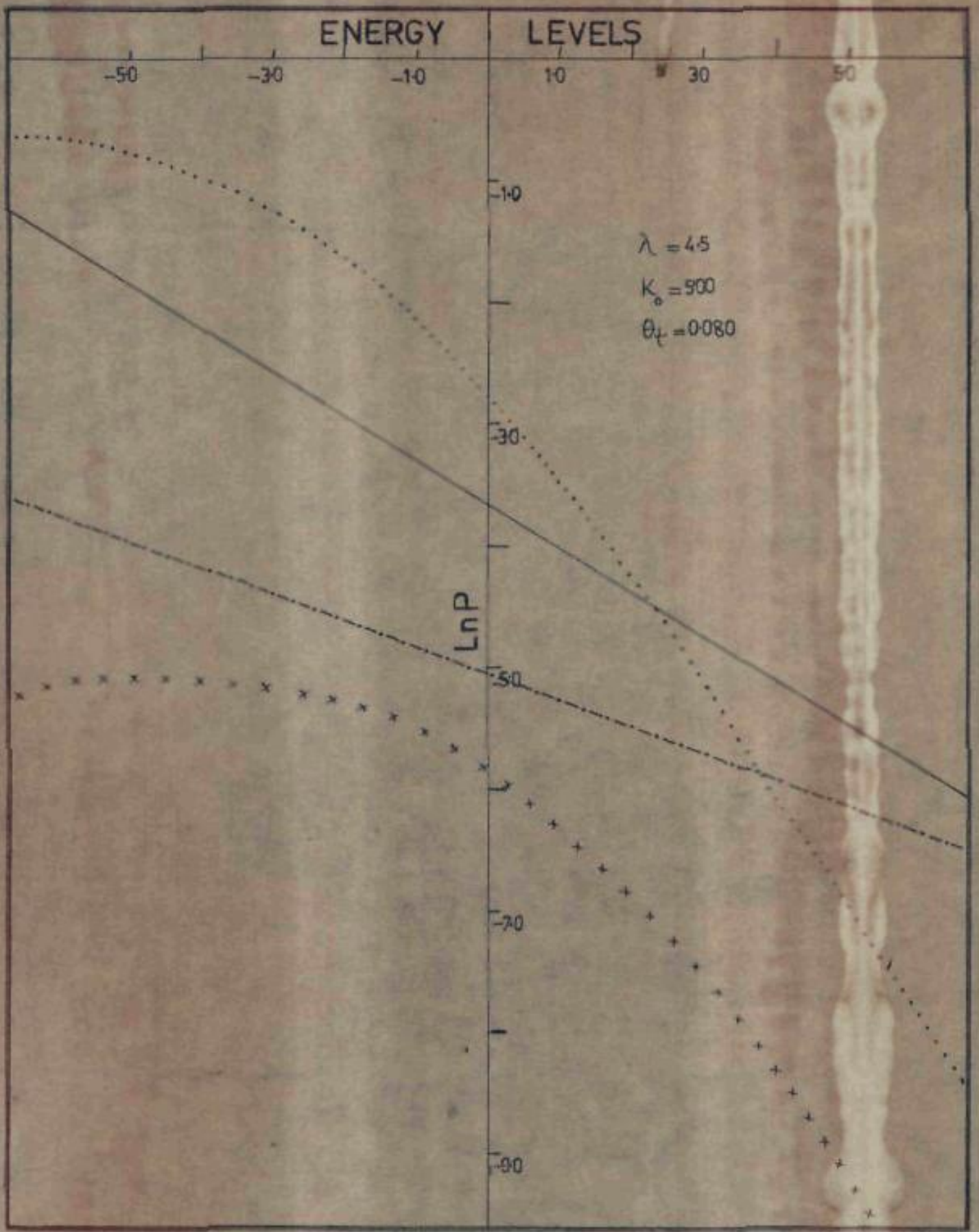
ENERGY LEVELS
-50
-30
-10
10
30
50
-10
-30
-50
-70
-90
LnP
λ = 4·5
K₀ = 900
θ_t = 0·080

FIG :-1·22

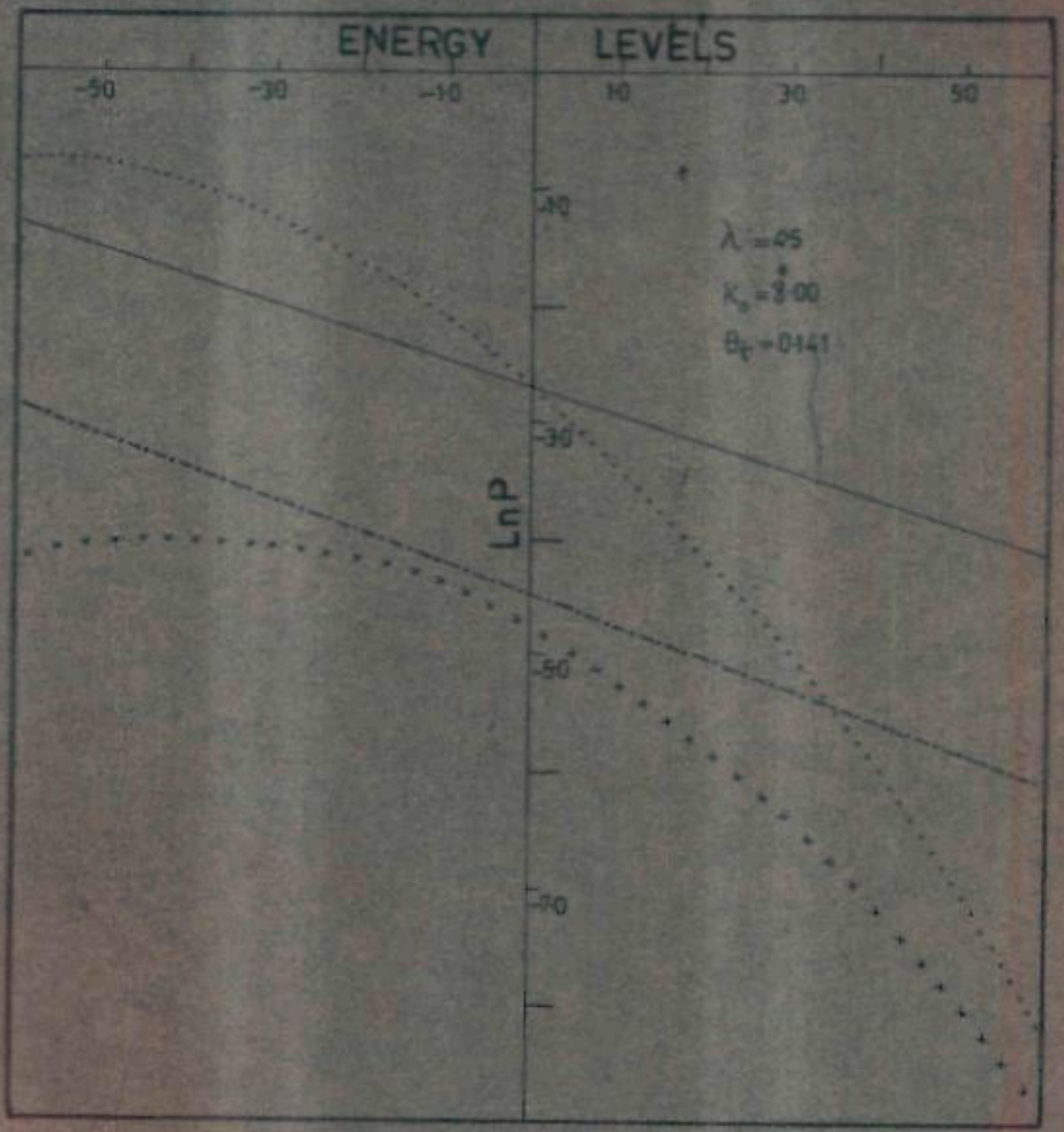

FIG :-1·23

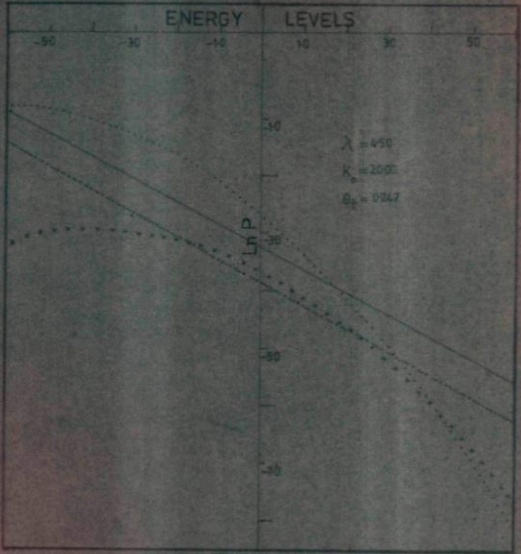

FIG :- 1·24

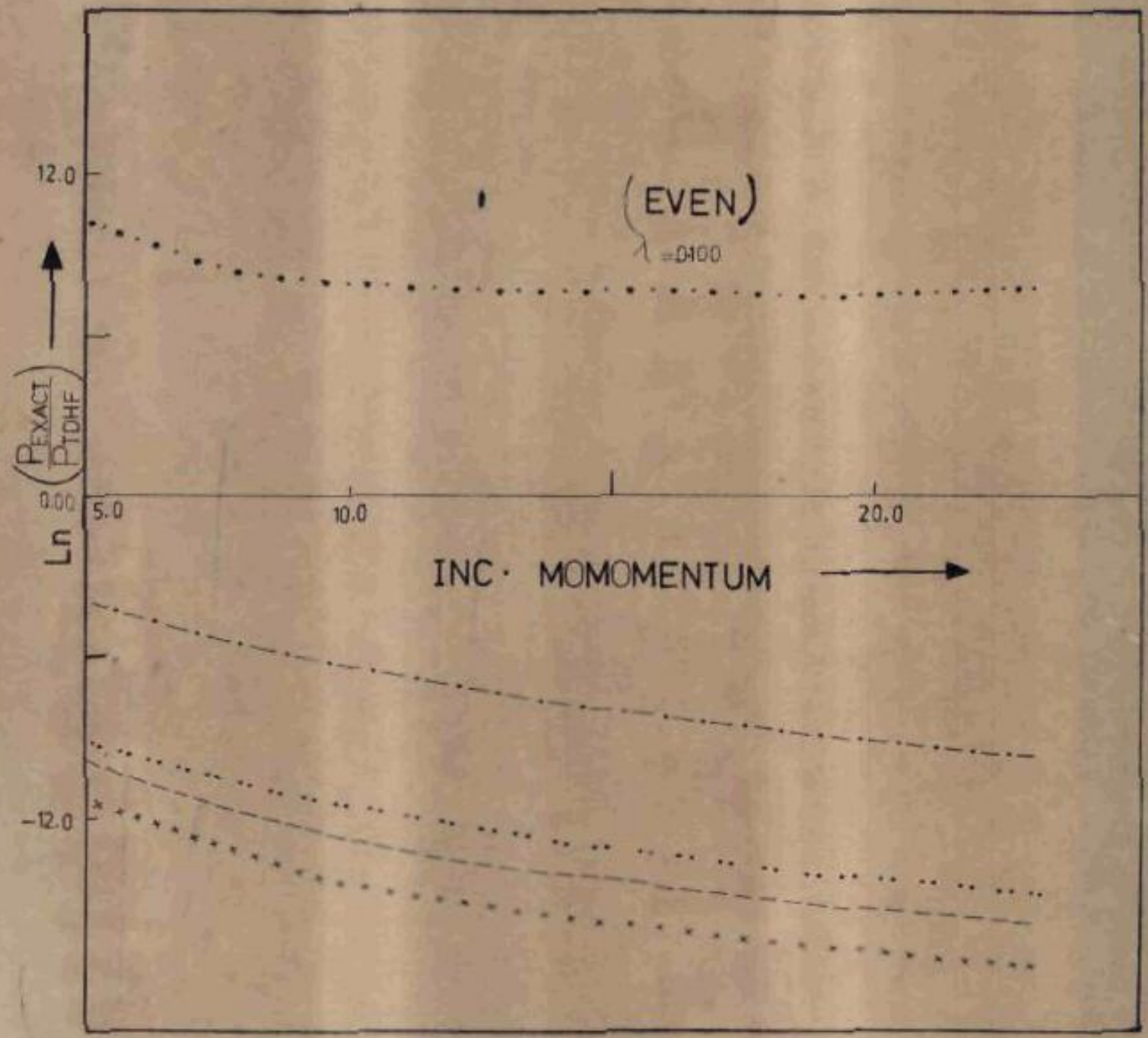
12.0
(EVEN)
λ =0100
Ln (PEXACT / PTDHF)
0.00
5.0
10.0
20.0
INC· MOMOMENTUM
-12.0

FIG :-1·25

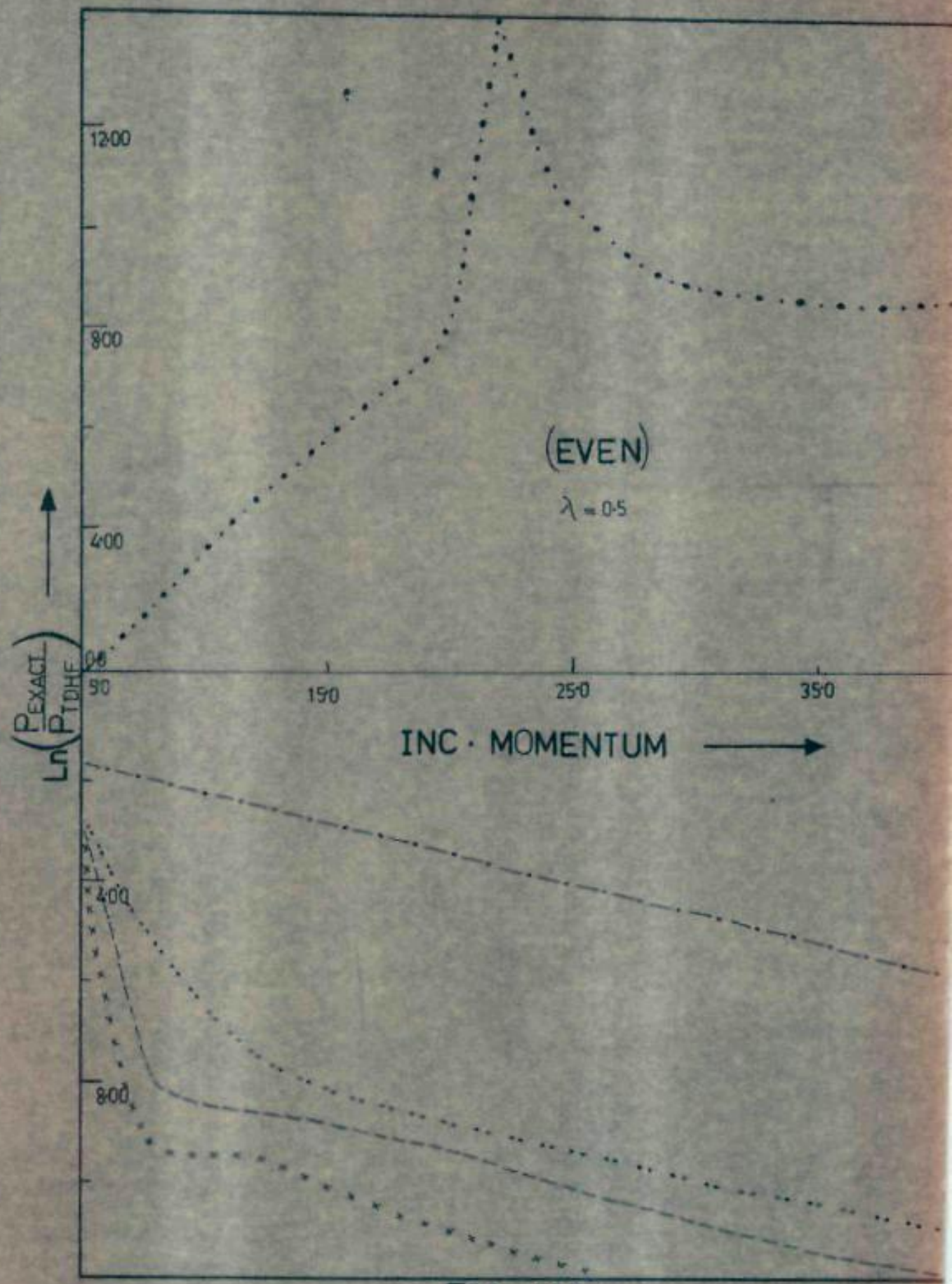
1200
800
400
00
(EVEN)
λ = 0·5
Ln(P_EXACT / P_TDHF)
90
150
250
350
INC · MOMENTUM
400
800

FIG :–1·26

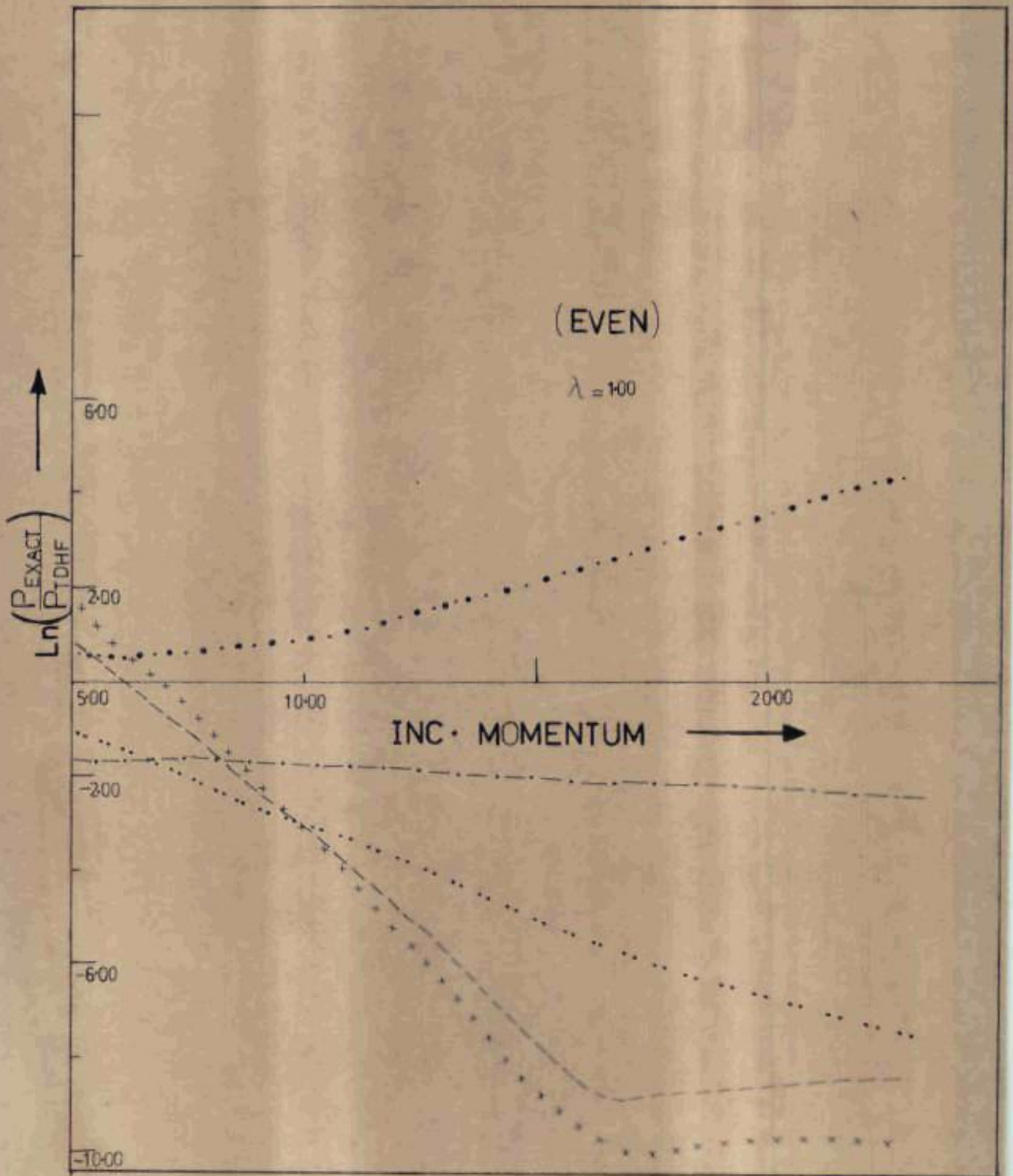
(EVEN)
λ = 1·00
6·00
2·00
-2·00
-6·00
-10·00
5·00
10·00
20·00
INC· MOMENTUM
Ln(P_EXACT / P_TDHF)

FIG :-1·27

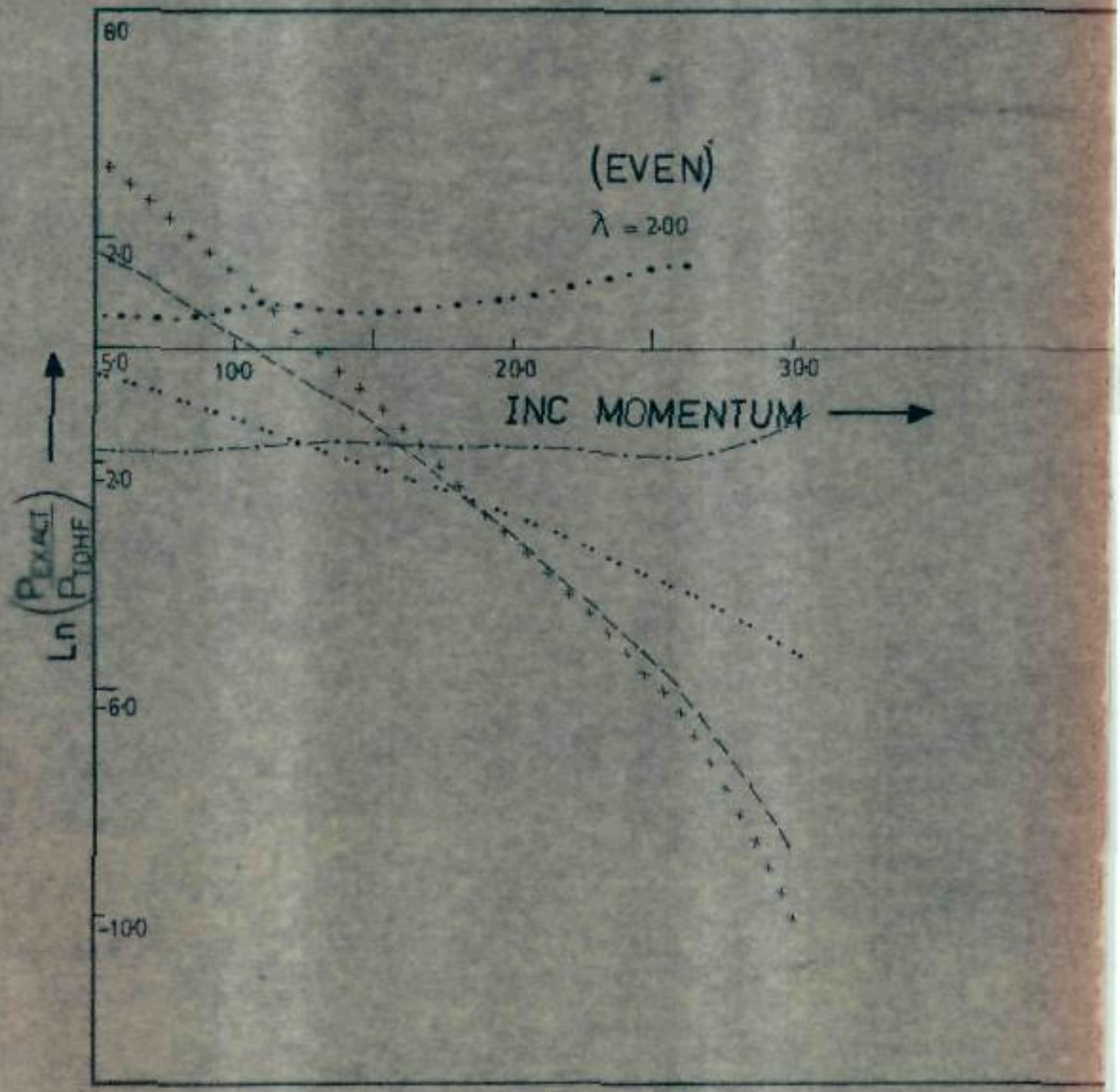
60
(EVEN)
λ = 2·00
20
5·0
10·0
20·0
30·0
INC MOMENTUM
-2·0
-6·0
-10·0
Ln (P EXACT / P IOHF)

FIG :- 1·28

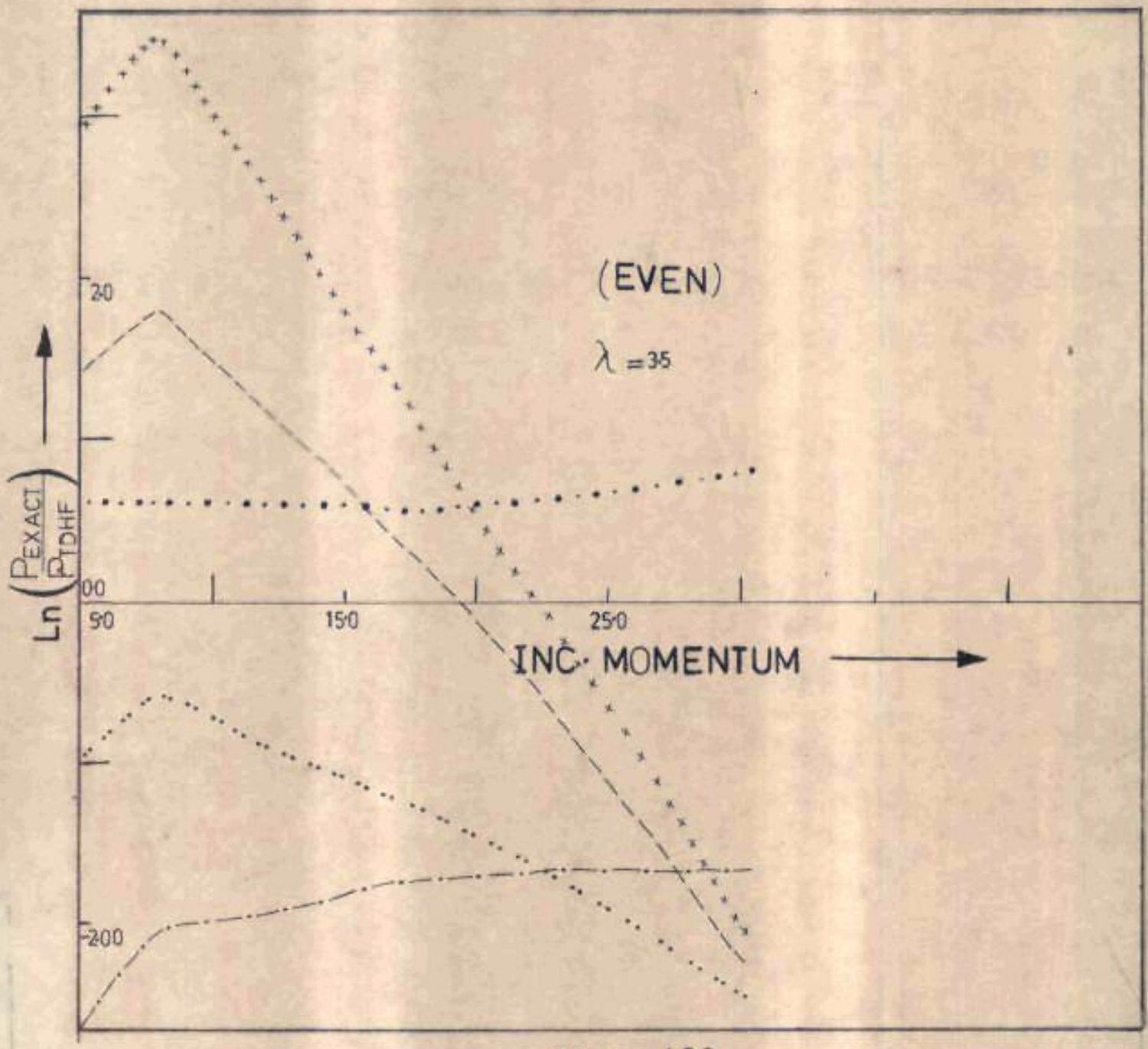

FIG :—1·29

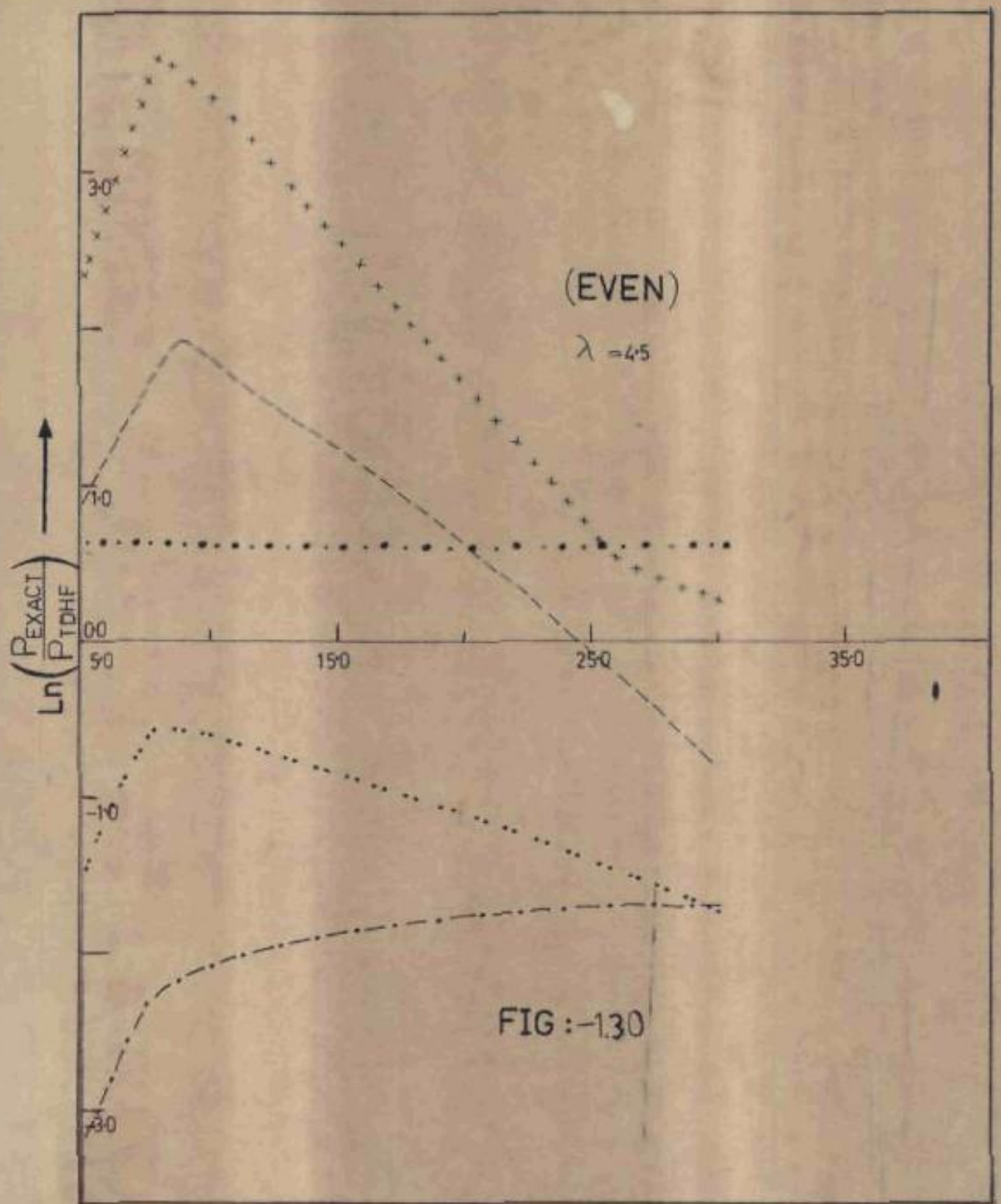

FIG :-1.30

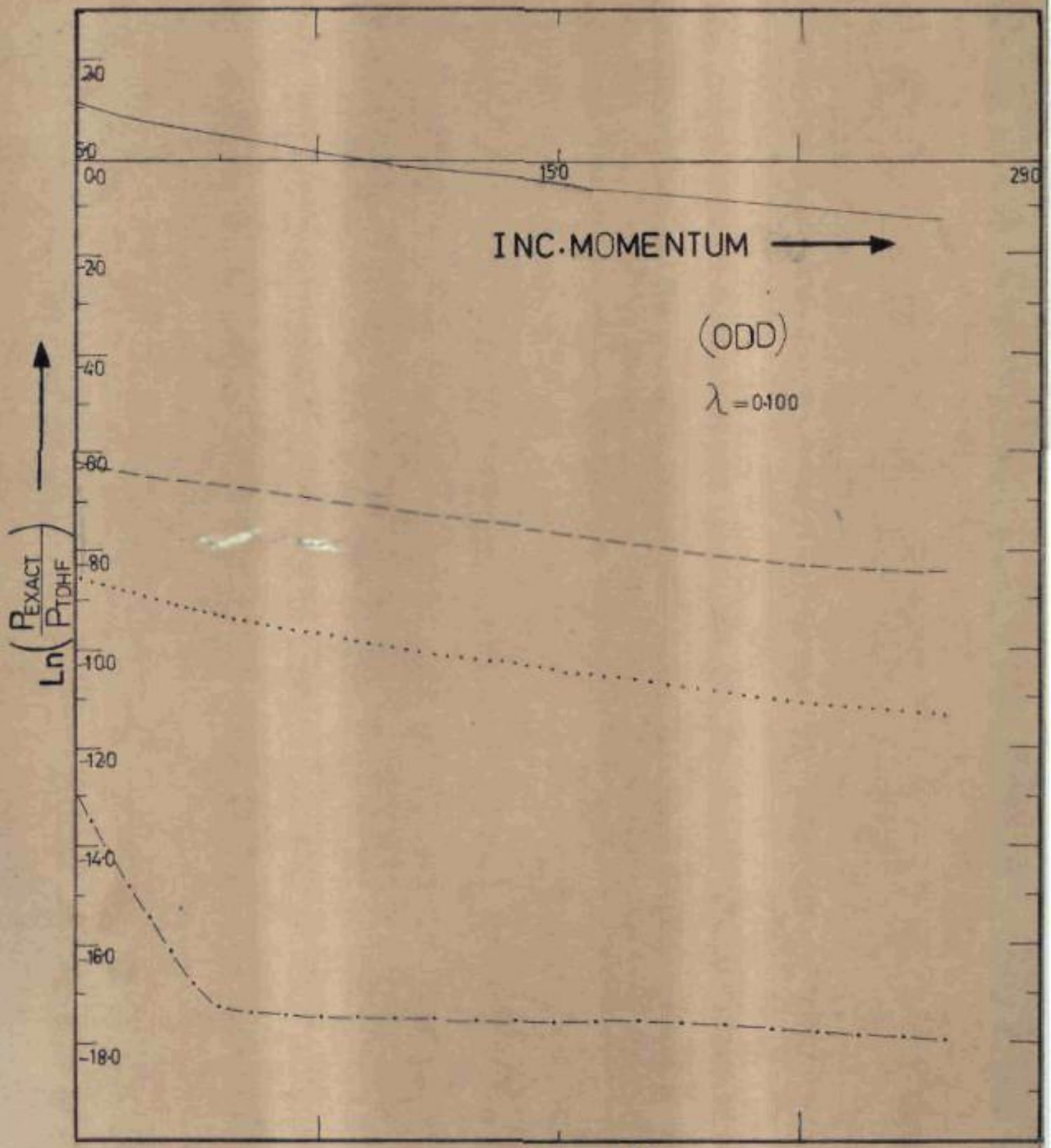
INC. MOMENTUM
(ODD)
λ = 0·100
Ln (P_EXACT / P_TDHF)
-20
-40
-60
-80
-100
-120
-140
-160
-180
150
290

FIG :—1·31

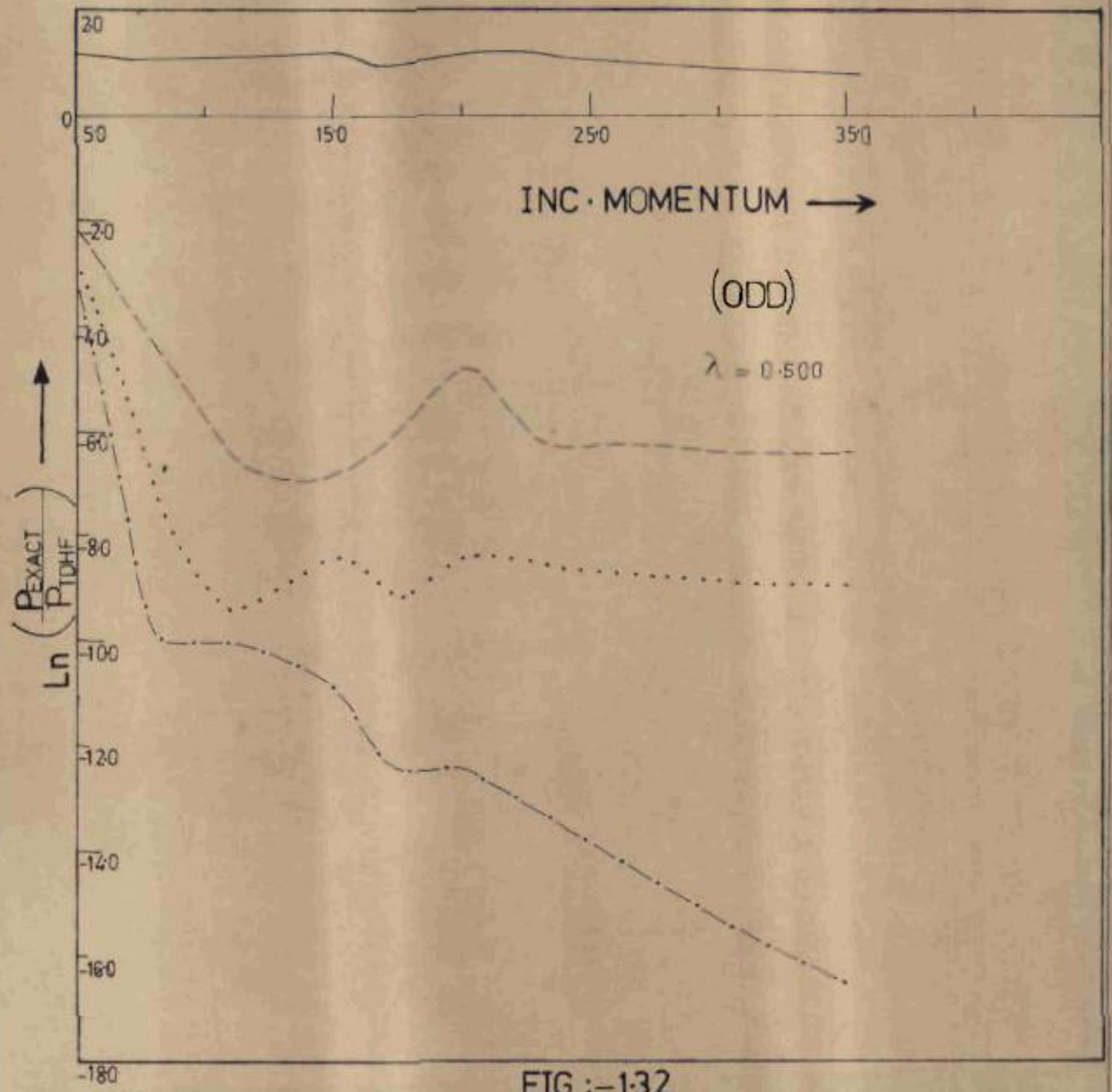
20
0
50
150
250
350
INC · MOMENTUM ⟶
(ODD)
λ = 0·500
-20
-40
-60
-80
-100
-120
-140
-160
-180
Ln (P_EXACT / P_TDHF)

FIG :-1·32

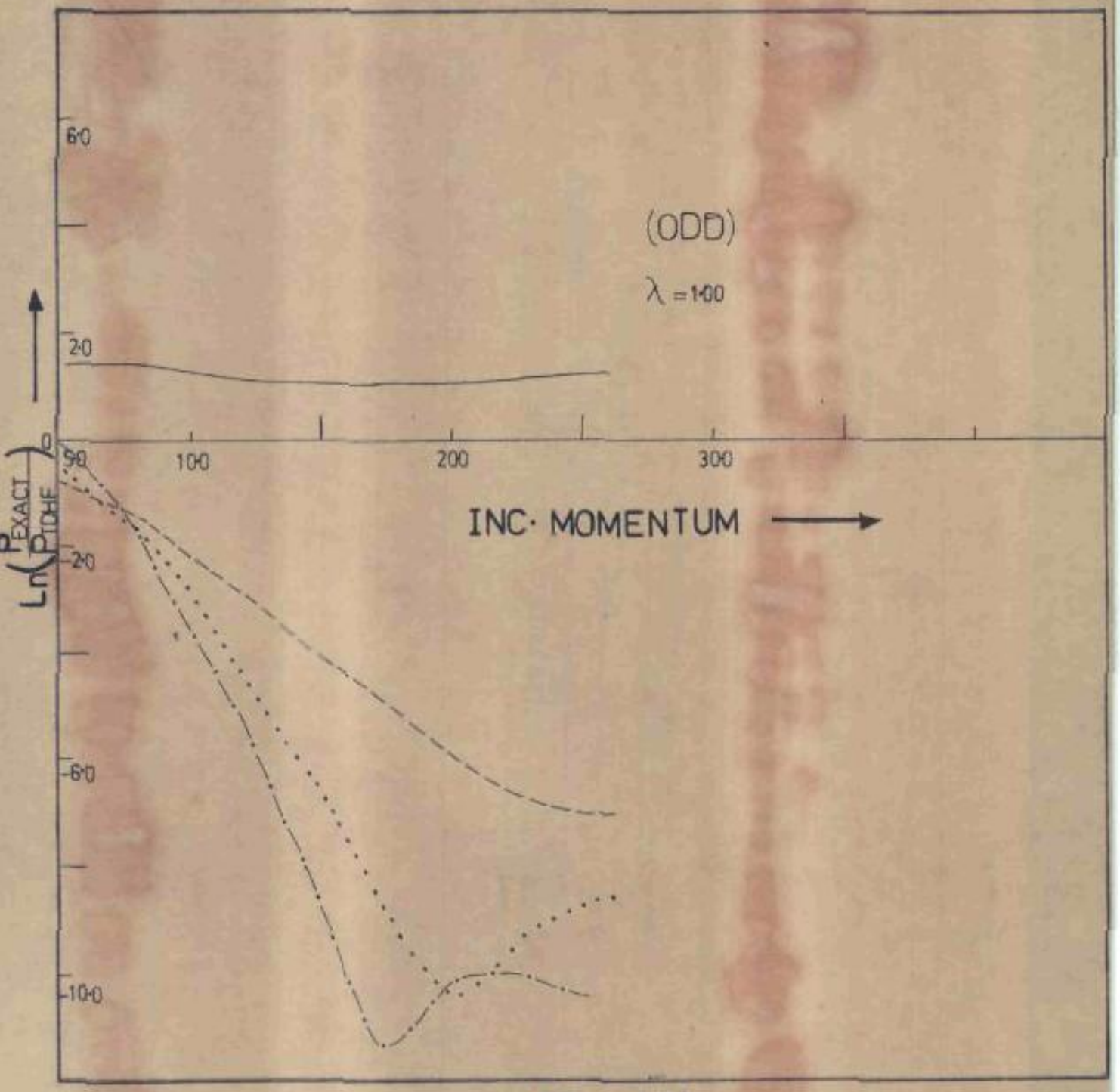
6·0
2·0
(ODD)
λ = 1·00
90
100
200
300
INC· MOMENTUM
Ln(P_EXACT / P_TDHF)
2·0
-6·0
-10·0

FIG :-1·33

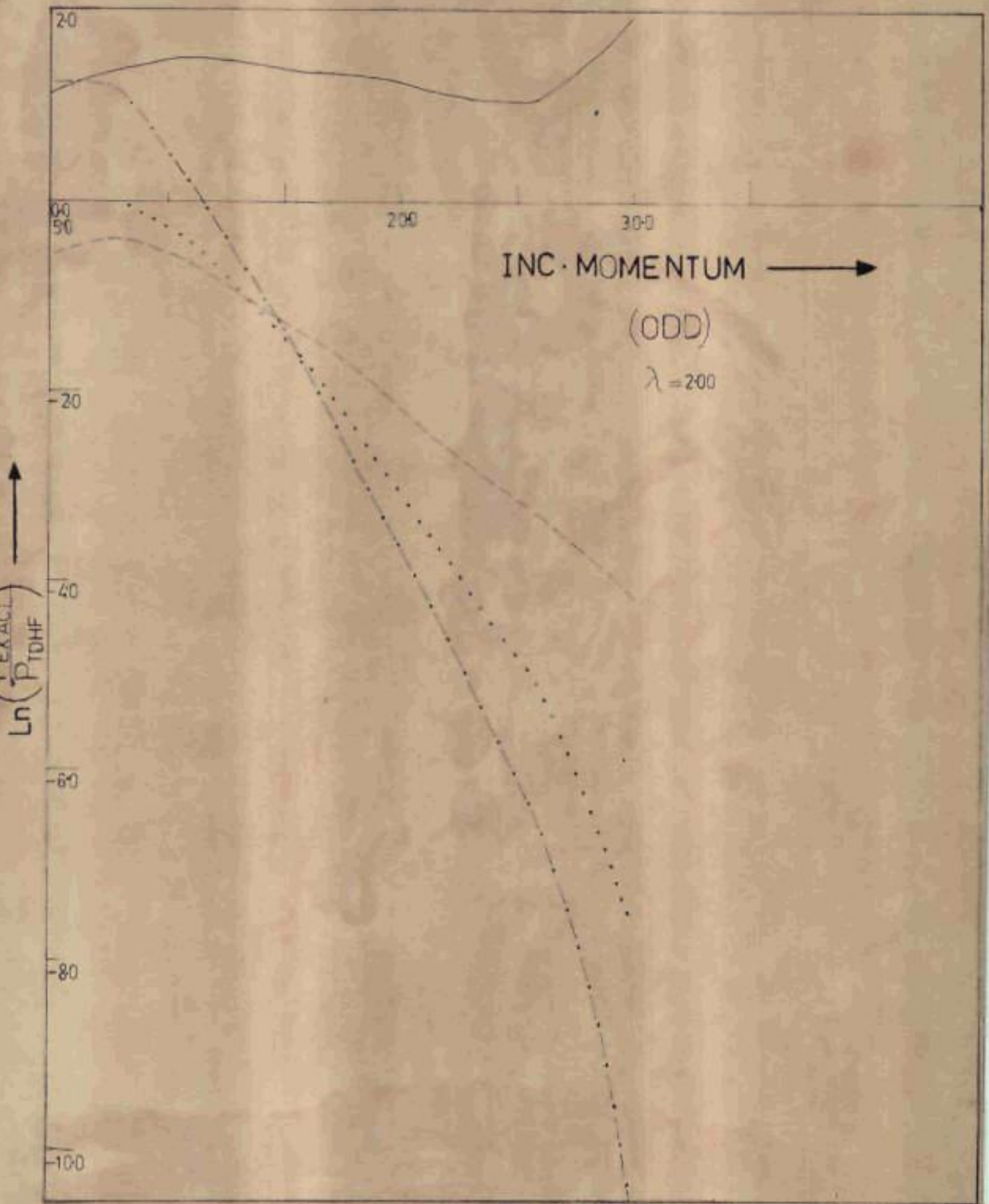
20
00
50
200
300
INC · MOMENTUM
(ODD)
λ = 200
-20
-40
-60
-80
-100
Ln(P_EXACT / P_TDHF)

FIG :- 134

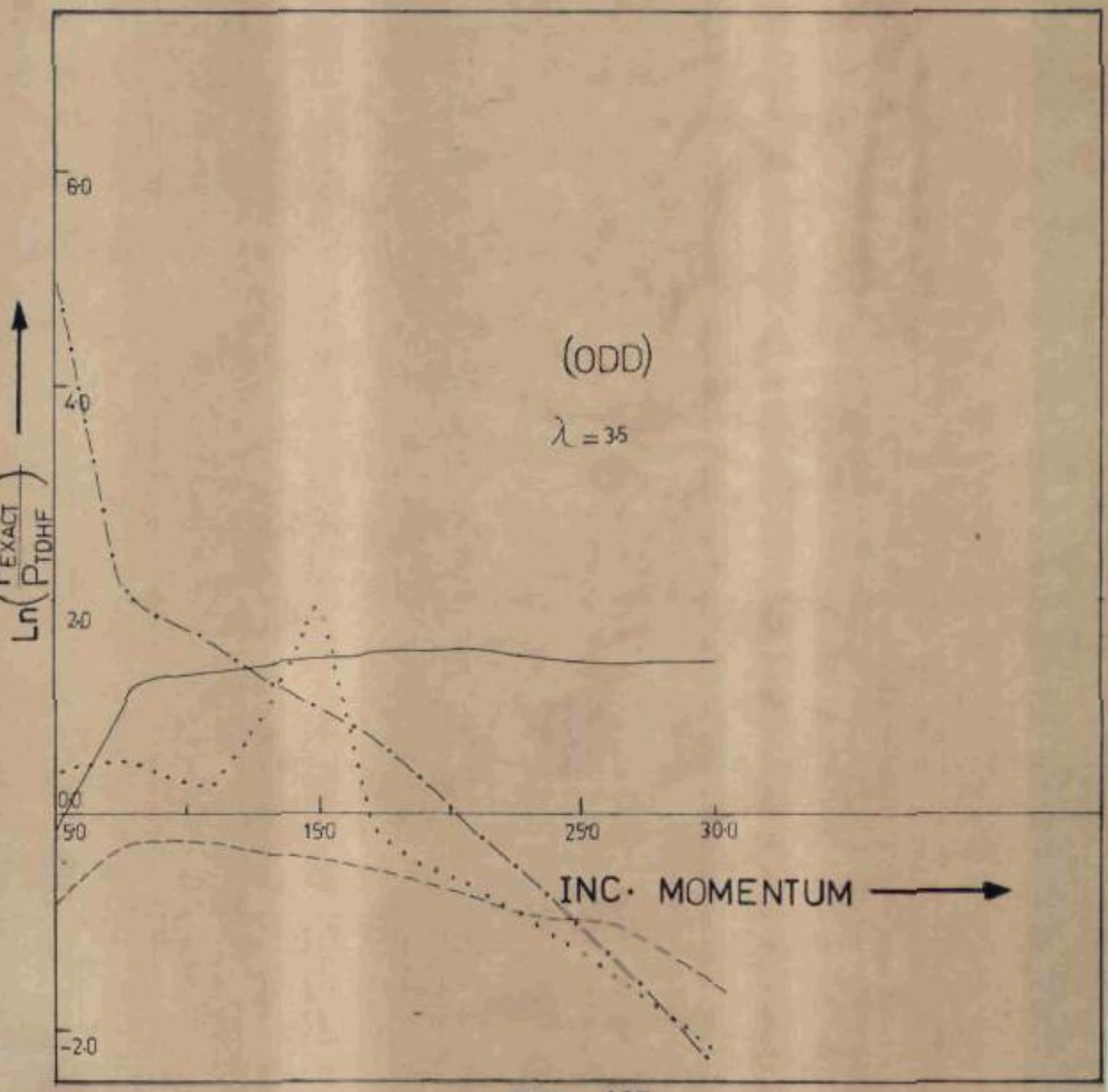
6·0
4·0
2·0
0·0
-2·0
(ODD)
λ = 35
Ln(P_EXACT / P_TDHF)
50
150
250
300
INC· MOMENTUM

FIG :- 1.35

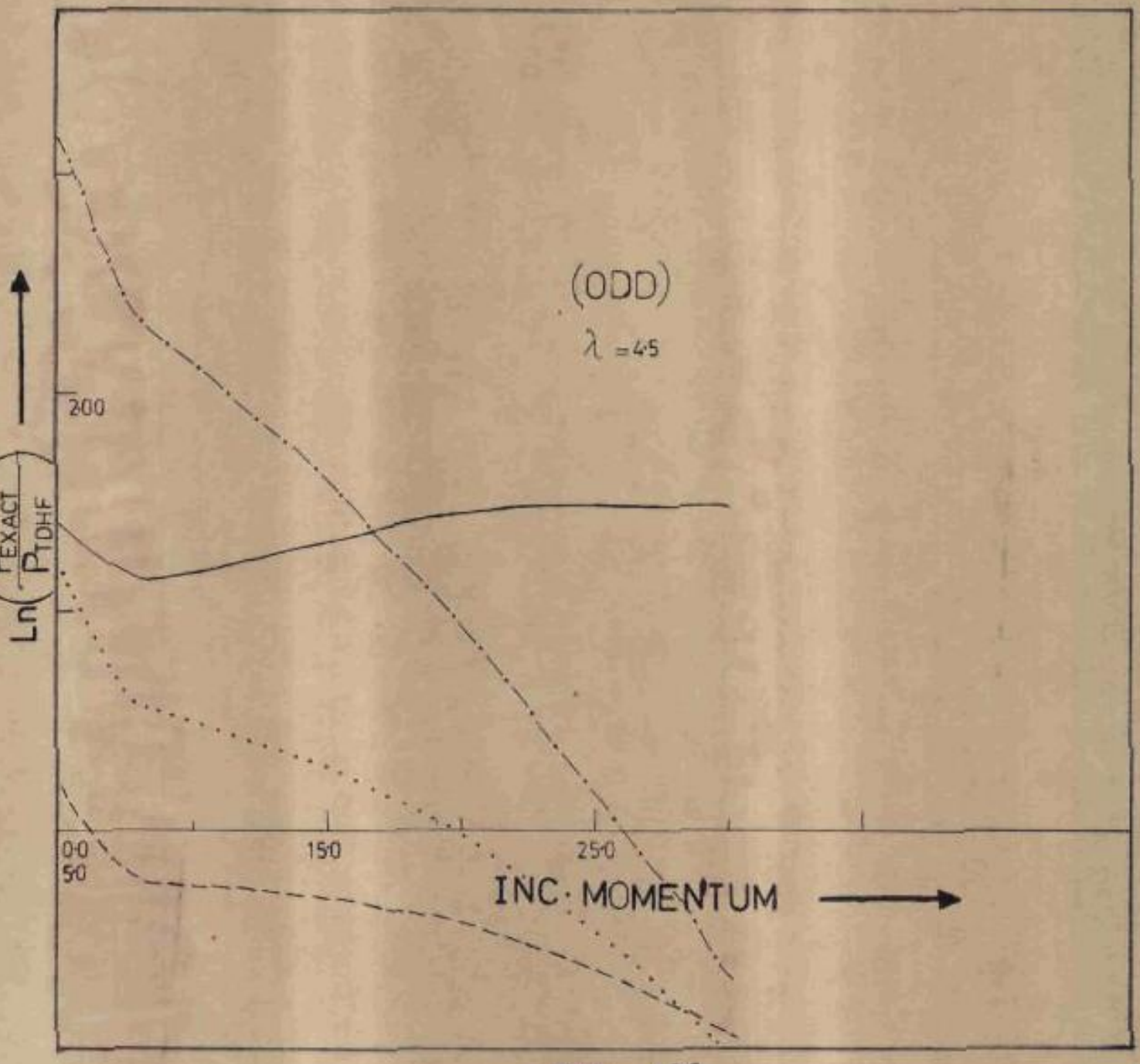

FIG :– 1·36

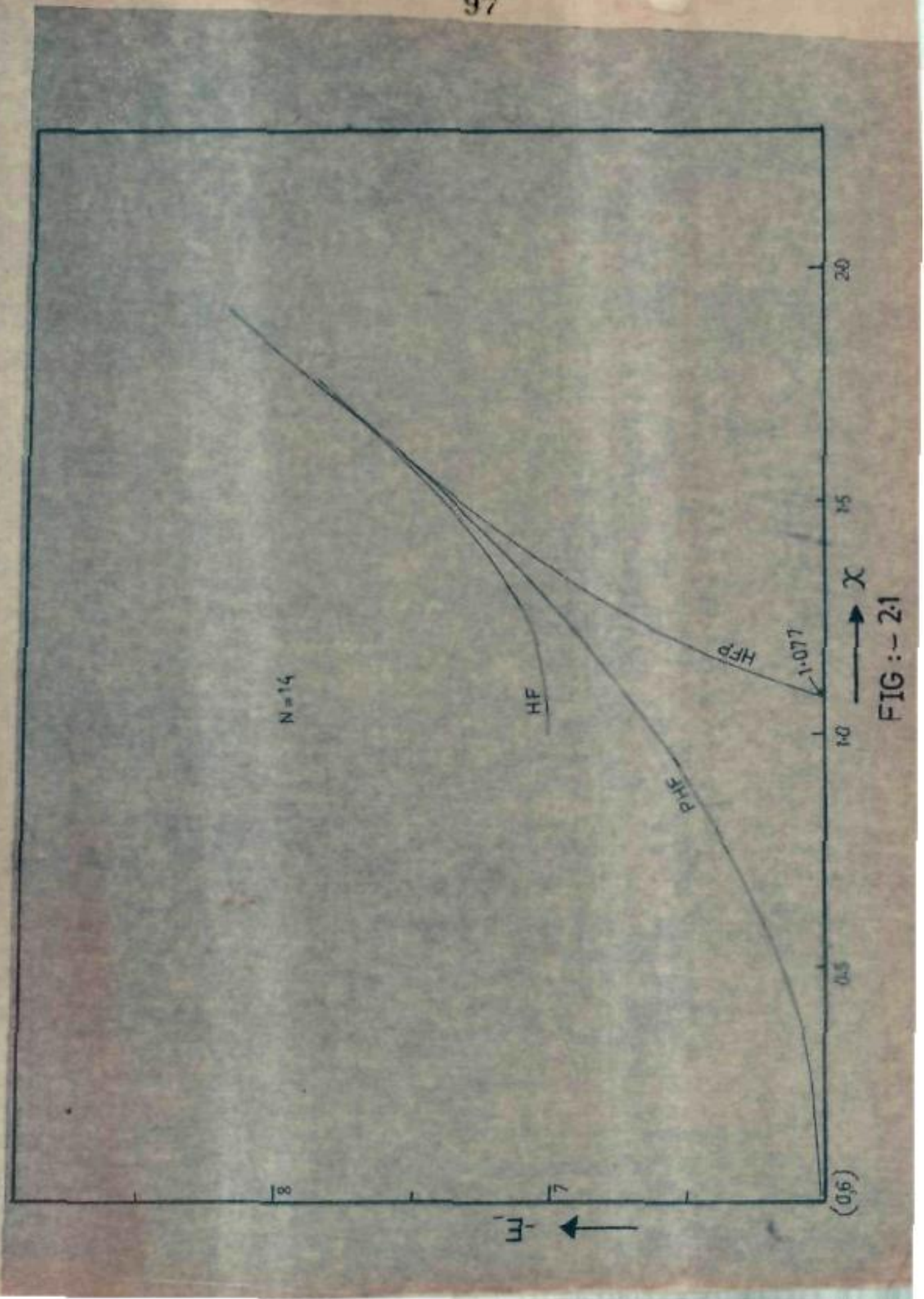

FIG :- 2.1

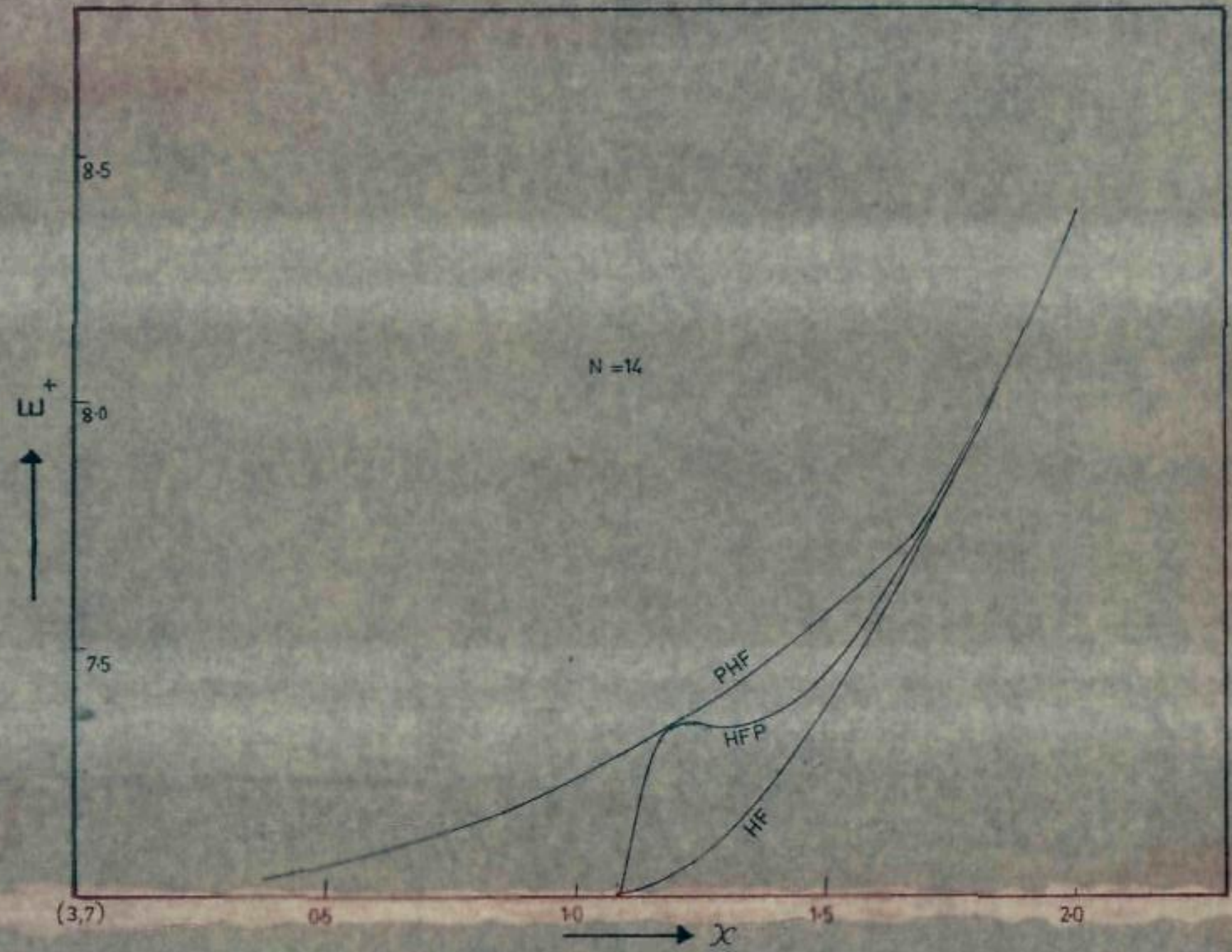

FIG :- 2·2

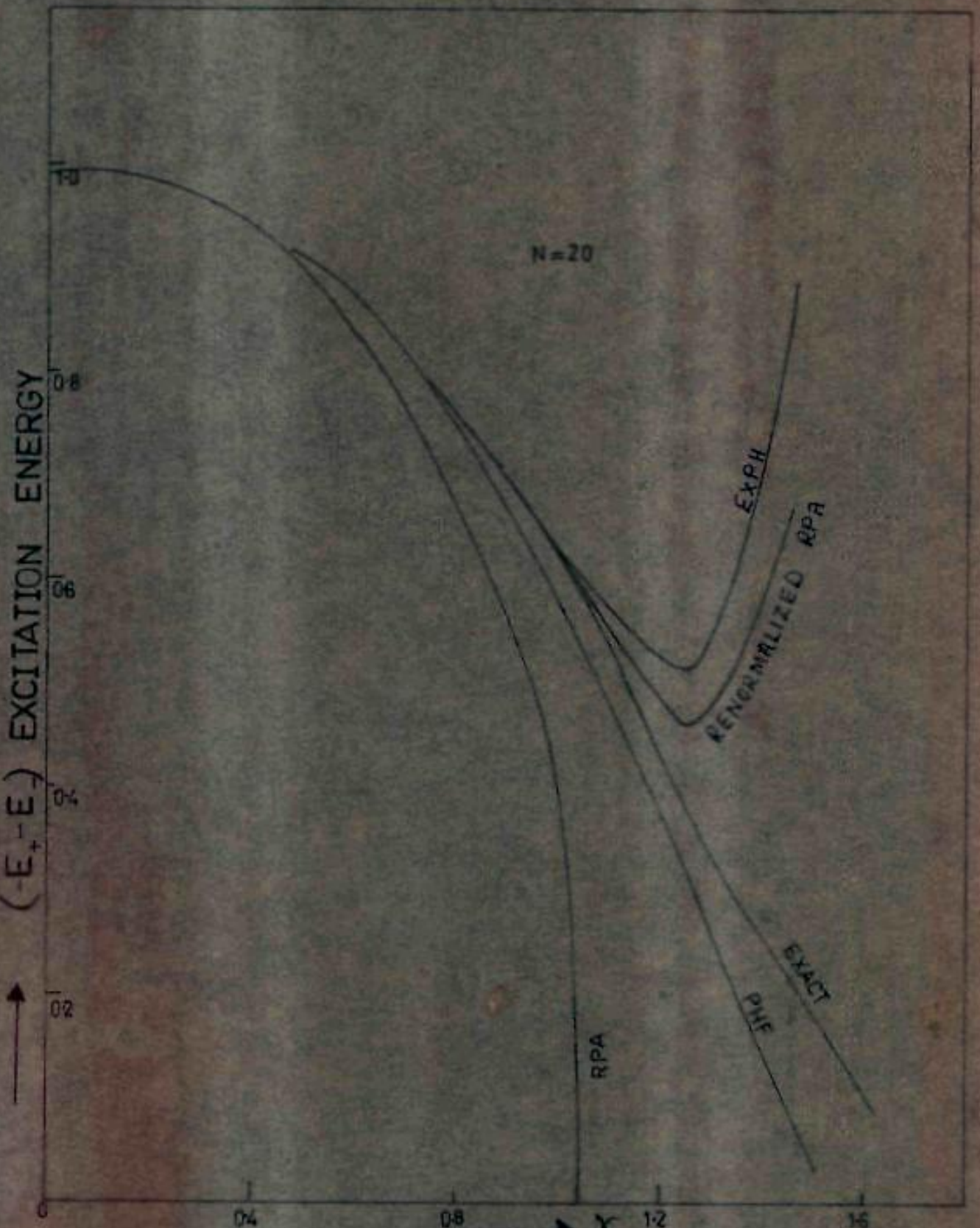
N=20
EXPH
RENORMALIZED RPA
EXACT
THF
RPA
$(-E_+ - E_-)$ EXCITATION ENERGY
X
0
0·4
0·8
1·2
1·6
0·2
0·4
0·6
0·8
1·0

FIG:-2·3

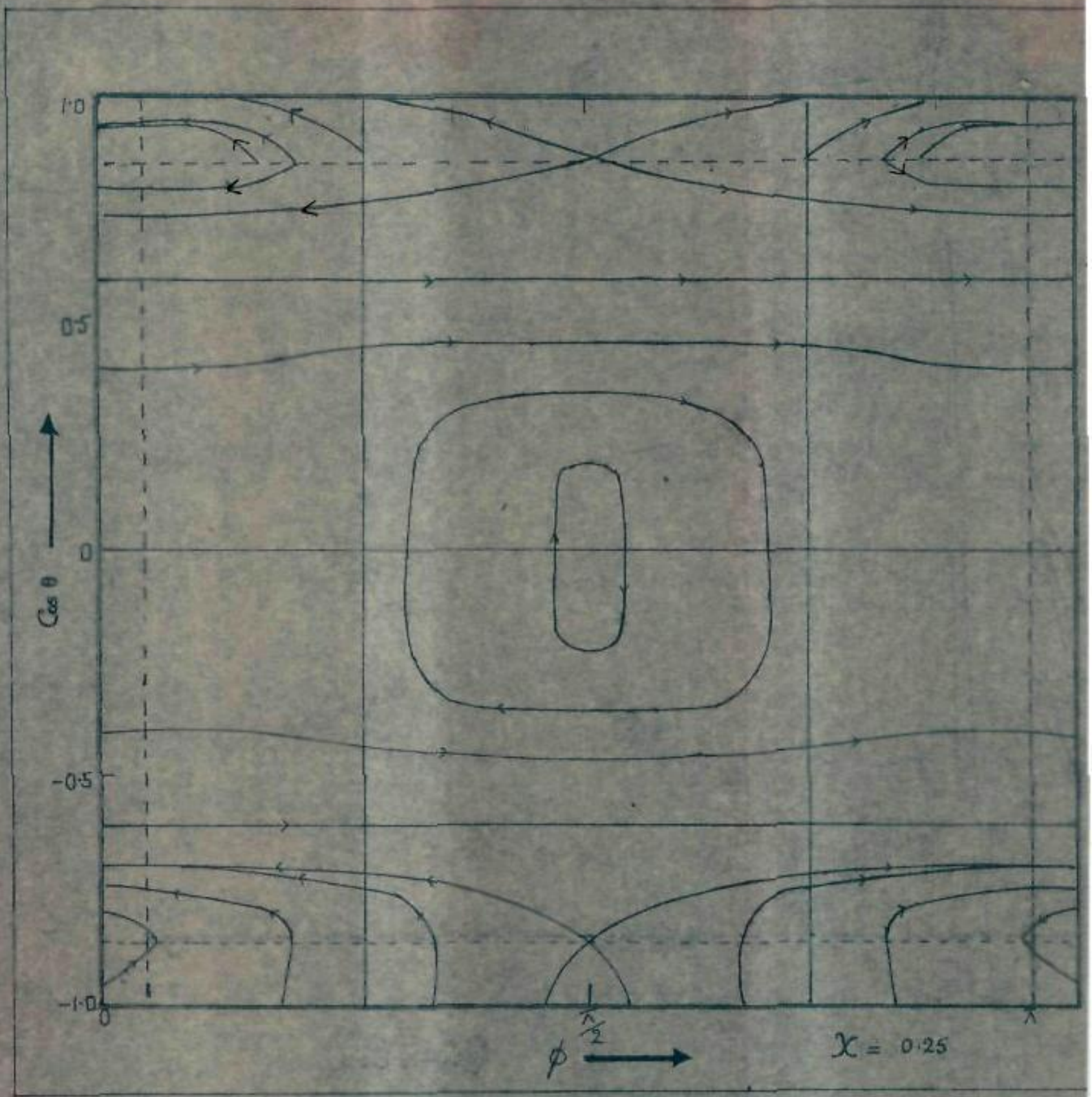

FIG :- 2·4

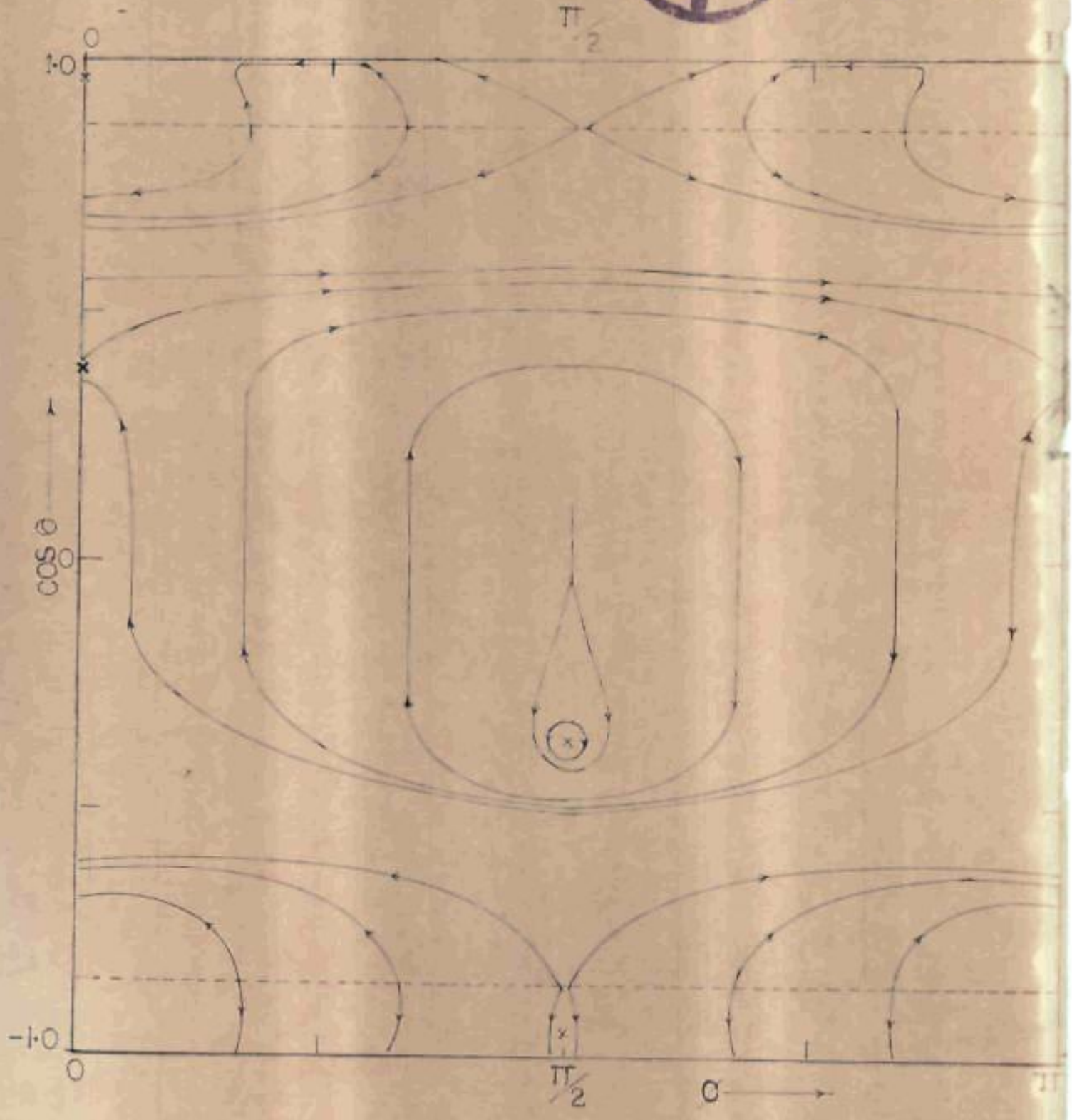

FIG.:-2·5

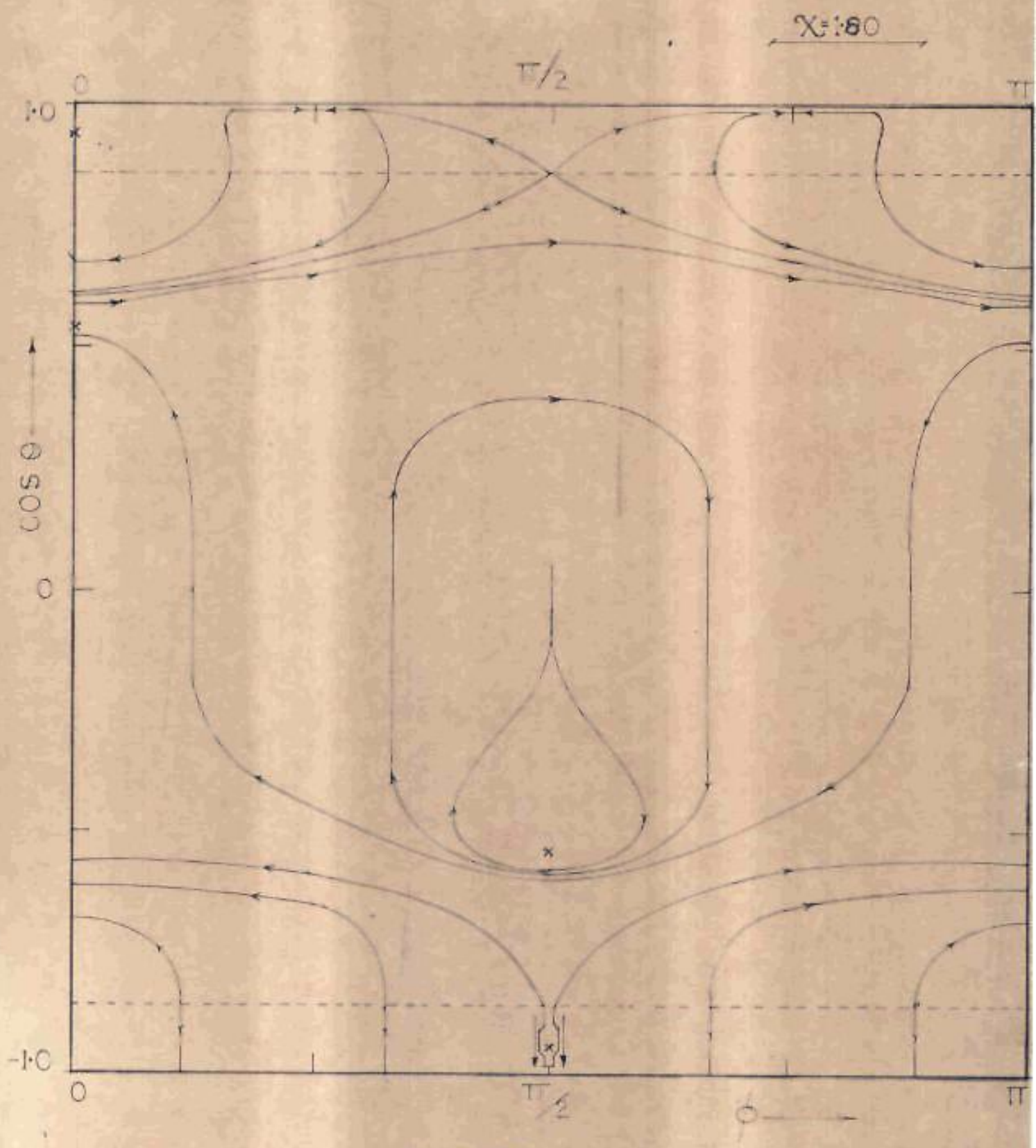

FIG.: 26

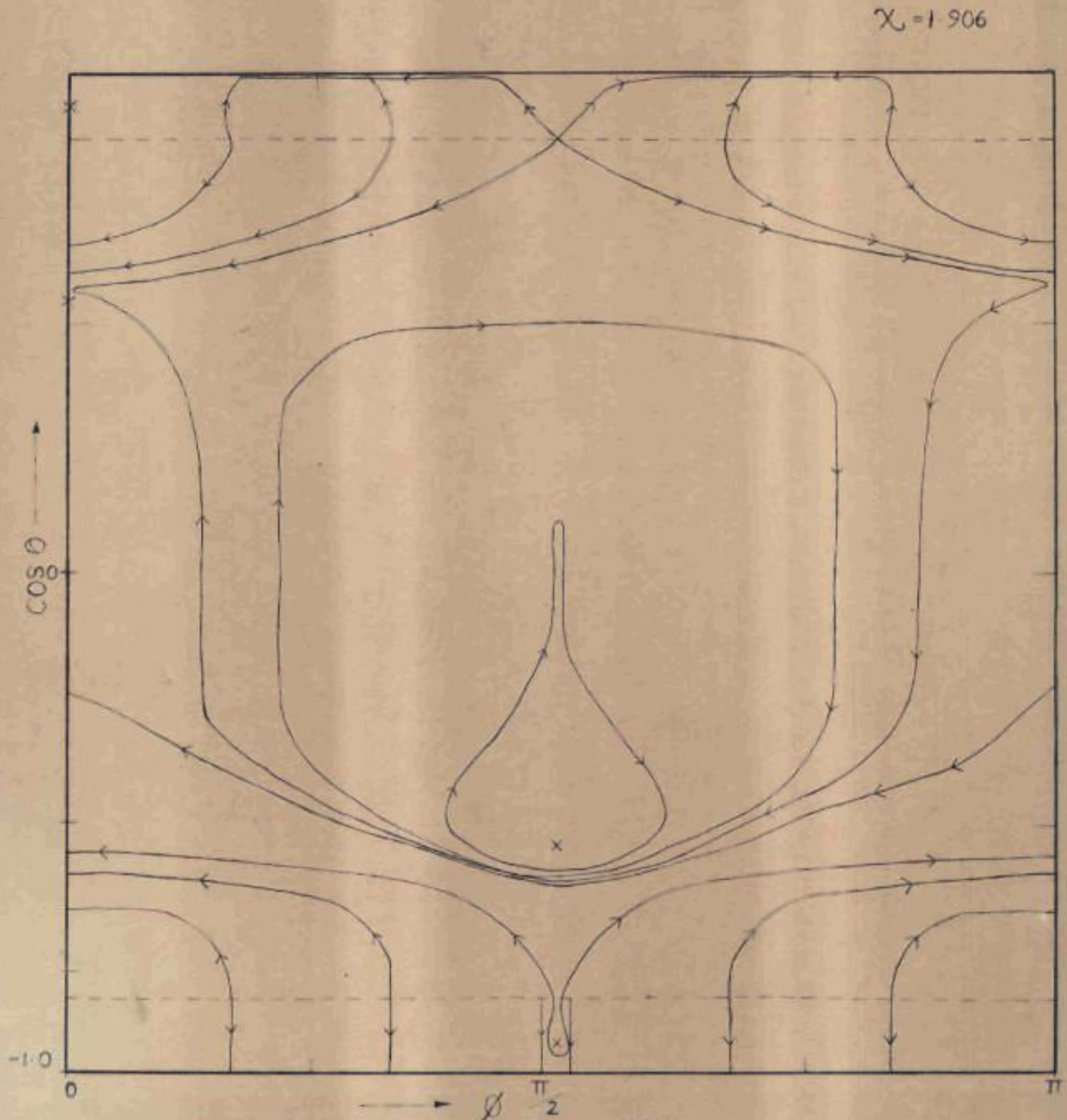

FIG 2·7

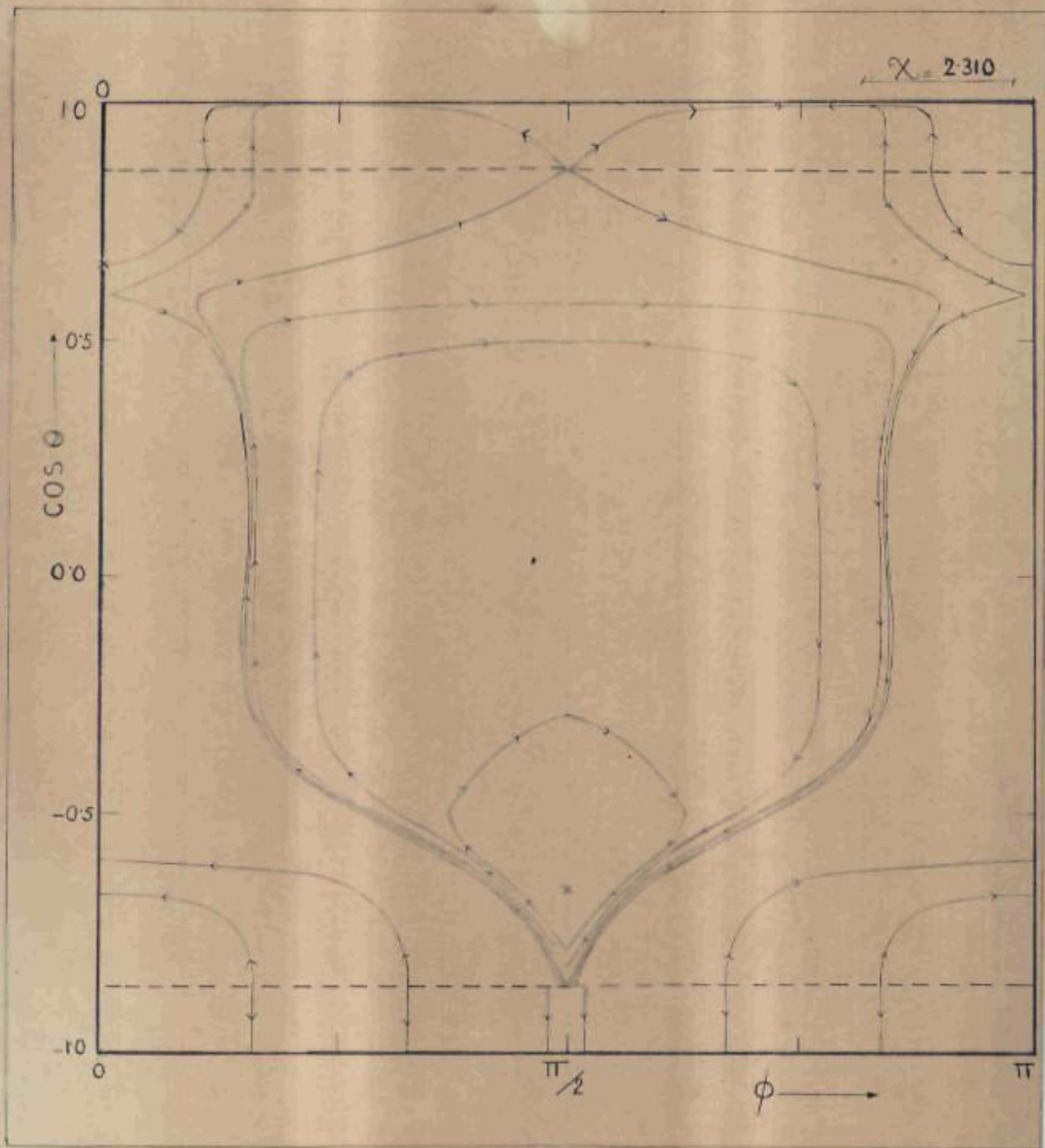

FIG:- 2·8

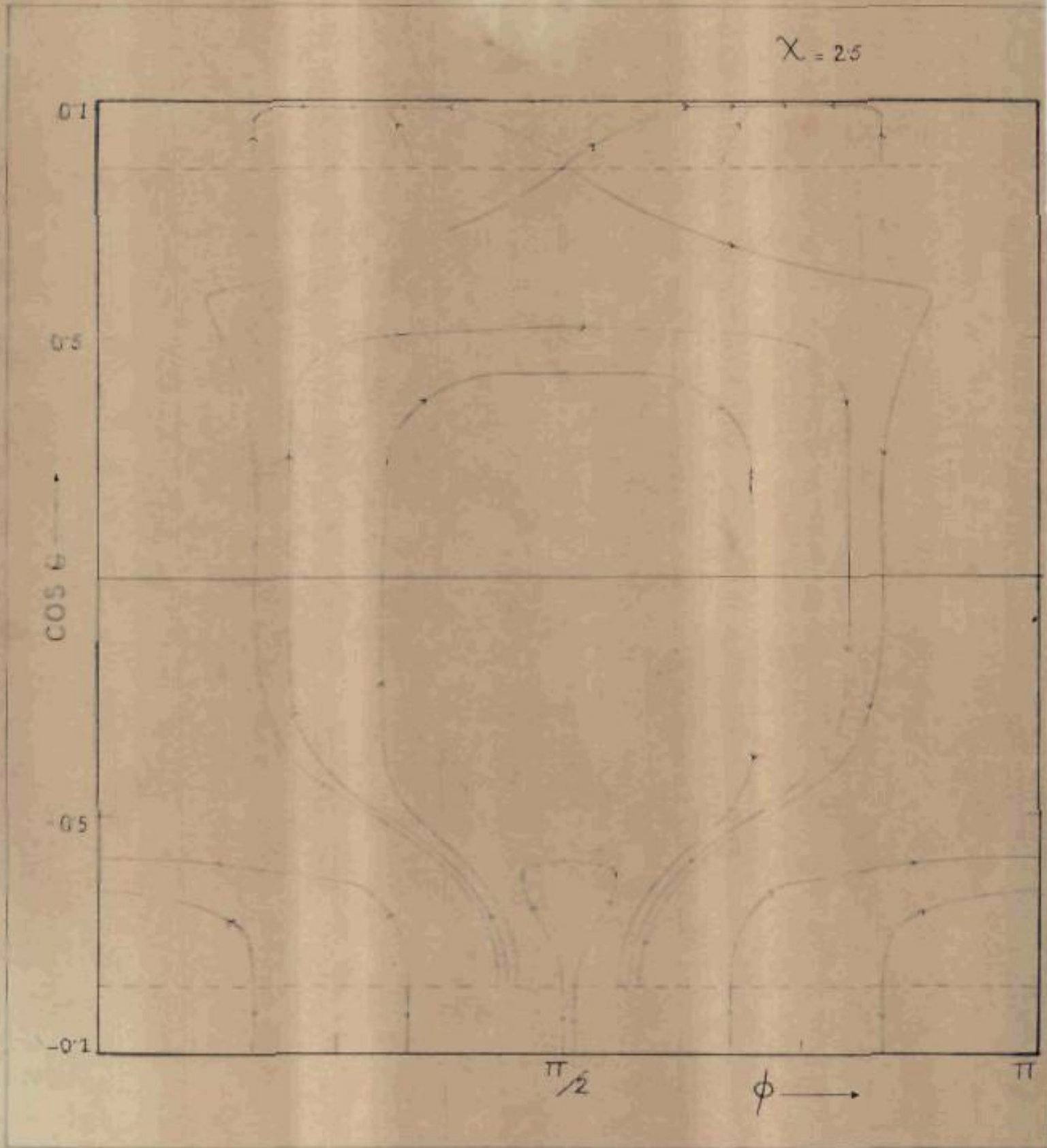

FIG. — 2·9

Captions to Tables

Table 1.1 —— 1.3:— The logarithms of the probability distribution

$$P_M = |\langle \Psi_{TDHF} | M \rangle|^2$$

for several values of M.

Table 1.4 —— 1.9:— Logarithms of the probability distribution of various eigenstates in the exact calculations and TDHF calculations.

Table 1.10 —— Table 1.14:—
A comparison of the energy loss in exact calculations, TDHF approximation, and PTDHF approximations.

Table 2.1 :— The excitation energy of the odd parity states obtained from various calculations viz exact Hartree-Fock theory, Projected Hartree-Fock theory, and projection after variation (i.e. HFP) theory respectively.

Table 2.2:— The same as 2.1 but with even parity states.

Table 2.3:— a display of the fixed points for various strength of the interaction parameter.

TABLE : 1.1 $\theta = 0.10$

LOGARITHMS OF THE PROBABILITY DISTRIBUTION P_m FOR SEVERAL M VALUES.

M VALUES	$L_n P_m$ VALUES
- 4	- 0.00002
- 3	- 12.009
- 2	- 24.845
- 1	- 38.239
0	- 52.104
1	- 66.414
2	- 81.195
3	- 96.536
4	- 112.703

TABLE : 1.2 $\theta = 0.55$

LOGARITHMS OF THE PROBABILITY DISTRICUTION P_m FOR SEVERAL M VALUES.

M VALUES	$L_n P_m$ VALUES
- 4	- 0.00002
- 3	- 8.600
- 2	- 18.026
- 1	- 28.009
0	- 38.466
1	- 49.368
2	- 60.739
3	- 72.669
4	- 85.428

TABLE : 1.3 $\theta = 1.00$

LOGARITHMS OF THE PROBABILITY DISTRIBUTION P_m FOR SEVERAL m VALUES

m VALUES	$Ln P_m$ VALUES
- 4	- 0.00002
- 3	- 7.407
- 2	- 15.635
- 1	- 24.424
0	- 33.681
1	- 43.389
2	- 58.565
3	- 64.300
4	- 75.862

TABLE : 1.4 INTERACTION STRENGTH $\lambda = 0.5$

THE LOGARITHMS OF THE PROBABILITY DISTRIBUTION OF THE STATES (E_i)

INCIDENT MOMENTUM (K_o)	5.0		35.0	
STATES (E_i)	EXACT CALCULATION	TDHF CALCULATION	EXACT CALCULATION	TDHF CALCULATION
- 5.36970	- 0.569	- 1.566	- 0.044	- 8.405
- 3.23577	- 2.603	- 0.872	- 7.626	- 2.432
0.00000	- 5.047	- 2.251	- 11.917	- 1.447
3.23577	- 6.681	- 4.255	- 13.429	- 2.064
5.36970	- 8.009	- 5.861	- 15.997	- 2.947
- 5.04042	- 4.089	- 2.328	- 3.158	- 3.922
- 1.75502	- 4.268	- 2.151	- 8.136	- 1.718
1.75502	- 6.309	- 3.430	- 10.646	- 1.551
5.04042	- 8.716	- 5.399	- 19.146	- 2.454

TABLE :-1·5 INTERACTION STRENGTH λ = 1·0

THE LOGARITHMS OF THE PROBABILITY DISTRIBUTION OF THE STATES (E_i)

INCIDENT MOMENTUM (K_o)	5·00		8·00		17·00	
STATES (E_i)	EXACT CALCU-LATION	TDHF CALCU-LATION	EXACT CALCU-LATION	TDHF CALCU-LATION	EXACT CALCU-LATION	TDHF CALCU-LATION
-5·36970	0·503	-1·091	-0·578	-1·318	-0·415	-3·083
-3·23577	-2·443	-0·781	-2·493	-0·823	-3·284	-1·216
0·00000	-3·627	-2·583	-4·567	-2·408	-7·527	-1·722
3·23577	-4·214	-4·904	-6·096	-4·559	-12·097	-3·174
5·36970	-4·885	-6·685	-7·393	-6·246	-14·516	-4·491
-5·04042	-1·492	-2·909	-1·145	-2·527	-1·203	-2·283
-1·75502	-3·654	-2·927	-3·856	-2·450	-6·345	-1·557
1·75502	-4·984	-4·396	-5·555	-3·825	-10·802	-2·360
5·04042	-6·474	-6·530	-7·531	-5·876	-15·214	-3·951

TABLE : 1.6

INTERACTION STRENGTH λ = 2.00

THE LOGARITHMS OF THE PROBABILITY DISTRIBUTION OF THE STATES (E_i)

INCIDENT MOMENTUM (K_o)	5.00		11.00	
STATES (E_i)	EXACT CALCULATION	TDHF CALCULATION	EXACT CALCULATION	TDHF CALCULATION
- 5.36970	- 0.354	- 0.932	- 0.523	- 1.116
- 3.23577	- 2.595	- 0.754	- 2.480	- 0.785
0.00000	- 3.171	- 2.728	- 3.927	- 2.562
3.23577	- 3.412	- 5.197	- 4.822	- 4.863
5.36970	- 3.773	- 7.064	- 5.771	- 6.632
- 5.04042	- 2.384	- 3.513	- 1.375	- 2.851
1.75502	- 5.205	- 5.137	- 4.77	- 4.317
5.04042	- 6.065	- 7.333	- 6.208	- 6.442

CALCULATION TYPE	INCIDENT MOMENTUM (K₀)				INCIDENT MOMENTUM (K₀)			
	EXACT CALCULATION	SERIES CALCULATION	EXACT CALCULATION	TYPE CALCULATION	EXACT CALCULATION	SERIES CALCULATION	EXACT CALCULATION	TYPE CALCULATION
	. . . .		. . . .	. . . .		. . . .	. . . .	

TALLY DISTRIBUTION FOR SQUARES (Q) OF THE PROBABILITY DISTRIBUTION OF SQUARES (Q) THE PROBABILITY [illegible]

INTERACTION [illegible] | INTERACTION [illegible] | [illegible]

TABLE :- 1.7 INTERACTION STRENGTH λ = 2.00

THE LOGARITHMS OF THE PROBABILITY DISTRIBUTION OF THE STATES (E_i)

INCIDENT MOMENTUM (K_o)	15.00		17.00	
STATES (E_i)	EXACT CALCULATION	TDHF CALCULATION	EXACT CALCULATION	TDHF CALCULATION
- 5.36970	- 0.574	- 1.268	- 0.58	- 1.372
- 3.23577	- 2.476	- 0.813	- 2.513	- 0.833
0.00000	- 4.459	- 2.444	- 4.756	- 2.371
3.23577	- 5.976	- 4.630	- 6.586	- 4.488
5.36970	- 7.287	- 6.335	- 8.044	- 6.155
- 5.04042	- 1.171	- 2.588	- 1.119	- 2.471
- 1.75502	- 3.766	- 2.532	- 3.955	- 2.372
1.75502	- 5.396	- 3.928	- 5.793	- 3.725
5.04042	- 7.321	- 5.997	- 7.942	- 5.758

TABLE : 1.8a

INTERACTION STRENGTH $\lambda = 3.5$

THE LOGARITHMS OF THE PROBABILITY DISTRIBUTION OF THE STATES (E_i)

INCIDENT MOMENTUM (K_o)	23.00		30.00	
STATES (E_i)	EXACT CALCULATION	TDHF CALCULATION	EXACT CALCULATION	TDHF CALCULATION
- 5.36970	- 0.558	- 1.186	- 0.580	- 1.389
- 3.23577	- 2.462	- 0.798	- 2.516	- 0.837
0.00000	- 4.211	- 2.506	- 4.785	- 2.36
3.23577	- 5.475	- 4.751	- 6.666	- 4.467
5.36970	- 6.659	- 6.489	- 8.148	- 6.128
- 5.04042	- 1.244	- 2.712	- 1.116	- 2.455
- 1.75502	- 3.621	- 2.690	- 3.971	- 2.396
1.75502	- 5.074	- 4.119	- 5.834	- 3.697
5.04042	- 6.799	- 6.218	- 8.012	- 5.724

TABLE 1.8 b — INTERACTION STRENGTH λ = 3.5

THE LOGARITHMS OF THE PROBABILITY DISTRIBUTION OF THE STATES (E_i)

INCIDENT MOMENTUM (K_o)	5.00		8.00		17.00	
STATES (E_i)	EXACT CALCU-LATION	TDHF CALCU-LATION	EXACT CALCU-LATION	TDHF CALCU-LATION	EXACT CALCU-LATION	TDHF CALCU-LATION
- 5.36970	- 0.234	- 0.834	- 0.325	- 0.916	- 0.493	- 1.074
- 3.23577	- 0.388	- 0.788	- 2.788	- 0.751	- 2.513	- 0.778
0.00000	- 3.776	- 2.829	- 3.316	- 2.744	- 3.796	- 2.598
3.23577	- 3.959	- 5.404	- 3.439	- 5.229	- 4.544	- 4.933
5.36970	- 4.433	- 7.339	- 3.598	- 7.107	- 5.392	- 6.722
- 5.04042	- 3.268	- 4.484	- 2.433	- 3.614	- 1.480	- 2.954
- 1.75502	- 4.754	- 4.612	- 4.003	- 3.707	- 3.479	- 2.979
1.75502	- 5.461	- 6.194	- 4.815	- 5.252	- 4.620	- 4.455
5.04042	- 5.831	- 8.431	- 5.44	- 7.455	- 5.907	- 6.595

TABLE : 1.9 INTERACTION STRENGTH $\lambda = 4.5$

THE LOGARITHMS OF THE PROBABILITY DISTRIBUTION OF THE STATES (E_i)

INCIDENT MOMENTUM (K_o)	5.00		8.00		20.00	
STATES (E_i)	EXACT CALCU-LATION	TDHF CALCU-LATION	EXACT CALCU-LATION	TDHF CALCU-LATION	EXACT CALCU-LATION	TDHF CALCU-LATION
- 5.36970	- 0.175	- 0.81	- 0.282	- 0.87	- 0.471	- 1.054
- 3.23577	- 4.047	- 0.734	- 2.945	- 0.744	- 2.544	- 0.774
0.00000	- 4.441	- 2.856	- 3.35	- 2.791	- 3.713	- 2.615
3.23577	- 4.57	- 5.461	- 3.395	- 5.326	- 4.351	- 4.967
5.36970	- 5.079	- 7.414	- 3.479	- 7.234	- 5.115	- 6.766
- 5.04042	- 3.688	- 5.091	- 2.842	- 3.998	- 1.565	- 3.008
- 1.75502	- 5.039	- 5.229	- 4.342	- 4.11	- 3.476	- 3.041
1.75502	- 5.605	- 6.823	- 5.101	- 5.676	- 4.548	- 4.526
5.04042	- 5.901	- 9.07	- 5.578	- 7.898	- 5.725	- 6.674

TABLE : 1.10 INTERACTION STRENGTH λ = 0.1

INCIDENT MOMENTUM (K_o)	ENERGY LOSS OBTAINED FROM EXACT CALCULATIONS	TDHF CALCULATIONS	PTDHF CALCULATIONS
5.00	0.633E-01	0.882E-02	0.672E-01
15.00	0.732E-02	0.152E-03	0.585E-01
20.00	0.413E-02	0.520E-04	0.584E-01

TABLE : 1.11

INTERACTION STRENGTH λ = 0.50

ENERGY LOSS OBTAINED FROM

INCIDENT MOMENTUM (K_o)	EXACT CALCULATIONS	TDHF CALCULATIONS	PTDHF CALCULATIONS
5	0.7659E + 00	0.6944E + 00	0.7528E + 00
11	0.2579E + 00	0.1740E + 00	0.2324E + 00
20	0.9353E - 01	0.229E - 01	0.8133E + 00
30	0.4388E - 01	0.420E - 02	0.626E - 01
40	0.2518E - 01	0.2439E - 02	0.608E - 01

TABLE : 1.12 INTERACTION STRENGTH λ = 1.00

INCIDENT MOMENTUM (K_o)	ENERGY LOSS OBTAINED FROM EXACT CALCULATIONS	TDHF CALCULATIONS	PTDHF CALCULATIONS
5	0.1539E + 01	0.8675E + 00	0.9259E + 00
11	0.6605E + 00	0.6362E + 00	0.6945E + 00
17	0.3766E + 00	0.3303E + 00	0.3887E + 00
23	0.2399E + 00	0.1522E + 00	0.2106E + 00
26	0.197E + 00	0.1010E + 00	0.1594E + 00

TABLE :-1.13 INTERACTION STRENGTH $\lambda = 2.00$

ENERGY LOSS OBTAINED FROM

INCIDENT MOMENTUM (K_o)	EXACT CALCULATIONS	TDHF CALCULATIONS	PTDHF CALCULATIONS
5	0.2153E + 01	0.9336E + 00	0.9919E + 00
11	0.1318E + 01	0.8577E + 00	0.916E + 00
17	0.8732E + 00	0.7608E + 00	0.819E + 00
23	0.6236E + 00	0.6072E + 00	0.6655 + 00
30	0.4463E + 00	0.6263E - 01	0.1209E + 00

TABLE : 1.14 INTERACTION STRENGTH λ = 4.5

ENERGY LOSS OBTAINED FROM

INCIDENT MOMENTUM (K_o)	EXACT CALCULATIONS	TDHF CALCULATIONS	PTDHF CALCULATIONS
5	0.7313E + 00	0.9872E + 00	0.1046E + 01
8	0.2165E + 01	0.9605E + 00	0.1019E + 01
15	0.1827E + 01	0.9082E + 00	0.9666E + 00
20	0.1529E + 01	0.8823E + 00	0.9407E + 00
26	0.1249E + 01	0.852E + 00	0.9104E + 00
30	0.1102E + 01	0.8278E + 00	0.8862E + 00

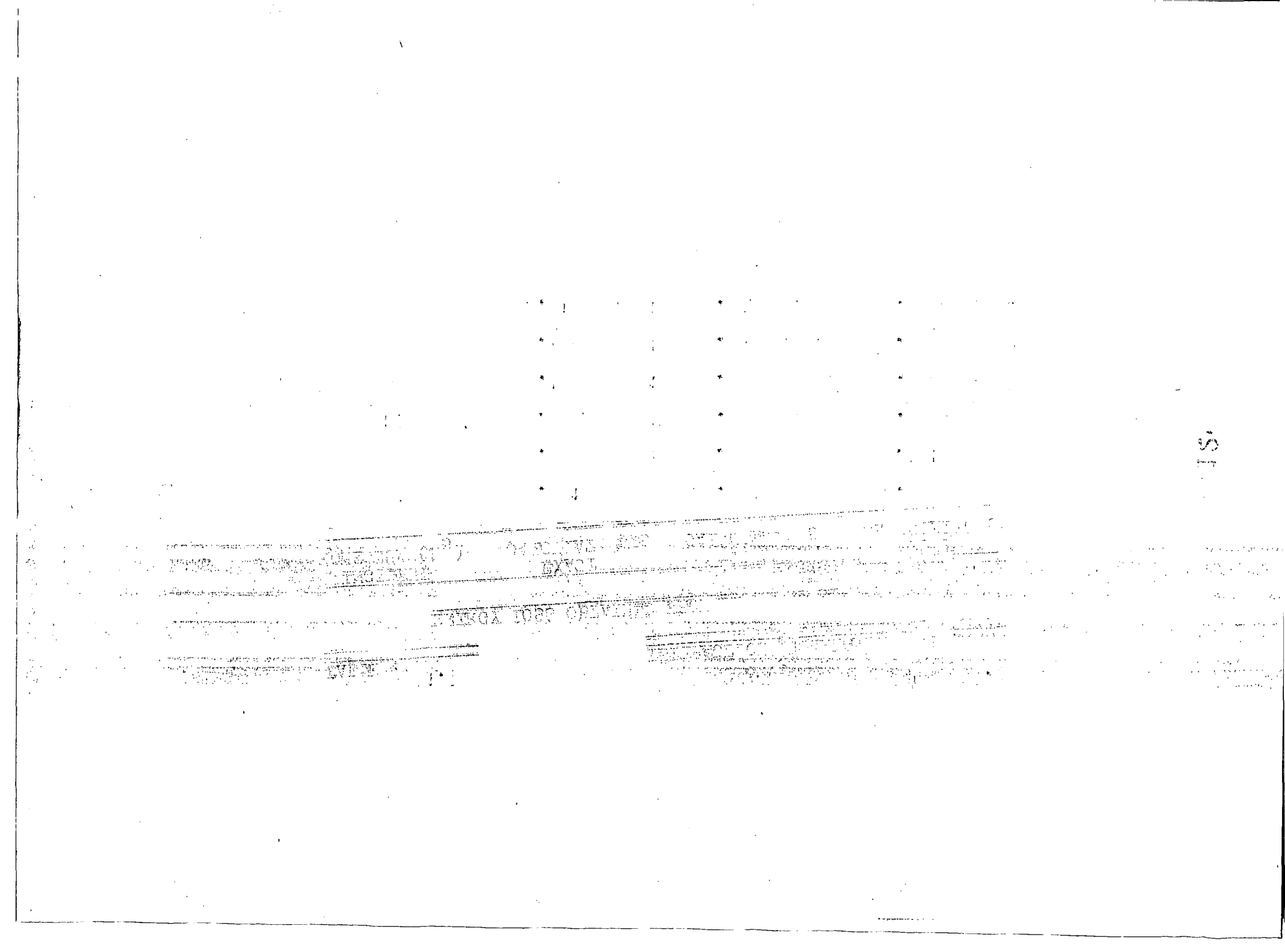

TABLE : 2.1 N = 14

ODD PARITY STATES (E_-)

χ	ζ	E_{EXACT}	E_{HF}	E_{PHF}	E_{HFP}
2	0.54	8.517	8.385	8.381	8.381
1.9	0.56		8.159	8.153	8.153
1.8	0.58		7.944	7.934	7.933
1.7	0.61		7.742	7.726	7.723
1.6	0.64		7.556	7.529	7.519
1.5	0.67		7.388	7.343	7.320
1.4	0.69		7.242	7.169	7.112
1.3	0.72		7.124	7.007	6.873
1.2	0.74		7.041	6.858	6.562
1.1	0.77		7.002	6.721	6.124
1.0	0.79	6.622	7.012	6.596	-941.22
0.8	0.83	6.393		6.381	
0.6	0.875	6.219		6.215	
0.4	0.92	6.096		6.095	
1.05			7.002		-2246.89
1.077			7.000		6.000

TABLE : 2.2 N = 14

EVEN PARITY STATES(E_+)

χ	ξ	E_{EXACT}	E_{HF}	E_{PHF}	E_{HFP}
2	0.55	8.636	8.385	8.388	8.388
1.9	0.58			8.166	
1.8	0.62		7.944	7.957	7.954
1.7	0.71			7.772	
1.6	0.84		7.556	7.659	7.591
1.5	0.86		7.388	7.567	7.454
1.4	0.88		7.242	7.486	7.366
1.3	0.90		7.124	7.413	7.342
1.2	0.905		7.041	7.349	7.347
1.1	0.92		7.001	7.290	7.130
1.0	0.925	7.270		7.239	
0.8	0.94	7.163		7.151	
0.6	0.955	7.088		7.084	
0.4	0.971	7.038		7.037	
1.077			7.000		7.000
1.15			7.015		7.295
1.17			7.024		7.326

122

TABLE 2.3

INTERACTION PARAMETER χ	FIXED POINTS ξ_1	ξ_2
0.25	0.989	0.096
0.50	0.980	0.188
0.95	0.966	0.346
1.05	0.963	0.376
2.50	0.926	0.659

REFERENCES

1. Ullah, N., and Nesbet, R.K. Nucl. Phys. 39, (1962) 239.
2. Negele J.W. Phys. Rev. C 1, (1970) 1260.
3. Brueckner K.A., Gammel, J.L. et al Phys. Rev. 110 (1958) 431.
4. Baranger M., and Kumar K. Nucl. Phys. A 122 (1968) 241.
5. Nucl. Phys. A 110 (1968) 490.
5. Bethe H.A. Ann. Rev. Nucl. Sci 21 (1971) 93.
6. Faesseler A.Z. Physik 218, (1961) 394.
7. Ripka G. Advances in Nuclear Physics Vol. I ed. Baranger and Vogt (1968).
8. Faessler A. et al Z. Physik 212 (1968) 1.
   Sauer P.U. Nuovo Cim 57 B, (1968) 62.
9. TDHF and Beyond Lecture Notes in Physics, edited by K. Goeke and P.G. Reinhard.
10. Bardeen J.L., Cooper N., and Schrieffer J.R. Phys Rev 108, (1957) 1175.
11. Bogolyobov N.N. Soviet Phys Usp 2, (1959) 236.
12. Baranger M. Phys Rev 122, (1961) 992.
13. Valantin J.G., Phys Rev 122, (1961) 1012.
14. Dirac P.A.M. Proc. Camb. Phil. Soc. 26 (1930) 376.
15. Ferrel R.A. Phys Rev 107, (1957) 849.
16. Goldstone J. and Gottfried Nuovo Cim 13, (1959) 849.
17. Ehrenreich H. and Cohen M.H. Phys Rev 115, (1959) 786.
18. Bonche P., Koonin S.E. et al Phys Rev C 13, (1976) 1226.
19. Zyrianov P.S. and Eleonoski V.M., J.E.T. P 3, (1956) 620.

[illegible]

20. Wheeler J.A. Phys. Rev 52, (1937) 1083, 1107.

21. Belyaev S.T. Nucl. Phys. 64, (1965) 17.

22. Davies K.T.R. et al Phys Rev C 6, (1976) 2385.

23. A. de Shalit and H. Feshback, Theoretical Nuclear Physics, (Wiley New York 1974) Vol. 1, P 541.

24. Engel Y.M. et al Phys A 249, (1975) 215.

25. Wong C.Y. et al Nucl Phys A 256, (1975) 469.

26. Levit S. et al Phys. Rev C 21, (1980) 1603.

27. Alhassid Y. and Koonin S.E. Phys Rev C 23, (1981) 1590.

28. Negele J.W. in Theoretical Methods in Medium Energy and Heavy Ion Physics, Koonin S.E. Progress in Part and Nucl Phys 4 (1980) 283.

29. Lipkin H.J. et al Nucl. Phys A 62, (1965) 188, 199, 211.

30. Agassi D. and Lipkin H.J. Nucl Phys A 86, (1966) 321.

31. Mayer M.G. Phys. Rev 78, (1950) 22.

32. Bohr A. et al Phy Rev 110, (1958) 936.

33. Bogolyobov N.N. Nuovo Cim 7, (1958) (Ser 10) 794.

34. Pal M.K. Nucl Phys A 349, (1980) number (3), (4), 433.

35. Koonin S.E. and Nix J.R. Phys Rev C 13, (1976) 209.

36. Bloch C. and Messiah A. Nucl Phys A 39, (1962) 95.

37. Schutte J.D. and Bleuler K. Nucl Phys A 119, (1968) 221.

38. Agassi D. Nucl Phys A 116, (1968) 49.

39. Griffin J.J. et al Phys Rev C 21, (1979) 1098.

40. Parikh J.C. and Pave D.J. Phys Rev 175, (1968) 1293.

41. Griffin J.J. and Wheeler J.A. Phys Rev 108, (1957) 311.

42. Peierls R.E. and Yoccuz J. Proc. Phys Soc A 70, (1957) 381.

43. Peierls R.E. and Thouless P.J. Nucl Phys 38, (1962) 154.

44. Verhaar B.J. Nucl Phys 41, (1963) 53; 45 129.
Verhaar B.J. Nucl Phys 54, (1964) 641.

45. Rouhaninejad H. and Yoccuz J. Nucl Phys 78, (1966) 353.

46. Davies K.T.R. et al Phys Rev Lett 41, (1978) 632.

47. Flocard H. et al Phys Rev C 17, (1978) 1682.

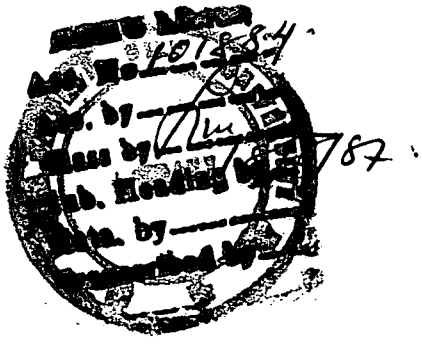

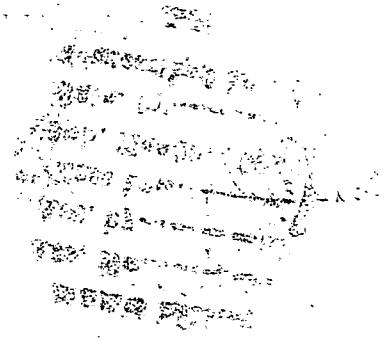

APPENDIX (A)

* Exactly Solvable Microscopic. Model for Deep Inelastic Collisions.

Energy Dissipation in Heavy Ion Reactions has been receiving attention in the last few years. There are several approximation methods developed for their study. Quite a number of dissipative concepts like friction, viscosity etc. are introduced and several attempts were made to relate them with microscopic quantum mechanical description (e.g. use of Time Dependent Perturbation theory (Beck and Gross 1973) to obtain expression for frictional forces proportional to the velocities).

The validity of these concepts and approximation methods is not clear. If an exactly solvable quantum mechanical model Hamiltonian for the description of Heavy Ion Reactions is available, it can be used to test the adequacy of these approximation methods.

In Section 1 we propose such a model based on the famous Lipkin Meshkov Glick Hamiltonian (Lipkin et al 1965). The method of obtaining exact solution is given in Section 2. The results are given in Section 3.

1. The Model : - The two nuclei A & B are moving in a one dimensional path, after collision they go away with part of translational Kinetic Energy transfered into internal excitation.

* This is a condensed version of the M. Phil thesis submitted in 1981.

The Hamiltonian can be written as

$$H = T_{rel} + H_A + H_B + V_{int} \quad \text{-----(1)}$$

i.e. the sum of Kinetic Energy, two intrinsic Hamiltonians of the nuclei and interaction between the nuclei are the usual Lipkin Model Hamiltonians described below.

In the Lipkin Model each nucleus consists of fermions distributed in two single particle energy levels $\pm \varepsilon/2$ denoted by $\sigma = \pm 1$, each having a degeneracy Ω. The N degenerate states are distinguished by a quantum number p. The two body interaction changes the Quantum number σ only but not p explicitly, in second quantized form the Hamiltonian can be written as

$$H_0 = \frac{\varepsilon}{2} \sum_{p,\sigma} a^\dagger_{p\sigma} a_{p\sigma} + \frac{V}{2} \sum_{pp'\sigma} a^\dagger_{p\sigma} a^\dagger_{p'\sigma} a_{p'-\sigma} a_{p-\sigma} \quad \text{-----(2)}$$

In all, there are 2^N eigenstates of this Hamiltonian and in a DIC, starting with the ground state, the nucleus could get excited into several of those states. However, because of internal symmetries of the Hamiltonian, there is a considerable reduction in the dimensionality. The Hamiltonian can be written in a very simple form using quasi spin operators defined through

$$J_+ = \sum_p a^\dagger_{p+1} a_{p-1} \; ; \; J_- = (J_+)^\dagger$$

$$J_z = \frac{1}{2} \sum_{p\sigma} \sigma a^\dagger_{p\sigma} a_{p\sigma} \; ; \; J_x = \frac{1}{2}(J_+ + J_-)$$

$$J_y = \frac{1}{2i}(J_+ - J_-)$$

These operators satisfy the usual angular momentum algebra, then the Hamiltonian can be expressed as

$$H_o = \mathcal{E} J_z + \frac{V}{2}\left(J_+^2 + J_-^2\right)$$
$$\text{or,} \quad H_o = \mathcal{E} J_z + V\left(J_x^2 + J_y^2\right) \qquad \text{-----(4)}$$

From the single particle part of the Hamiltonian it is clear that $J = \frac{N}{2}$ and that starting from the ground state, the nucleus can get excited to any of the $(2J = N)$ excited states only. Thus effectively, the dimensionality is cut down considerably.

Evaluation of energy levels and eigenfunctions involves diagonalization of matrices of dimensions only.

In order to distinguish the quasi spins of the two nuclei, we express H_A & H_B in terms of different quasi spin operators.

$$H_A = \mathcal{E} L_3 + V\left(L_x^2 - L_y^2\right)$$
$$H_B = \mathcal{E} S_3 + V\left(S_x^2 - S_y^2\right) \qquad \text{-----(5)}$$
$$\text{and} \quad [L_i, S_j] = 0$$

The interaction between the nucleons of A with the nucleons of B is quite similar to the interaction term in (5)

$$V_{int} = V\left(L_x S_x - L_y S_y\right) f(x) \qquad \text{-----(6)}$$

Where V denotes the strength of the interaction and is the form factor. For convenience we can choose f as follows :

$$f(x) = 2 \quad |x| < a$$
$$= 0 \quad |x| > a \qquad \text{------ (7)}$$

Then within the range of interaction the Hamiltonian takes the form

$$H = \xi J_3 + V(J_x^2 - J_y^2) + T_{rel}$$

where $J_i = L_i + S_i$ ------- (8)

2. Method of Solution.

The eigenstates of H_A are obtained by numerical diagonalisation

$$H_A \phi_i = \varepsilon_i \phi_i \quad \text{-----} \quad (9)$$

Outside the range of interaction we have

$$\left.\begin{aligned} H|s\rangle &= E_s|s\rangle \\ |s\rangle &= \phi_i(A)\phi_j(B) \\ E_s &= \varepsilon_i + \varepsilon_j \end{aligned}\right\} \text{-----} (10)$$

The incident state is described by

$$\psi_{inc} = I_0 \exp(ik_0 x)|s=0\rangle \text{-----} (11)$$

Initial kinetic energy is $\hbar^2 k^2 / 2m$. After scattering, the general wave function outside the range of interaction is a linear combination of states like

$$\left.\begin{aligned} &A_s \exp(ik_s x)|s\rangle \text{ for } x > a \\ &B_s \exp(-ik_s x)|s\rangle \text{ for } x < -a \end{aligned}\right\} \text{-----} (12)$$

Within the range of interaction the eigenstates are obtained by diagonalisation of H in equation (8)

$$H|\alpha\rangle = W_\alpha|\alpha\rangle \text{-----} (13)$$

The wave function can be written as

$$\Psi = I_0 \exp(ik_0 x)|0\rangle + \sum_s R_s \exp(-ik_s x)|s\rangle \quad x<0$$

$$= \sum_s T_s \exp(ik_s x)|s\rangle \quad x>0 \qquad ----(19)$$

R_s & T_s represent amplitudes of reflected and transmitted waves. Equations (16) & (17) are still valid. With the use of delta function explicit evaluation of $E\ W_{\alpha}\ |\alpha\rangle$ becomes unnecessary, and this simplifies the equations considered.

The continuity condition on the wave functions gives us $\quad T_s = I_0 \delta_{s0} + R_s \qquad ----- (20)$

The derivative boundary condition gives us

$$ik_s T_s - i\left[\delta_{s0} k_0 I_0 - k_s R_s\right]$$

$$= \frac{2m}{\hbar^2} \sum_t \langle s|Va(L_x S_x - L_y S_y)|t\rangle T_t \qquad ----(21)$$

From equation (20) we have $R_s = T_s - I_0\ \delta_{s0}$ substituting of this in equation (21) give us a set of linear equations for T. In order to get an idea of dimensionality for $N=8, J=4$ and each nucleus has 9 eigenstates; the states $|s\rangle$ are 81 in number, i.e. equation (21) is a set of linear equations in 81 variables T_t.

However because of the inherent symmetries of the problem the dimension can be reduced further. First since H_0 contains only J_z and J_+^2 and J_-^2 its eigenstates have components with either even $m(J_z)$ or odd m values only and not both. For convenience we call these states even and odd states.

However because of the inherent symmetries of the problem the dimension can be reduced further. First since H_0 contains only J_z^2 and J_+^2 and J_-^2 (and eigenstates) have components with either even or odd m values only and not both, for convenience we call these states even and odd states.

The continuity condition on the wave function gives us

The wave function can be written as

$$[illegible] \qquad (20)$$

From equation (20) we have $[illegible]$ substituting of this in equation (21) give us a set of linear equations for $[illegible]$ represent amplitudes of reflected and transmitted waves. Equations (16) & (17) are still valid. With the use of delta function explicit evaluation of $[illegible]$ becomes unnecessary, and this simplifies the equations considered.

In order to get an idea of dimensionality for N=2, J=4 and each nucleus has 9 eigenstates; the states $|S\rangle$ are 81 in number, i.e. equation (21) is a set of linear equations in 81 variables $[illegible]$.

However because of the inherent symmetries of the problem the dimension can be reduced further. First since H_0 contains only J_z^2 and J_+^2 and J_-^2 (and eigenstates) have components with either even or odd m values only and not both, for convenience we call these states even and odd states.

The continuity condition on the wave function gives us

The wave function can be written as

$$[illegible] \qquad (20)$$

From equation (20) we have [illegible]

in 81 variables [illegible].

considered.

However [illegible]

Within the range of interaction the wave function is a linear combination of functions like $\exp(\pm i K_\alpha x)|\alpha\rangle$

Where $K_\alpha = \left[k_0^2 + \frac{2m}{\hbar^2}(E_0 - W_\alpha)\right]^{1/2}$, $k_s = \left[k_0^2 + \frac{2m}{\hbar^2}(E_0 - E_s)\right]^{1/2}$ ----- (14)

The wave function in these three regions is written with appropriate coefficients, and appropriate boundary conditions are used at $x = \pm a$. If the incident beam is coming from left we have

$$\psi = I_0 e^{ik_0 x}|0\rangle + \sum_s R_s e^{-ik_s x}|s\rangle \quad , x < -a$$

$$= \sum_\alpha \left[A_\alpha e^{iK_\alpha x} + B_\alpha e^{-iK_\alpha x}\right]|\alpha\rangle, \quad |x| < a$$

$$= \sum T_s e^{ik_s x}|s\rangle \qquad x > a \quad ----(15)$$

The continuity of the wave function and its first derivative would give the required equations to determine A_α, B_α and T_s , R_s . The probability of excitation to an excited state by an energy $E_s - E_0$ is given by

$$P_s = \frac{k_s}{k_0} \frac{|T_s|^2 + |R_s|^2}{I_0^2} \quad ------ (16)$$

The average energy loss is given by

$$E_{loss} = \sum_s P_s (E_s - E_0) \quad ------ (17)$$

Generalization of this model for three dimensional motion is straight forward. However in the numerical calculations, the V_{int} is taken to be

$$H_{int} = Va\left[L_x S_x - L_y S_y\right]\delta(x) \quad ----(18)$$

The incident state is an even-even state. Since the interaction has terms like $L_+ S_+$ and $L_- S_-$ it connects even-even states to odd-odd states and vice versa, even-odd states never get excited, this reduces the dimension of the problem to 41. It is possible to iterate eq^n (21) once and obtain a set of 25 (or 16) equations having only even-even (or odd-odd) states only. Denoting even-even states with labels i, j, ... and odd-odd states with labels m, n, and introducing notation

$$M_{im} = \frac{2m}{\hbar^2} \langle i | Va(L_x S_x - L_y S_y) | M \rangle \quad ----(22)$$

we have

$$2i\left[k_i T_i - \delta_{io} I_o K_o\right] = \sum_j \left[\sum_m \frac{M_{im} M_{mj}}{2i k_m}\right] T_j \quad ---(23)$$

After solving this set of 25 linear equations, the other 16 amplitudes can be calculated using eq^n (21).

Since the two nuclei are considered to be identical the probability of excitation to state ϕ_i (A) ϕ_j(B) should be the same as ϕ_j(A) ϕ_i(B). In fact the two amplitudes are closely related, this reduces the dimensionality to 15. A similar procedure using the odd-states reduces the dimension to 10 and brings the problem within the reach of microcomputer.

The energy loss is obtained by use of equations (16) and (17).

3. THE RESULTS.

Calculations are done with N = 4 & N = 8, $\hbar = 1$ and $2m = 1$. For the preliminary calculations with N = 4, we choose $\frac{NV}{c} = 1$. From the structure of the equations (22) and (23), the amplitudes depend on $\frac{k}{a}$ only, we have chosen Va = 1. Table 1 gives the energy loss variation with incident momentum, the energy loss at first decreases reaches a minimum and again increases. The occupation probabilities (P_i) of the several energy levels for typical values of incident momentum (k_o) are presented in table (2) and for each given k_o, P_i decrease approximately exponentially, as E_i increases thus suggesting a Boltzmann distribution of the occupation probabilities. This indicates more or less complete thermalization and only the state $E_i = 1.25$ has occupation probabilities higher than the expected Boltzmann distribution.

In table (3) the effective temperatures and the measures of the goodness of the fit for several k_o values are given.

For smaller values of the ranges parameter λ , the energy loss monotonically decreases with the increase in the value of the incident momentum. However for large values of λ , the energy loss shows a maximum.

The occupation probabilities of the excited states, for different values of the range parameter λ , are shown in table (4) and figures 1 and 2.

For smaller values of the range parameter $\lambda = V_a/\varepsilon$ the occupation probabilities again show an exponential dependence on energy as seen in figure (1). However for larger values of λ , there is deviation from the Boltzmann distribution, as seen in figure (2).

The odd states approximately follow a different Boltzmann distribution as compared to the even states. These results demonstrate the capabilities of the model Hamiltonian to handle nuclei with considerably larger number of nucleons even on a computer of limited capabalities.

It is expected that even for nuclei with N = 40, and using a finite range instead of a delta function, calculation of a single scattering will take few minutes. In fact three dimension generalization of this model can be done trivially though it is expected to consume more time.

This model offers an opportunity for testing several approximation methods such as Time Dependent Perturbation theory. (Beck & Gross 1973). Time Dependent Hartree-Fock theory (Koonin & Negele 1977), Linear response theory (Hofmann 1977) and others. The occurence of the Boltzmann distribution, is very interesting.

For N = 8, that fact that for weaker interaction the occurence of single Boltzmann distributions and occurence of two separate Boltzmann distribution for even and odd states is another interesting feasures, perhaps in addition to the general heating of the nucleus, a collective odd parity excitation might have taken place.

References.

Beck R and Gross D H E 1973. Phys. Lett. B47, 143.

Hofmann, H. Fizika 1977 9 441.

Koonin, S.E. and Negele, J.W. 1977 Phys. Rev. C15 1359

Lipkin H.Q. Meshkov N and Glick, A.J. 1965, Nucl. Phys. 62, 188.

- - - - - -

TABLE 1

Dependence of the energy loss (E_{loss}) on the incident momentum (K_o) for N = 4

K_o	E_{loss}
5	0.0595
6	0.0421
7	0.0301
8	0.0221
9	0.0356
10	0.1767

TABLE 2

Probabilities of Excitations (P_i)

K_o =	5	6	7	8	9	10
E_i =						
- 2.17	0.7644 + 00	0.2123 + 00	0.8481 + 00	0.8678 + 00	0.8963 + 00	0.9180 + 00
- 1.25	0.1886 + 00	0.1583 + 00	0.1329 + 00	0.11191 + 00	0.9497 - 01	0.8120 - 02
0	0.3780 - 01	0.2501 - 01	0.1680 - 01	0.1150 - 01	0.8070 - 02	0.6860 - 03
1.25	0.750 - 02	0.378 - 02	0.194 - 02	0.1050 - 02	0.5880 - 03	0.343 - 03
2.17	0.1710 - 02	0.599 - 03	0.2420 - 03	0.1130 - 03	0.5830 - 04	0.377 - 04

TABLE 3

The effective temperatures for several k_o values is given.

k_o	Regression coefficient	Inverse temperature
5	-0.972	1.357
6	-0.9987	1.619
7	-0.9939	1.727
8	-0.9989	2.013
9	-0.9992	2.175
10	-0.9496	2.356

TABLE 4

The Occupation Probabilities of the excited states.

E_i	$\lambda = 1.5$ $k_o = 4.615$	$\lambda = 1.5$ $k_o = 14.115$	$\lambda = 3.5$ $k_o = 4.615$
-4.23	0.536 + 00	0.723 + 00	0.571 + 00
-3.47	0.153 + 00	0.197 + 00	0.569 - 01
-2.40	0.111 + 00	0.519 - 01	0.676 - 01
-1.23	0.370 - 01	0.175 - 01	0.168 - 01
0	0.584 - 01	0.675 - 02	0.450 - 01
1.23	0.136 - 01	0.261 - 02	0.657 - 02
2.40	0.437 - 01	0.116 - 02	0.393 - 01
3.47	0.582 - 02	0.31 - 03	0.249 - 02
4.23	0.450 - 01	0.11 - 03	0.560 - 01

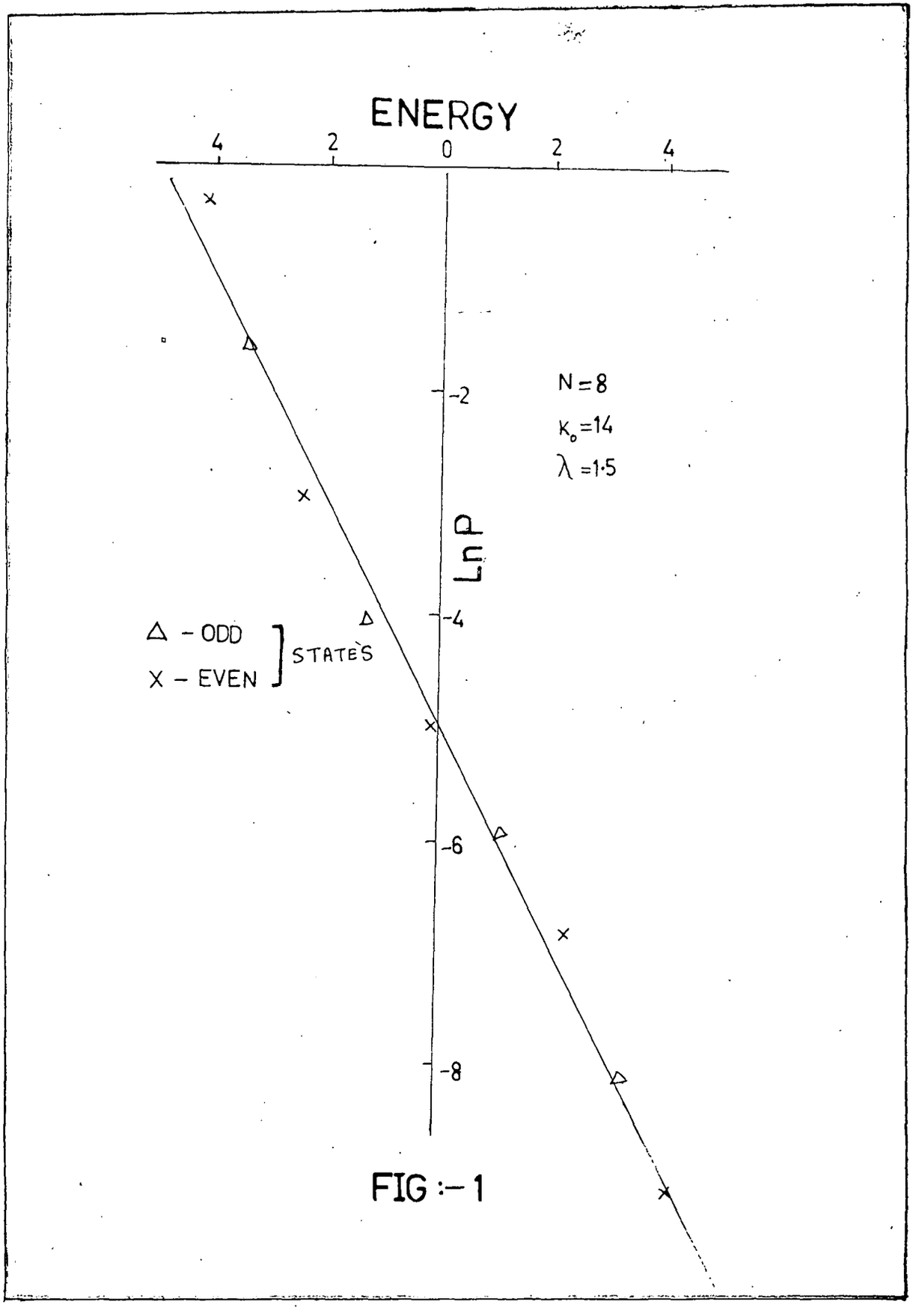

FIG :- 1

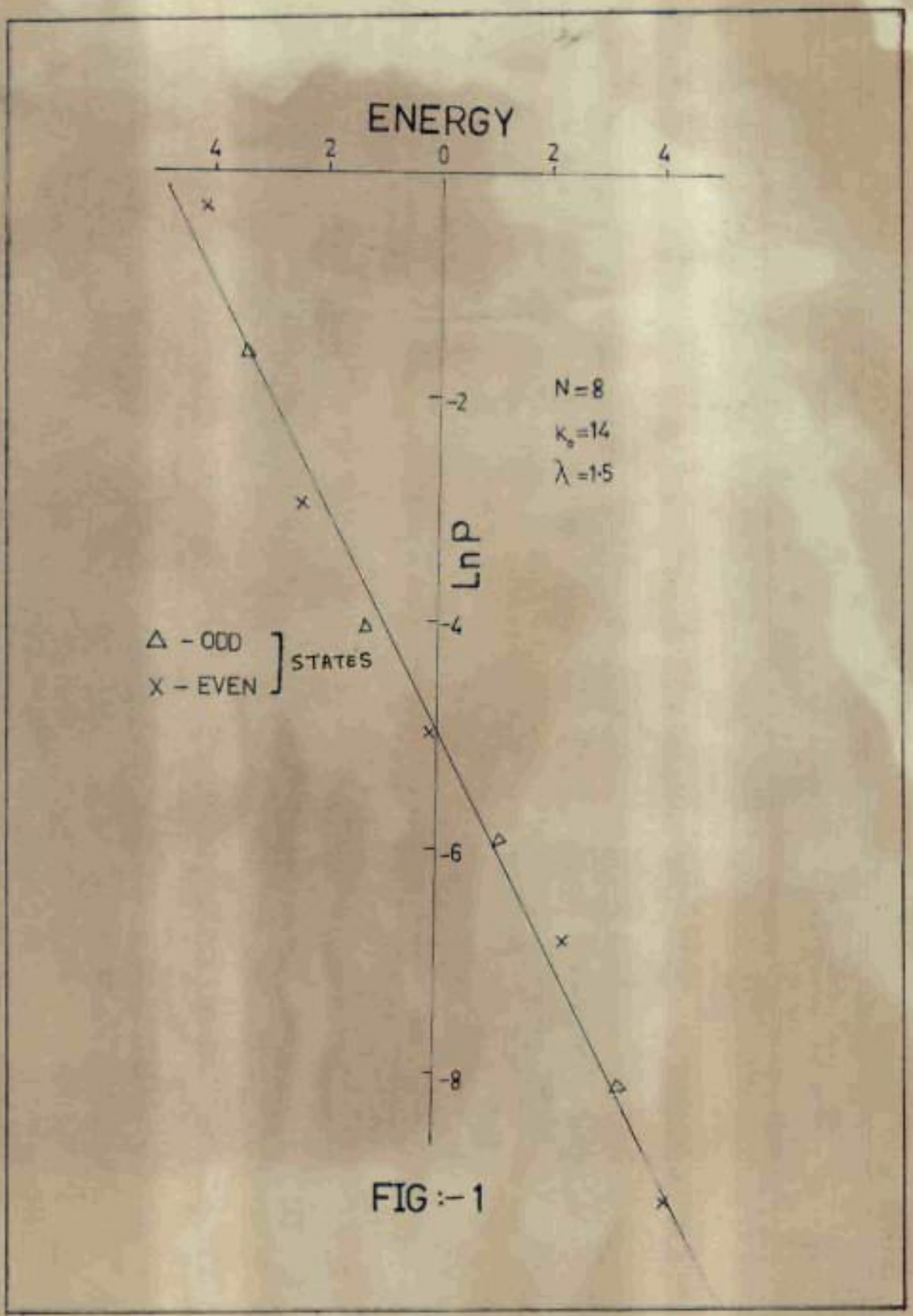

FIG :- 1

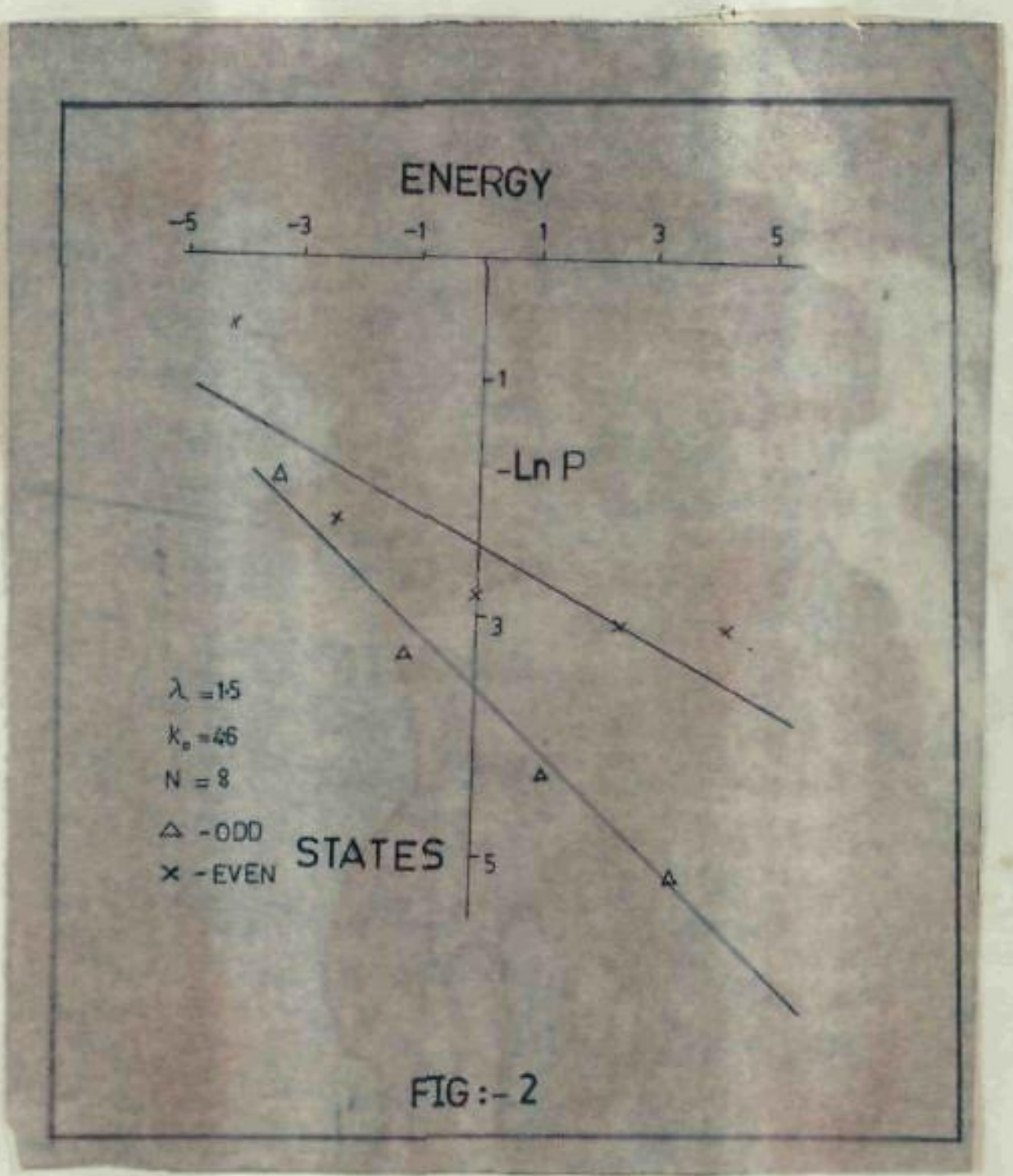

FIG :- 2